สภาพย่อยสลายได้ทางชีวภาพและสมบัติเชิงกลของวัสดุเชิงประกอบไมโครคริสตัลลีนเซลลูโลสที่ปรับสภาพด้วยไซเลน/พอลิแล็กทิกแอซิด

นายธนวัฒน์ ทะยอมใหม่

วิทยานิพนธ์นี้เป็นส่วนหนึ่งของการศึกษาตามหลักสูตรปริญญาวิทยาศาสตรมหาบัณฑิต
สาขาวิชาวิทยาศาสตร์พอลิเมอร์ประยุกต์และเทคโนโลยีสิ่งทอ ภาควิชาวัสดุศาสตร์
คณะวิทยาศาสตร์ จุฬาลงกรณ์มหาวิทยาลัย
ปีการศึกษา 2554

ลิขสิทธิ์ของจุฬาลงกรณ์มหาวิทยาลัย
บทคัดย่อและแฟ้มข้อมูลฉบับเต็มของวิทยานิพนธ์ตั้งแต่ปีการศึกษา 2554 ที่ให้บริการในคลังปัญญาจุฬาฯ (CUIR)
เป็นแฟ้มข้อมูลของนิสิตเจ้าของวิทยานิพนธ์ที่ส่งผ่านทางบัณฑิตวิทยาลัย
The abstract and full text of theses from the academic year 2011 in Chulalongkorn University Intellectual Repository(CUIR)
are the thesis authors' files submitted through the Graduate School.

BIODEGRADABILITY AND MECHANICAL PROPERTIES OF SILANE TREATED MICROCRYSTALLINE CELLULOSE /POLY(LACTIC ACID) COMPOSITES

Mr.Tanawat Tayommai

A Thesis Submitted in Partial Fulfillment of the Requirements
for the Degree of Master of Science Program in Applied Polymer Science and Textile Technology
Department of Materials Science
Faculty of Science
Chulalongkorn University
Academic Year 2011
Copyright of Chulalongkorn University

Thesis Title	BIODEGRADABILITY AND MECHANICAL PROPERTIES OF SILANE TREATED MICROCRYSTALLINE CELLULOSE /POLY(LACTIC ACID) COMPOSITES
By	Mr. Tanawat Tayommai
Field of Study	Materials Science
Thesis Advisor	Associate Professor Duangdao Aht-Ong, Ph.D

Accepted by the Faculty of Science, Chulalongkorn University in Partial Fulfillment of the Requirements for the Master‘s Degree.

……..Dean of the Faculty of Science
(Professor Supot Hannongbua, Dr.rer.nat.)

THESIS COMMITTEE

……..Chairman
(Assistant Professor Sirithan Jiemsirilers, Ph.D.)

……..Thesis Advisor
(Associate Professor Duangdao Aht-Ong, Ph.D)

……..Examiner
(Associate Professor Pranut Potiyaraj, Ph.D)

……..Examiner
(Associate Professor Kawee srikulkit, Ph.D)

……..External Examiner
(Associate Professor Paiparn Santisuk)

ธนวัฒน์ ทะยอมใหม่: ภาพย่อยสลายได้ทางชีวภาพและสมบัติเชิงกลของวัสดุเชิงประกอบไมโครคริสตัลลนเซลลูโลสที่ปรับสภาพด้วยไซเลน/พอลิแล็กทิกแอซิด
(BIODEGRADABILITY AND MECHANICAL PROPERTIES OF SILANE TREATED MICROCRYSTALLINE CELLULOSE /POLY(LACTIC ACID) COMPOSITES)
อ.ที่ปรึกษาวิทยานิพนธ์ : รศ.ดร.ดวงดาว อาจองค์, 106 หน้า

พลาสติกย่อยสลายได้ทางชีวภาพเสริมแรงด้วยเส้นใยธรรมชาติ ได้ถูกนำไปใช้งานในหลายด้านไม่ว่าจะเป็น งานโครงสร้าง ไปจนถึงอุตสาหกรรมอาหาร ซึ่งการใช้เส้นใยธรรมชาติเป็นสารเสริมแรงนั้นมีข้อดีในหลายๆ ด้าน เมื่อเปรียบเทียบกับเส้นใยอนินทรีย์ เช่นเส้นใยแก้ว ยกตัวอย่างเช่น ทำให้วัสดุมีน้ำหนักเบา เส้นใยสามารถหาทดแทนได้ มีราคาถูก ปล่อยก๊าซคาร์บอนไดออกไซด์ต่ำ ไม่ขัดถูกับเครื่องจักรในกระบวนการผลิต เป็นมิตรต่อสิ่งแวดล้อม และยังสามารถย่อยสลายได้ ดั้นนั้นในงานวิจัยนี้ จึงทำการศึกษาการเตรียมวัสดุเชิงประกอบของพอลิแล็กทิกแอซิดเสริมแรงด้วยไมโครคริสตัลลีนเซลลูโลสจากเส้นใยมะพร้าว เพื่อลดราคา และปรับปรุงสมบัติ ของพอลิแล็กทิกแอซิด โดยไมโครคริสตัลลีนเซลลูโลสจากใยมะพร้าวสามารถเตรียมได้จากการสกัดลิกนิน ฟอกขาว และไฮโดรลิซิสด้วยกรด จากนั้นทำการปรับปรุงพื้นผิวด้วย 3-อะมิโน ไตรเอททอกซี ไซเลน เพื่อเพิ่มความเข้ากันได้ระหว่างเส้นใยและพอลิเมอร์ การเตรียมวัสดุเชิงประกอบสามารถทำได้โดยใช้เครื่องอัดรีดแบบเกลียวคู่ โดยมีอัตราส่วนของไมโครคริสตัลลีนเซลลูโลสที่อัตราส่วนต่าง ๆ และมีไบ-โอแม็ก เป็นสารเติมแต่ง จากการทดลองพบว่า การเติมไมโครคริสตัลลีนเซลลูโลสร้อยละ 5 โดยน้ำหนัก และผสมไบโอแม็ก 2 ส่วนในร้อยส่วนของพอลิแล็กทิกแอซิด ให้สมบัติเชิงกลที่ดีที่สุด สมบัติทางความร้อนของวัสดุเชิงประกอบที่เตรียมได้มีค่าลดลง เมื่อมีการเพิ่มอัตราส่วนไมโครคริสตัลลีนเซลลูโลส แต่สามารถปรับปรุงสมบัติดังกล่าวได้โดยการใช้ 3-อะมิโน ไตรเอททอกซี ไซเลนปรับปรุงพื้นผิว การทดสอบความสามารถในการย่อยสลาย พบว่า พอลิแล็กทิกแอซิด และวัสดุเชิงประกอบที่เตรียมได้ที่มีไมโครคริสตัลลีนเซลลูโลสร้อยละ5 และ มี สารปรับปรุงพื้นผิว สามารถย่อยสลายได้ร้อยละ 80.1 และ 78.2 ตามลำดับหลังจากทำการทดสอบ 40 วัน ตามมาตรฐาน ISO 14855-2 และร้อยละ 37.6 และ 42.1 ตามมาตรฐาน ISO 14852 และจากการฝังดินพบว่า น้ำหนักของวัสดุเชิงประกอบลดลง เมื่อวันทดสอบและอัตราส่วนไมโครคริสตัลลีนเซลลูโลสที่เพิ่มขึ้น แต่วัสดุเชิงประกอบไม่สามารถย่อยสลายได้ในน้ำทะเลภายใน 30 วัน

ภาควิชา วัสดุศาสตร์ ลายมือชื่อนิสิต.....
สาขาวิชา วิทยาศาสตร์พอลิเมอร์ประยุกต์และเทคโนโลยีสิ่งทอ ลายมือชื่อ อ.ที่ปรึกษาวิทยานิพนธ์.....
ปีการศึกษา 2554

5272329023: APPLIED POLYMER SCIENCE AND TEXTILE TECHNOLOGY
KEY WORD: POLYLACTIC ACID / BIODEGRADABILITY / SILANE

TANAWAT TAYOMMAI: BIODEGRADABILITY AND MECHANICAL PROPERTIES OF SILANE TREATED MICROCRYSTALLINE CELLULOSE /POLY(LACTIC ACID) COMPOSITES. THESIS ADVISOR: ASSOC. PROF. DUANGDAO AHT-ONG, Ph.D. 106 pp.

Biodegradable plastic reinforced natural fiber composites are finding applications in many fields ranging from construction industry to food industry. The use of natural bio based fillers as reinforcements in composites has several advantages over inorganic fillers including lower density, renewability, low cost, lower CO_2 emissions, reduced abrasion, and thus machine wear during production processes, eco-friendliness, and biodegradability. In this research, polylactic acid (PLA)/ microcrystalline cellulose (MCC) composites were investigated as a means to reduce the material cost and enhance the material properties. The coir fiber was prepared by 3 steps process namely delignification, bleaching, and hydrolysis, respectively, to obtain MCC. The MCC was then surface treated by 5 wt.% of 3-aminopropyl triethoxy silane (APS). After that, PLA was mixed with MCC at various ratios by twin-screw extruder and fabricated into test specimens by compression molding. The Biomax® was used as the modification resin. The results shows that, the polylactic acid with 5 wt.% of microcrystalline cellulose and blend with 2 phr of Biomax® exhibited the best mechanical properties compared with all prepared composites. Thermal stability of PLA composites were decrease with increasing MCC content but it can be improved by treated the MCC by APS. The percentage of biodegradation of neat PLA and PLA-5MCC-Si-Bi and %biodegradation reached the values of 80.1% and 78.2%, respectively, at 40 days of test period according to ISO 14855-2. In aqueous medium, the percentage of biodegradation of neat PLA and PLA-5MCC-Si-Bi reached the value of 37.6% and 42.1 %, respectively, according to ISO 14852. The weight remaining of PLA composites buried in landfill was decreased with increasing MCC content and degradation time. Surprisingly, the PLA composites were not degraded under real seawater condition in 30 days.

Department: Materials Science Student's signature……...
Field of study: Applied Polymer Science and textile technology Advisor's signature……..
Academic year: 2011

ACKNOWLEDGMENTS

The author would like to thank many people for kindly providing the knowledge of this study, the most important thing for this completed is the advice and professional aid of my advisor. I would like to express my gratitude and appreciation to my advisor Associate Professor Dr. Duangdao Aht-Ong.

I wish to express my grateful thank to Assistant Professor Dr.Sirithan Jiemsirilers, chairman of this thesis committee for her valuable advice. I also would like to express my appreciation to Associate Professor Paiparn Santisuk, Associate Professor Dr.Pranut Potiyaraj, and Associate Professor Dr. Kawee Srikulkit for seving as my thesis committee member and for their invaluable suggestions and guidance.

In addition, the author would like to acknowledge the financial support of this research from Nation Innovation Agency through research grant No. D4-52. The financial support and scholarship from National Center of Petroleum, Petrochemicals, and Advanced Materials, Chulalongkorn University are highly appreciated.

I truly thank many helping hands throughout my study including students in the Department of Materials Science, Faculty of Science, Chulalongkorn University for their friendship and assistance.

Finally, I would like to express my greatest appreciation to my family for their support and encouragement.

LIST OF ABBREVIATIONS

APS	3-Aminopro triethoxy silane
MCC	Microcrystalline cellulose
PLA	Polylactic acid
SEM	Scanning electron microscope
DSC	Differential scanning calorimetry
TGA	Thermo gravimetric analysis
XRD	X-ray diffrectometor
PLA-Bi	Polylactic acid blend with Biomax®
MCC-Si	Silane treated microcrystalline cellulose

CONTENTS

Page

Page

LIST OF TABLES

LIST OF FIGURES

Page

Page

Page

CHAPTER 1

Introduction

1.1 Background

Advanced technology in the field of petrochemical-based polymers has brought many benefits to mankind. However, it is becoming more obvious that the ecosystem is much disturbed and damaged as a result of the non-degradable plastic materials for disposable items. The environmental impact of plastic wastes is increasing global concerns, and alternative disposal methods are limited. Incineration of the plastic wastes always produces a large amount of green house gases and creates global warming, and sometimes produces toxic gases, which again contribute to global pollution. On the other hand, satisfactory landfill sites are also limited. Also, the petroleum resources are finite and becoming limited. For this reason, there is an urgent need to develop renewable source-based environmental benign plastic materials, especially in short-term packaging and disposable applications that would not involve the use of toxic or noxious components in their manufacture and could allow the composting of naturally occurring degradation products. One of the most promising polymers in this direction is PLA because it is made from agricultural products and is readily biodegradable. PLA is not a new polymer; however, recent developments in the manufacturing of the monomer economically from agricultural products have placed this material at the forefront of the emerging biodegradable plastics industries.

PLA is a linear aliphatic thermoplastic polyester. High molecular weight PLA is generally produced by the ring-opening polymerization of the lactide monomer. Lactide is a cyclic dimer prepared by the controlled depolymerization of lactic acid oligomer, which in turn is obtained by the fermentation of corn, sugar cane, sugar beat, and so on [1,2]. PLA has comparable mechanical performance to those petroleum-based polyesters, especially high elasticity modulus and high stiffness, thermoplastic behavior, biocompatibility, and good shaping and molding capability. PLA is classified as a water-sensitive polymer because it degrades slowly compared

with water-soluble or water-swollen polymers [3]. Its thermal and mechanical properties are superior to those of the other biodegradable aliphatic polyesters, such as poly(butylenes succinate) (PBS), poly(3-hydroxybutyrate) (PHB), and poly(capro lactone) (PCL) [4].

As with other biopolymers, PLA remains relatively costly when compared with commodity thermoplastics such as polyethylene and polypropylene but a cost level competitive with polyethylene terephthalate (PET) is considered feasible. Possibly because the polymer has only recently been available in bulk to any great degree, there has so far been relatively little research on PLA as a matrix in natural fibre biocomposites.

The use of natural biobased fillers as reinforcements in composites has several advantages over inorganic fillers including lower density, renewability, low cost, lower CO_2 emissions, reduced abrasion, and thus machine wear during production processes, eco-friendliness, and biodegradability [5]. For these reasons, biofiller-reinforced biodegradable polymer biocomposites have been increasingly used to fabricate products such as automotive interiors, electronic products, and packaging [6]. Cellulose fibers such as cotton, banana [7] have been used as reinforcing fillers in biodegradable polymer. These fillers are completely biodegradable in a wide range of environments. In particular, cellulose fiber has attracted attention as an alternative to wood fiber and flour. Coconut palms are grown in more than 80 countries of the world, with a total production of 61 million tones per year [8]. Thailand is the sixth coconut production of the world. Coir (the fiber from the husk of the coconut) is used in ropes, mats, brushes, sacks, and as stuffing fiber for mattresses [9]. Therefore, there has been considerable research aimed at increasing the use of coir as reinforcements for composite materials.

The interest in using natural fibers in composites has increased in recent years due to their lightweight, nonabrasive, nontoxic, low cost, and biodegradable properties. However, lack of good interfacial adhesion, low melting point, and poor resistance to moisture absorption, make the use of natural fiber reinforced composites less attractive. Pretreatments of the fiber can clean the fiber surface, chemically modify the surface, stop the moisture absorption process and increase the surface

roughness [10]. As the natural fibers bear hydroxyl groups from cellulose and lignin, therefore, they are amenable to modification. The hydroxyl groups may be involved in the hydrogen bonding within the cellulose molecules thereby reducing the activity towards the matrix. Chemical modifications may activate these groups or can introduce new moieties that can effectively interlock with the matrix. Mercerization, isocyanate treatment, acrylation, permanganate treatment, acetylation, silane treatment and peroxide treatment with various coupling agents and other pretreatments of natural fibers have achieved various levels of success in improving fiber strength, and fiber-matrix adhesion in natural fiber reinforced composites. Simple chemical treatments can be applied to the fibers to change surface tension and polarity through modification of fiber surface [11].

1.2 Objective of Research

The goal of this research was to improve properties of polylactic acid by reinforcing with microcrystalline cellulose from agricultural wastes. Therefore, the coir fiber waste was used to prepare microcrystalline cellulose by acid hydrolysis. Then, the prepared microcrystalline cellulose was used as reinforcement in polylactic acid at various ratios. The coir microcrystalline cellulose/polylactic acid composites were prepared by mixing the composition using a twin-screw extrusion and fabricating by compression molding. 3-aminopropyl triethoxy silane and Biomax® strong 120 were used to improve interfacial adhesion and elongation of composites, respectively. The effect of microcrystalline cellulose content fiber surface treatment and additive on mechanical, physical, thermal and degradability properties of composites were investigated. As mentioned, the primary mechanism of degradation of PLA is hydrolysis, catalyzed by temperature, followed by bacterial attack on the fragmented residues. Many studies concern biodegradation of PLA in different environments such as aquatic system, soil, and compost. Therefore, the real condition (land fill, sea water) and simulated condition (ISO 14855-2, ISO 14852) were used to investigate the biodegradability of polylactic acid/microcrystalline cellulose composites. For the rail condition, percentage of weight remaining, molecular weight, and morphology of polylactic acid/microcrystalline cellulose composites was used to determine the biodegradability of its. The percentage of biodegradability of polylactic

acid/microcrystalline cellulose composites in simulated conditions was calculated by percentage of carbon dioxide release from microorganism.

CHAPTER 2

Literature review

3.1 Composites

Composites are combinations of (at least two) materials: matrix and reinforcement [12,13,14]. The matrix material surrounds and supports the reinforcement materials by maintaining their relative positions. The reinforcements are embedded and arranged in specific internal configurations to obtain mechanical or other properties. The reinforcing materials, which consist of one or more chemically distinct constituents, can be metal, ceramic, or polymer. Due to the broad diversity of matrix and reinforcement materials available, the properties of the composite materials can combine the best of each component to maximize the properties (stiffness, strength-to-weight ratio, tensile strength, etc.) and minimize others properties such as weight and cost. Naturally, reinforcing materials are stiff and strong while the polymer matrix is usually a ductile or tough material. If the composite is designed and fabricated correctly, it combines the strength of the reinforcement with the toughness of the polymer matrix to achieve a combination of desirable properties that cannot be achieved with any single component material [15].

3.1.1 Classification

The major classes of structural composites can be categorized as polymer matrix composites (PMCs), metal matrix composites (MMCs) and ceramic matric composites (CMCs) [16].

- Polymer Matrix Composites

PMCs are the most developed class of composites materials that they have widespread application, can be fabricated into large complex shapes, and have been accepted in variety of aerospace and commercial application. They are made of components such as carbon or glass fiber bound together by a polymer matrix. These reinforced plastic are a synergistic combination of high-performance fiber and matrices

- Metal Matrix Composites

These composites consist of metal alloys reinforced with continuous fibers, whiskers, or particulates. Because of their use of metal as matrix materials, they have a higher temperature resistance than PMCs but in general are heaver. They are not as widely use as PMCs but are finding increasing application in many areas such as transportation.

- Ceramic Matrix Composites

Ceramic materials have a natural high-temperature resistance but also have basic limitation in structural application owing to their propensity for brittle fracture. The incorporation of reinforcement, for example, ceramic fiber reinforcement into the ceramic matrix can improve the forgivability of the material by allow cracking to be retarded by the fiber-matrix interfaces. CMCs are a class if structural materials with reinforcements such as SiC fiber embedded in a ceramic matrix such as Al_2O_3, Si_3N_4 or SiC.

3.1.2 Polymer Matrix Composites

Polymer composites are a well-established class of materials in which particles or fibers – used as reinforcing component are dispersed in the polymer matrix. The schematic of PMCs is shown in Figure 2.1. The fiber provides the high strength and modulus, whereas the matrix spreads the loads as well as offering to weather and corrosion. Composites strength is almost directly proportional to the basic fiber strength and can be improved at the expense stiffness. High-modulus organic fibers have been made with simple polymer by arranging the molecules during processing, with results in a straightened molecular structure. The advantages of PMCs can therefore be summarized as [14]:

- High strength-to-weight ratio
- High creep resistance
- High tensile strength at elevated temperatures
- High toughness.

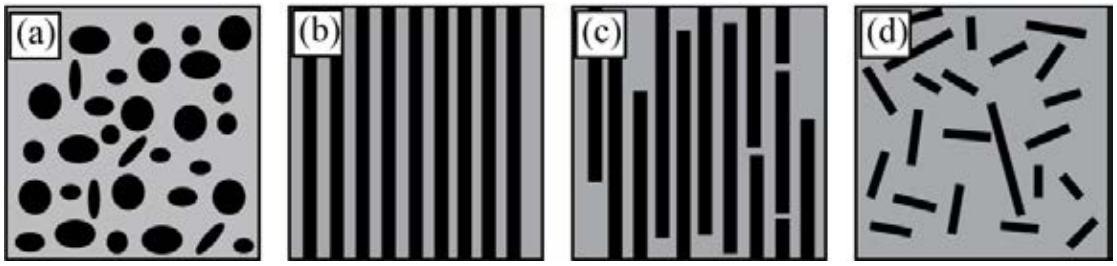

Figure 2.1 Schematic representations of polymer composites: a) particle reinforcement b) fiber reinforcement with continuous and aligned fibers; c) with discontinuous and aligned fibers; d) with discontinuous and randomly oriented fibers.

The strengthening mechanisms of the composites depend primarily on the amount, arrangement, geometry and type of reinforcement in the polymer matrix. Polymer composites can be divided into two main categories (Figure. 2.1), normally referred to as [13,15]:

– Particle-reinforced polymer composites (PRPCs)

Particles used to reinforce polymers include ceramics and glasses such as small mineral particles, quartz or glass powder, metal particles such as Ni, Cu, Ag, Al or Fe, and occasionally also organic particles of wood, rice hulls or starch [13]. Most mineral particles such as $CaCO_3$ are normally used to increase the modulus of the matrix, to increase wear and abrasion resistance and surface hardness, to improve performance at higher temperatures, to reduce friction and shrinkage, and to decrease the permeability of the matrix. Sometimes they are just used to reduce cost of the final. In contrast, metal particles are mainly used to improve the electrical conductivities of most insulating polymer matrices.

– Fiber-reinforced polymer composites (FRPCs)

Fibers, although strong and tough, are generally not very stiff because they are very small in diameter. Therefore, it would be impossible for a structure to be made only from small fibers. Adding a matrix material connect the fibers together to form a structure, so that force can be transferred from one fiber to another to sharing the load. Adding reinforcing fibers will expansions the modulus of the matrix material. The orientation of the fibers relative to one another, the fiber concentration and their distribution all have a significant effect on the strength and other properties of the composites [17].

3.2 Biodegradable polymer

3.2.1 Classification

It is not easy to decide how to classify biodegradable polymers. They can be sorted according to their chemical composition, synthesis method, processing method, economic importance, application, etc. Each of these classifications provides different and useful information. Figure. 2.2 shows a classification of biodegradable polymers in four families by the origin of the raw materials. Except the fourth family, which is of fossil origin, most polymers (family 1–3) are obtained from renewable resources (biomass) [18].

The first family is agro-polymers (e.g. polysaccharides) obtained from biomass by extraction. The second and third families are polyesters, obtained by fermentation from biomass or from genetically modified plants (e.g. PHA, polyhydroxyalkanoate) respectively and by synthesis from monomers obtained from biomass (e.g. polylactic acid). The fourth family is polyesters, totally synthesized by the petrochemical process such as polyesteramide; polycaprolactone; aliphatic or aromatic copolyesters). A large number of these biodegradable polymers are commercially available for example polylactic acid. They show a large range of properties and they can compete with available non-biodegradable polymers in the same industrial fields such as packaging.

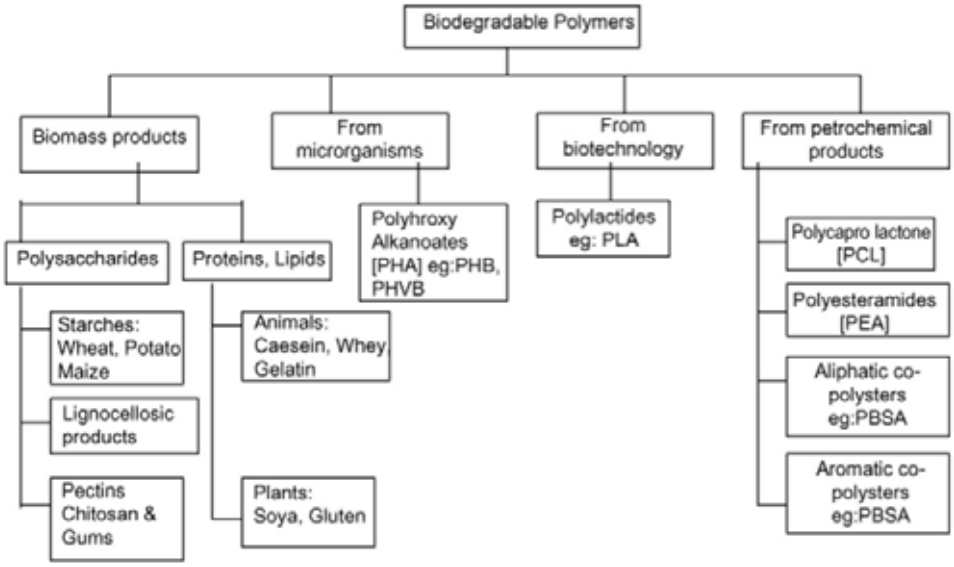

Figure 2.2. Classification of biodegradable polymer [18].

3.2.2 Polylactic acid

Polylactic acids or Polylactide are terms used to indicate the same biodegradable aliphatic polyester [19]. The difference in terminology indicates simply the synthesis method chosen to produce the polymer from lactic acid. The interesting of PLA is started in the 1930s with the work of Carothers but the molecular weight was too low and the mechanical properties were weak. In 1954, DuPont patented a PLA presenting higher molecular weight. PLA can be synthesized by the esterification of lactic acid, which was obtained by fermentation. Nowadays, the PLA cost decrease is due mainly to the improvement of the bacterial yield and synthesis technology [20].

3.2.2.1 Synthesis

Lactic acid is one of the simplest chiral molecules and exists as the two stereoisomers, L- and D-lactic acid. The L form differs from the D form in its effect on polarised light. For L-lactic acid, the plane is rotated in a clockwise (dextro) direction, whereas the D form rotates the plane in a anticlockwise (laevo) direction. Figure 2.3 illustrates these two forms [21].

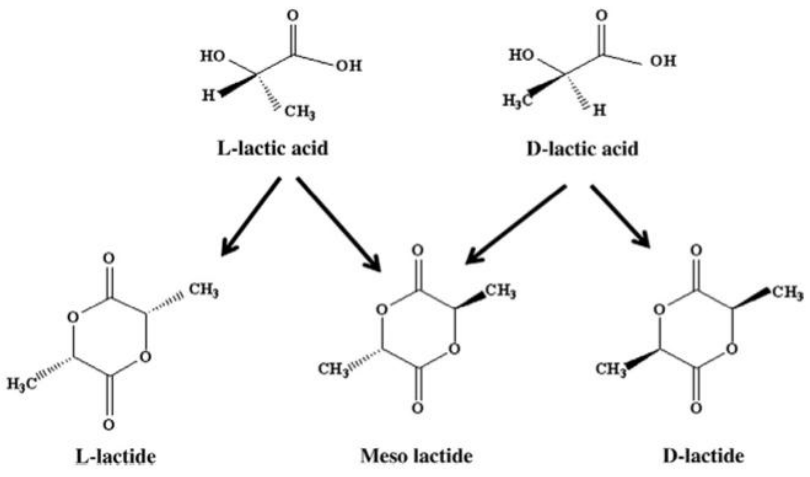

Figure 2.3 The stereo complex of lactic acid.

The both functional group (hydroxyl and carboxyl group) in lactic acid allows it to be synthesized directly to polyester via a condensation polymerization reaction. However, the conventional condensation polymerization of lactic acid does not obtained the molecular weight polymer and the polymerization time is very long. Addition of acidic catalysts, such as boric or sulfuric acid accelerates the esterification and trans-esterification processes, When the pre-condensates obtained by dehydratization up to 120 °C are heated to 180 °C in the presence of nonacidic trans-esterification catalysts, such as PbO, a moderate yield of relatively high-molecular weight PLA may result [22,23].

The general way to obtain the high-molecular weight polylactic acid is process by ring-opening polymerization of lactide. The intermediate lactide, a cyclic lactic acid dimer, is formed in the first step when the condensation product water is removed by evaporation during oligomerization. L-lactic acid, D-lactic acid or mixtures can be polymerized to low-molecular weight prepolymer, which is in then catalytically depolymerized through an internal trans-esterification, i.e., by ‗back-biting' reaction to lactide. Three stereoforms of lactide are possible: L-lactide, D-lactide, and meso-lactide (**Figure. 2.3**). In the second step, purified L-lactide, D-lactide, DL-lactide (50:50 mixture of L and D isomers), or meso-lactide monomer is converted into the corresponding high-molecular weight polyester by catalytic ring- opening polymerization. A stannous octoate catalyst carried out ring-opening polymerization most commonly, but for laboratory demonstrations tin (II) chloride is often employed. The schematic of PLA synthesis root is shown in Figure 2.4.

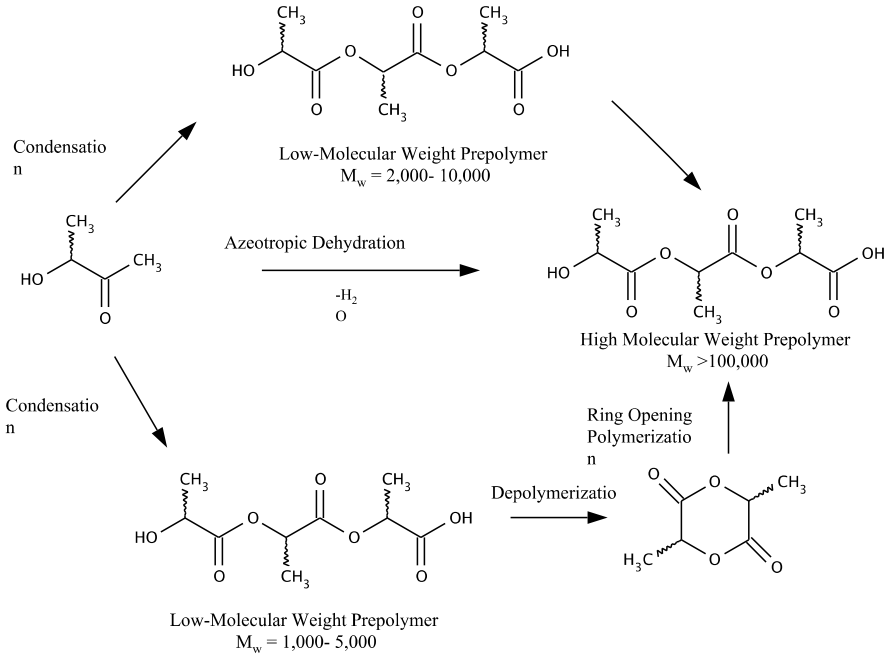

Figure 2.4 PLA synthesis root.

3.2.2.2 Properties

Poly (lactic acid) exists as a polymeric helix, with an orthorhombic unit cell. Properties of PLA depend on the component stereo isomers, processing temperature, annealing time and molecular weight. Poly-L-lactide (PLLA) is the product resulting from polymerization of L-lactide. PLLA has a crystallinity of around 37%, a glass transition temperature is in the range of 50–80 °C and a melting temperature around 173–178 °C. Because of the stereo regular chain microstructure, optically pure, polylactic acid, poly (L-lactide) (PLLA) and poly (D-lactide) (PDLA), are semi crystalline. The crystallization ability of polylactic acid decreases with chain stereo regularity. Crystallization of polylactic acid in the form of stereo complex also leads to a brittle mechanical behavior [22]. Polylactic acid is a clear, colorless thermoplastic when quenched from high temperature and is similar to polystyrene. Polylactic acid can be processed like most thermoplastics into fiber and film. The melting temperature of PLLA can be increased 40–50 °C and its heat deflection temperature can be increased from approximately 60–190 °C by physically blending the polymer with PDLA (poly-D-lactide). The density of crystalline polylactic acid was reported as 1.36 $g.cm^{-3}$ and 1.25 $g.cm^{-3}$ for amorphous [23].

In general, PLA are soluble in dioxane, acetonitrile, chloroform, methylene chloride, 1,1,2-trichloroethane and dichloroacetic acid. Ethyl benzene, toluene, acetone and tetrahydrofuran only partly dissolve PLA when cold, though they are readily soluble in these solvents when heated to boiling temperatures. The fastest rates of crystallization for pure PLA are found in the temperature of 110–130 °C, which yields spherulitic crystalline morphology. PLA can be crystallized by slow cooling, annealing it above the T_g, or strain crystallized. All PLA are insoluble in water, some alcohols and alkanes. Table 2.1 shows some of the general properties of PLA.

Table 2.1 General properties of PLA 3001D [24]

Properties	Values
Physical properties	
Melt flow rate (g/10 min)	4.3–2.4
Density (g/cm3)	1.25
Haze	2.2
Yellowness index	20–60
Mechanical properties	
Tensile strength at yield (MPa)	53
Elongation at yield (%)	10–100
Flexular modulus (MPa)	350–450
Thermal properties	
HDT (°C)	135
Melting point	120–170

3.3 Natural fiber

Natural fibers are subdivided based on their origins, coming from plants, animals or minerals. All plant fibers are composed of cellulose while animal fibers consist of proteins (hair, silk, and wool). Plant fibers include bast (or stem or soft sclerenchyma) fibers, leaf or hard fibers, seed, fruit, wood, cereal straw, and other grass fibers. Natural fibers can be considered as naturally occurring composites consisting mainly of cellulose fibrils embedded in lignin matrix. The reinforcing efficiency of natural fiber is related to the nature of cellulose and its crystallinity. The main components of natural fibers are cellulose (α-cellulose), hemicellulose, lignin, pectins, and waxes. Table 2.2 is shown the chemical composition of natural fiber.

Table 2.2 Chemical composition of common natural fiber [25].

Fiber	Cellulose (%)	Hemicellulose (%)	Lignin (%)
Cotton	82.7	5.7	–
Jute	64.4	12	11.8
Flax	64.1	16.7	2.0
Ramie	68.6	13.1	0.6
Sisal	65.8	12.0	9.9
Oil palm EFB	65.0	–	19.0
Oil palm Frond	56.03	27.51	20.48
Abaca	56–63	20–25	7–9
Hemp	74.4	17.9	3.7
Kenaf	53.4	33.9	21.2
Coir	32–43	0.15–0.25	40–45
Banana	60–65	19	5–10

3.3.1 Cellulose

Cellulose is a natural polymer consisting of D-anhydro glucose ($C_6H_{11}O_5$) repeating units joined by 1,4-b-D-glycosidic linkages at C_1 and C_4 position [26]. Each repeating unit contains three hydroxyl groups. These hydroxyl groups and their ability to hydrogen bond performance a major role in directing the crystalline packing and also govern the physical properties of cellulose and the cellulose structure is shown in Figure 2.5. Solid cellulose consist of main two regions with the regions of high order or crystalline regions and regions of low order or amorphous regions. Cellulose is also formed of slender rod like crystalline micro fibrils. The crystal nature of naturally occurring cellulose is known, as Cellulose I. Cellulose is resistant to strong alkali but is easily hydrolyzed by acid to water-soluble sugars. Cellulose is relatively resistant to oxidizing agents.

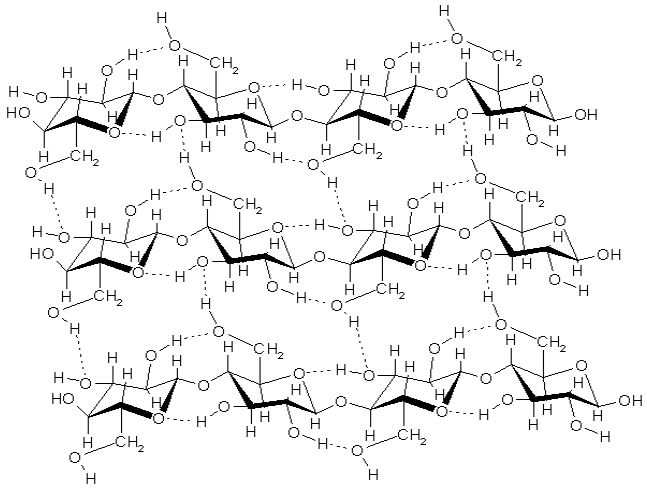

Figure 2.5 structure of cellulose

3.3.2 Microcrystalline Cellulose

Microcrystalline cellulose has been widely used especially in food, cosmetic, medical, and biodegradable composites as a reinforcing agent in polymer composites. The basic step for preparation MCC from plant has generally three steps these are delignification, bleaching and hydrolysis, the step of delignification and bleaching are remove lignin and other composition in fibers to produce cellulose micro fibrils. Moreover, lignin and other composition effects on hydrolysis reaction of cellulose micro fibrils because they are inhibit to the hydrolysis reaction. So they have to remove as much as possible.

MCC is prepared from removing of amorphous regions in cellulose micro fibrils. Under controlled condition, this transformation consists of the hydrolysis of amorphous regions within cellulose micro fibrils that is occurred on 1,4-b-D-glycosidic linkages, while leaving the integral micro or nano crystalline segment. However, size and shape of crystalline depend on type and nature of plants. The mechanism of hydrolysis condition to prepare crystalline cellulose is shown in Figure 2.6

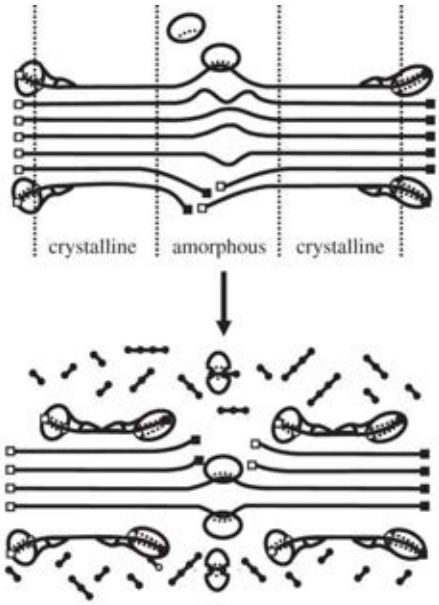

Figure 2.6 Hydrolysis of cellulose

In 1988, Paralikar and Bhatawdekar [26] prepared microcrystalline cellulose from bagasse pulp. The pulp was bleached with sodium chlorite and hydrolyzed with 2 N HCl at a boiling temperature for 15 min. The microcrystalline cellulose consists of cellulose 98%, moisture 3.7% and ash 0.05%. The weight loss during hydrolysis was about 18%. The particle length measured by light microscope and it was in the range of 30-40 um. These results showed that bagasse pulp could be use as the source of MCC.

After that in 2006, El-sakhawy et al [27] prepared MCC from local agricultural waste (rice straw and cotton stalks bleached pulp). Hydrolysis of bleached pulp was carried out using 2 N hydrochloric or sulfuric acid to study the

effect of the acid used in the properties of the produced microcrystalline cellulose such as morphology and particle size, they reported that microcrystalline is rod-like shape. All prepare microcrystalline cellulose sample has slightly lower particle size than the commercial MCC but wider particle size distribution. Furthermore, the effect of different acid used was shown that cotton stalk MCC samples with larger particle size was obtained in case of using sulfuric acid in the hydrolysis process.

3.4 Biodegradable Natural Fiber Composites

The combination of a plastic matrix and reinforcing fibers gives rise to composites having the best properties of each component. Since the plastics are soft, flexible and lightweight in comparison to fibers, their combination provides a high strength-to-weight ratio to the resulting composite [20]. Wood or plant fibers are of interest in polymer reinforcement for a number of reasons, especially their low cost, low weight and non-abrasiveness to processing equipment. In addition, natural fibers are CO_2-neutral when burned, have attractive acoustic and thermal insulation properties and have good specific mechanical properties.

PLA is attractive commercially material because it is biodegradable, can be produced from renewable resources and look like polystyrene in some of its properties. As with other biopolymers, PLA remains relatively costly when compared with commodity thermoplastics such as polyethylene and polypropylene but a cost level competitive with polyethylene terephthalate (PET) is considered feasible. Possibly because the polymer has only recently been available in bulk to any great degree, there has so far been relatively little research on PLA as a matrix in natural fiber biocomposites.

Jute-PLA composites have been made using a film stacking procedure and a combination of non-woven jute mats and extruded PLA films [28]. The fiber content was 40% w/w and the process involved use of a vacuum in the heating stage. The results of composite tensile tests showed that an approximate two times of tensile strength and about tree times of tensile modulus were achieved. However, the addition of jute fibers had little effect on impact strength and elongation, they were reduced slightly when compared with the neat PLA.

Oksman et al. [29] fed a hand-made flax roving through the side feeder of a twin-screw extruder in order to make flax-PLA composites. The fiber content was calculated based on the feeding speed and the weight of the roving/meter. The extrudate was compressed in mold in order to obtain specimens for tensile testing. Interestingly, it was found that the addition of flax fibers did not significantly improve the tensile strength, which the authors attributed to poor adhesion between flax and PLA. In contrast, the addition of fibers increased the tensile modulus but this subsequently decreased when the fiber addition level went up from 30% to 40%. The authors indicated that the compression molding process might have influenced fiber orientation with variations from one sample to another leading to the observed changes in tensile modulus. Further trials involved the use of triacetin as a plasticizer. Impact strength was improved at 5% triacetin content but did not improve further at higher plasticizer levels. Furthermore, triacetin addition caused a significant decrease in tensile modulus when plasticizer addition levels of 10 and 15% were employed. The authors suggested that triacetin changed the fiber structure making the fibers more brittle.

Injection-moulded flax-PLA composites were made as part of an EU FAIR project entitled –New functional biopolymer-natural fiber composites from agricultural resources" that examined the development and potential use of PLA composites in automotive applications [30]. Tensile strength was not increased when 20-40 wt.% flax was incorporated and this was explained by a lack of good fiber-PLA adhesion [31]. However, fibers were significantly shortened during processing and this could also partly explain the results. The Young's modulus of the composites increased linearly with flax content. Chemical treatment of the fibers and modification of the polymer by reactive extrusion were both studied as a means of enhancing composite properties but it was decided that the results did not justify the additional costs involved.

A commercial paper-like sheet of kenaf fiber was converted to a composite material by impregnation with a solution of a commercial L-PLA in dioxane solution [32]. Following this procedure, a composite material with 70% v/v fiber content was obtained. Tensile tests showed that a maximum tensile stress of

about 60 MPa was found for the best composite material, comparing with a value of about 20 MPa for the unreinforced polymer processed in the same way. Similarly, a tensile modulus of about 6 GPa for the kenaf-PLA composite compared with a value of just over 1 GPa for the unreinforced polymer. The authors concluded that good stress transfer from the resin to the matrix had been obtained.

In research by Shibata et al. [33], a flexural modulus of 5.5 GPa was achieved at 20 wt.% abaca fiber content in a PLA composite. This result compares with a flexural modulus of 3.5 GPa for the unreinforced polymer. A further increase in flexural modulus was obtained when using chemically modified (e.g., esterified) fibers. Flexural strength, at about 110 MPa, was not significantly improved by fiber addition.

It is well known that the properties of composites are significantly depending on the interface between the reinforced fibers and the matrix [34]. In most early research on the development of composite the fiber–matrix interface was considered to be critical for ensuring good composite mechanical properties [35] In order to enhance the mechanical properties of the composites, fibers have been treated with 3-aminopropyltriethoxysilane (APS) coupling agent. The structure of APS is shown in Figure 2.7. APS has ethoxy groups that hydrolyze in water or a solvent producing a silanol and next the silanol reacts with the OH group of the fiber which forms stable covalent bonds to the cell wall that are chemisorbed onto the fiber surface (as seen in Figure. 2.7) [36].

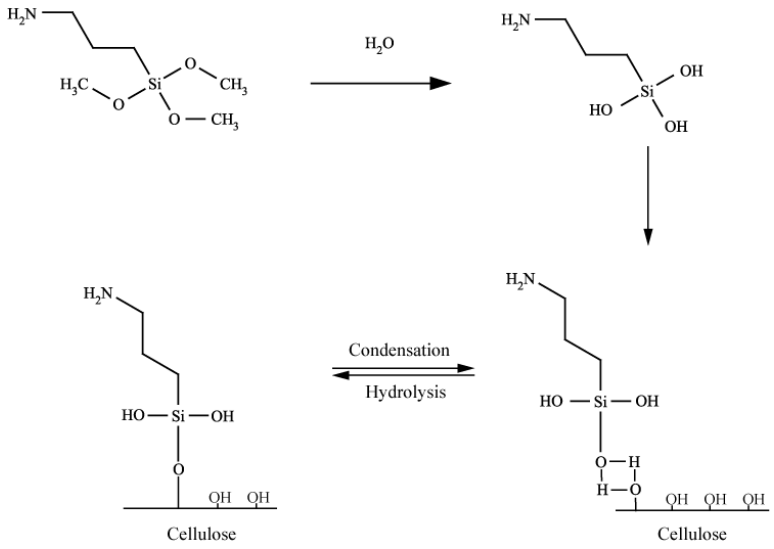

Figure 2.7 APS cellulose surface treatment reaction.

In 1996, Dupraz et al. [37] suggested that APS has the ability to bond to polylactic acid. During surface treatment, APS hydrolyzes and the resultant silanol groups can bond with the fiber surface. Amine groups from APS can form hydrogen bonds to COO-sites on the hydrolyzed PLA backbone.

In 2008, M.S. Huda et al. [38] prepared biocomposites from polylactic acid (PLA) and APS treated kenaf fibers and reported that the APS surface treated fiber reinforced composites had higher storage moduli than the untreated fiber reinforced composites, which suggested better adhesion between the treated kenaf fibers and the matrix. This improved adhesion results improved high temperature modulus and softening temperature than untreated fiber composites.

3.5 Biodegradation

There are several ways a polymer may degrade in the environment. These include biodegradation, photo degradation, oxidation, and hydrolysis. The general public as one and the same often interprets these processes though they lead to very different end results. It is often conceived that the breakdown of a plastic into small, invisible (to the naked eye) fragments is biodegradation, when in reality these fragments may remain in the environment over a significant period of time. Figure 2.8 summarizes the various modes of environmental polymer degradation.

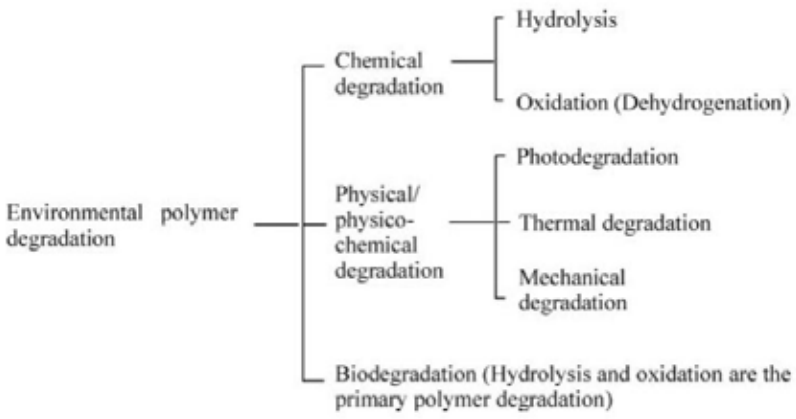

Figure 2.8. Environmental polymer degradation.

Biodegradable polymers are generally degraded through two steps of primary degradation and ultimate biodegradation. Primary degradation is the depolymerization or chain cleavage of the polymer to oligomers that can be assimilated by the microbes. Molecular weight reduction is mainly caused by hydrolysis or oxidative chain scission. Hydrolysis occurs using environmental water with the aid of an enzyme or under non-enzymatic conditions (abiotic). In this case, autocatalysis, heat, or catalytic metals are often responsible for the hydrolysis. Once depolymerized, sufficiently small-sized oligomeric fragments are formed. These fragments are transported into the cell for further assimilation to produce biomass, minerals, water, and CO_2 under aerobic conditions. Under anaerobic conditions, CH_4 is mainly produced in place of CO_2 and water. The schematic of biodegradation by microorganism is displayed in Figure 2.9.

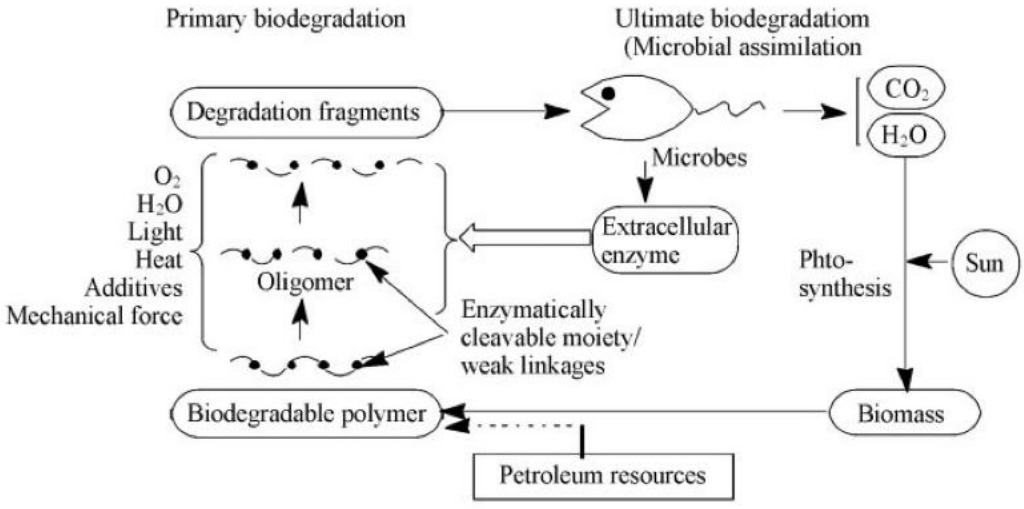

Figure 2.9. Biodegradation of biodegradation polymer by microorganisms [18]

3.5.1 Standard

Standard test procedures are available to evaluate the biodegradability of plastics. The American Society for Testing and Materials (ASTM), the Ministry of International Trade and Industry (MITI, Japan) and the Organization for Economic Cooperation and Development (OECD) have developed standard test procedures to evaluate the biodegradability of plastics. Most of these test methods measure the percent conversion of the carbon from the designed biodegradable plastic to CO_2 and CH_4 in aerobic and anaerobic environments, respectively. The absence of polymer and residue in the environment indicates complete biodegradation, whereas incomplete biodegradation may leave polymer and/or residue as a result of polymer fragmentation or metabolism in the biodegradation process. Failure in one test does not necessarily exclude biodegradation, it merely indicates that under the

3.5.1.1 ISO 14855-2: Determination of the ultimate aerobic biodegradability of plastic materials under controlled compositing condition - Method by analysis of evolved carbon dioxide. Part 2 Gravimetric measurement of carbon dioxide evolved in a laboratory-scale test [39].

This part of ISO 14855 specifies a method for determining the ultimate aerobic biodegradability of plastic materials under controlled composting condition by gravimetric measurement of the amount of carbon dioxide evolved. The method is designed to yield an optimum rate of biodegradation by adjusting the humidity, aeration and temperature of the composting vessel.

The method applies to the following materials:

- Natural and/or synthetic polymer and copolymer, and mixtures of these;
- Plastic materials that contain additive such as plasticizer or colorants;
- Water soluble polymer
- Materials that, under the test condition, do not inhibit the activity of microorganisms present in in inoculum.

If the teat material inhibit microorganism in the inoculum, another type of mature compost or pre-exposure compost can be used.

This method id designed to yield the optimum rate of biodegradability of plastic materials in mature compost by controlling the humidity aeration ratio and temperature in the composting vessel. It also aim to determine the ultimate biodegradability of the teat materials by using the small scale reactor. The degradation rate is periodically measured by determining the mass of the evolved carbon dioxide using adsorption column filled with soda lime and soda talc on an electronic balance.

The test materials is mixed with an inoculum derived from mature compost and with an inert materials such as sea sand, the sea sand plays an active part by acting as a holding body for humidity and microorganism. The test arrangements are present in Figure 2.10. The amount of carbon dioxide evolved is measurement at intervals on an electronic balance and carbon dioxide content is determined using the Equation 2.1. The degree of biodegradation, expressed as a percentage is calculated by comparing the amount of carbon dioxde evolved with the theoretical amount.

The CO_2 trapping reaction was done in a two steps reaction as mentioned below:

$NaOH \rightarrow CO_2 + NaHCO_3$ … Equation 2.1

then

$NaHCO_3 + NaOH \rightarrow Na_2CO_3 + H_2O$ … Equation 2.2

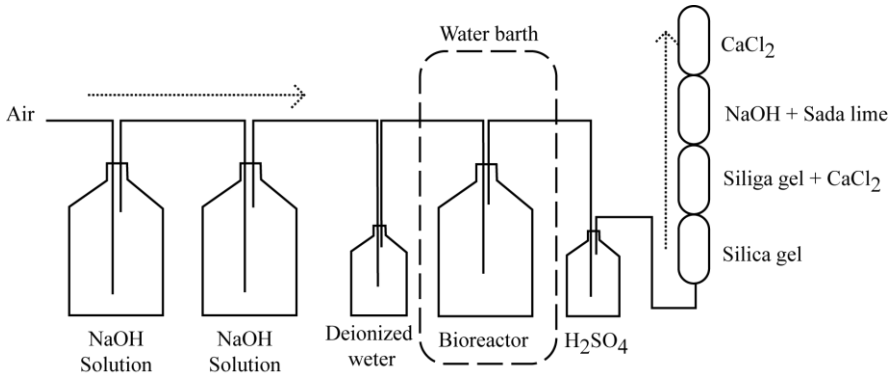

Figure 2.10 The schematic of GMR system

3.5.1.2 ISO 14852: Determination of the ultimate aerobic biodegradability of plastic materials in an aqueous medium - Method by analysis of evolved carbon dioxide [40].

This International Standard specifies a method, by measuring the amount of carbon dioxide evolved, for the determination of the degree of aerobic biodegradability of plastic materials, including those containing formulation additives. The test materials in exposed in a synthetic medium under laboratory condition to an inoculum from activated sludge, compost or soil.

If an unadapted activated sludge is used as the inoculum, the test simulated the biodegradation process which occur in a natural aqueous environment; if a mixed or pre-exproed inoculum is used, the method can be used to investigate the potential biodegradability of a test materials.

The conditions used in this International Standard do not necessarily correspond to the optimum condition allowing maximum biodegradation to occur, but the standard is designed to determine the potential biodegradability of the plastic materials or give an indication of their biodegradability in natural environment.

The method enables the assessment of the biodegradability to be improved by calculating a carbon balance.
The method applies to following materials:

- Natural and/or synthetic polymers, copolymer or mixtures thereof;
- Plastic materials, which contain additives such as plasticizer, colorants or other compounds.
- Water-soluble polymer.
- Materials that, under the test condition, do not inhibit the microorganisms present in the inoculum.

The Biodegradability of plastic materials in determined using aerobic microorganism in an aqueous system. The test mixture contains an inorganic medium, the organic test materials (the sole source of carbon

and energy) with a concentration between 100 mg/l and 2,000 mg/l of organic carbon, and activated sludge or a suspension of active soil or composted as the inoculum. The mixture is agitated in the test flasks and aerated with carbon dioxide free air over a period of time depending on the biodegradation kinetics, but not exceeding 6 mouths. The carbon dioxide evolved during the microbial degradation determine by titrimetric analytical method. The test arrangements are present in Figure 2.11.

The CO_2 produced reacts with the barium hydroxide ($Ba(OH)_2$) and precipitated as barium carbonate ($BaCO_3$) and the reaction is shown in Equation 2.3. The amount of CO_2 evolved is determined by titrating the remaining Ba(HO)2 with hydro chloric acid (HCl) (Equation 2.4).

$CO_2 + Ba(OH)_2 \rightarrow BaCO_3 + H_2O$ … Equation 2.3

then

$Ba(OH)_2 + 2HCl \rightarrow BaCl_2 + 2H_2O$ … Equation 2.4

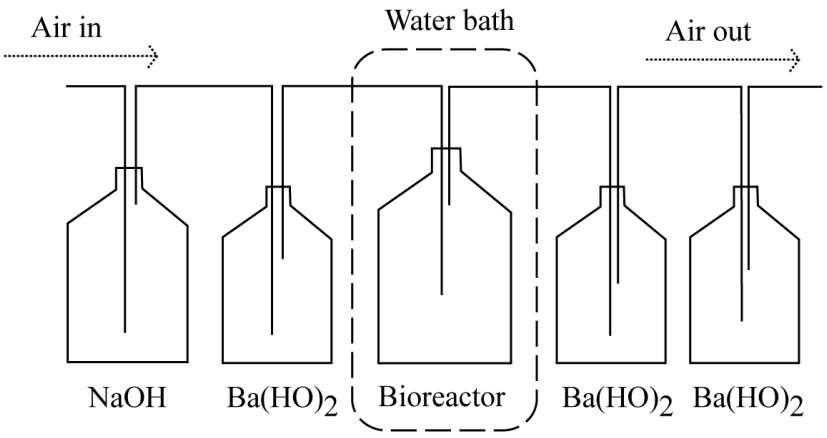

Figure 2.11 The schematic of aqueous medium test system

CHAPTER 3

Experimental

4.1 Materials and chemical

4.1.1 **Polymer matrix**

Poly(lactic acid) (PLA) resin grade number 3001D obtained from NatureWorks® LLC (Cargill-Dow), USA was used as matrix material. It has a specific gravity of 1.24 and MFI around 15 g/10 min (2.16 kg/190°C). The glass transition temperature and melting temperature of PLA are 62 °C and 160 °C respectively, as reported from technical data sheet published by the manufacturer. Its chemical structure is shown in Figure 3.1

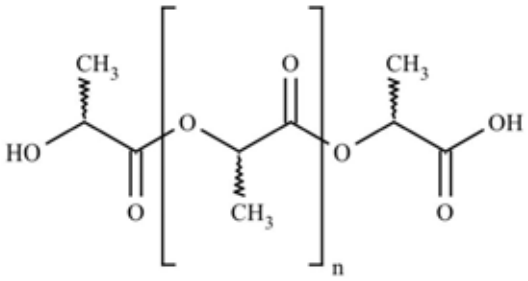

Figure 3.1 Chemical structure of Poly(lactic acid)

4.1.2 **Polymer modification**

Biomax® Strong 120 purchased from DuPont Company, USA, was used as PLA modification resin. The pellet is transparent with a density of 0.94 g/cm^3 and melting temperature of 72°C as reported from technical data sheet published by the manufacturer.

4.1.3 **Coir fiber**

Coir fiber was used to prepare microcrystalline cellulose, which was used as reinforcement.

4.1.4 **Sodium Hydroxide (NaOH)**

An analytical grade of sodium hydroxide, purchased from Fluka Co, Ltd., Thailand, was used as delignifying agent.

4.1.5 **Hydrochloric acid (HCl)**

An analytical grade of hydrochloric acid, purchased from Sigma Aldrich Co, Ltd., Thailand, was used as hydrolysis reagent.

4.1.6 **3-aminopropyltriethoxy silane ($H_2N(CH_2)_3Si(OC_2H_5)_3$)**

A surface modification reagent, 3-aminopropyltrimethoxy silane (Z-6011) supplied by DOW CORNING®, USA., was used to modify coir microcrystalline cellulose surface. The chemical structure of this reagent is shown in Figure 3.2.

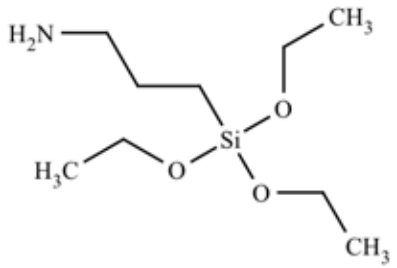

Figure 3.2 Chemical structure of 3-aminopropyltriethoxy silane

4.1.7 **Acetic acid (CH_3COOH)**

An analytical grade of acetic acid, purchased from Sigma Aldrich Co, Ltd., Thailand, was used as pH adjustment.

4.1.8 **Ethanol (C_2H_5OH)**

Absolute ethanol, purchased from Sigma Aldrich Co., Ltd., Thailand, was used as hydrolysis solvent for silane.

4.1.9 **Soda lime (NaOH, $Ca(OH)_2$, KOH, H_2O)**

An analytical grade of soda lime, supplied by Merck & Co., Inc., Thailand, was used as carbon dioxide trapping reagent

4.1.10 **Calcium chloride (CaCl)**

An analytical grade of calcium chloride anhydride granule, supplied by Merck & Co., Inc., Thailand, was used as moisture trapping reagent.

4.1.11 **Sodium hydroxide on support**

An analytical grade of Sodium hydroxide on support supplied (carbon porous char) by Merck & Co., Inc., Thailand, was used as carbon dioxide trapping reagent

4.1.12 **Sulfuric acid (H_2SO_4)**

Sulfuric acid purchased from Sigma Aldrich Co., Ltd., Thailand, was used as ammonia removing reagent.

4.1.13 **Silica gel**

Silica gel pellet, supplied by Merck & Co., Inc., Thailand, was used as moisture trapping reagent.

4.2 Instruments

The list of instruments used in this research is shown in Table 3.1

Table 3.1 Experimental instruments

Instruments	Model	Manufacturer
Twin screw Extruder	PRISM TSE 16 TC	Thermo election Co., USA
Hydraulic press	Scientific	Labtech Engineering, Thailand
Thermogravimetric analyzer	TGA/SDTA851^e	Mettler-Toledo, Switzerland
Differential scanning calorimeter	Diamond DSC	Perkin-Elmer, USA
Scanning electron microscope	JSM-5410 LV	JEOL, Japan
X-ray diffractometer	D8-Advance	Bruker, Germany
FT-IR spectrometer	Nicolet 6700	Thermo Scientific, USA
Gel permeation chromatography	RID-10A	Shimadzu, Japan
Universal testing machine	LR 100K	LLOYD, UK

4.3 Experimental procedure

Flow chart of the experimental process is shown in Figure 3.3

4.3.1 **Preparation of microcrystalline cellulose**

Coir fibers were cut into size 4-5 cm length before delignin with NaOH solution with concentration of 1.0 M. It was heated and stirred at 80°C for 2 hrs. The obtained fibers were washed with water prior to bleaching with 6% H_2O_2 in 15% w/v NaOH solution at 100°C for 1 hr. The bleached fibers were then washed with water until pH of the fiber became neutral. After that, the fibers were hydrolyzed with 0.1 M hydrochloric acid at 70°C for 2 hrs. Then, the fibers were washed with distilled water until the pH of the fiber became neutral and kept in the hot air oven at 80°C for 24 hrs. Finally, the fibers were ground by ball mill for 2 hours in order to get microcrystalline cellulose and kept in the desiccator for dying until being used.

4.3.2 **Surface modification of microcrystalline cellulose**

The obtained MCC was surface-modified by silane coupling agent using 3-aminopropyltriethoxy silane (APS). First, APS 5% on weight of MCC was hydrolyzed by the mixture solution of ethanol and water with ratio of 90:10 respectively. The pH was adjusted to 4.5 by a few drop of acetic acid, and then, it was stirred for 2 hours for hydrolysis reaction of silane group to silanol group. After that, the MCC was added into the solution, in which the liquor ratio is 1:10 and the mixture was then stirred for another 2 hrs. Next, the mixture was filtered and kept in the air to remove ethanol. Finally, the treated MCC was dried in an oven at 80°C for 24 hours before keeping in the desiccator until being used.

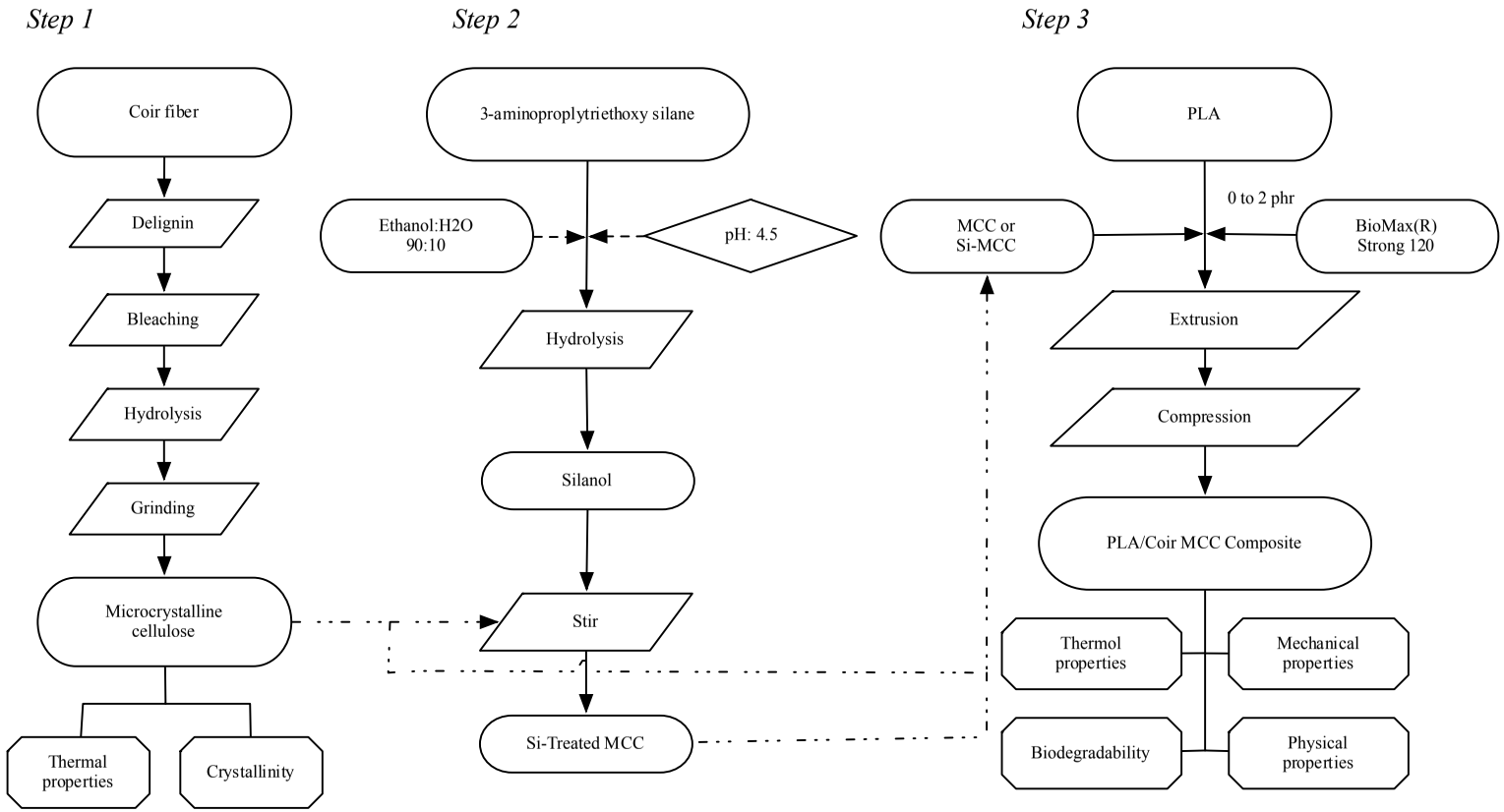

Figure 3.1 Experimental flow chart

3.1.1 **Preparation of PLA/MCC composites compound**

PLA, MCC, APS treated MCC, and Biomax® were dried in an oven at 60°C to remove any moisture that had been absorbed during the storage. The varied content of component was displayed in Table 3.2. The MCC content was loaded at 1.25, 2.5 5 and 10 wt.% and Biomax was used at 0 and 2 phr. The twin-screw extruder was used to mix PLA and its composites. The temperatures of the barrel from hopper to die were set at 160, 180, 180, 190 and 180°C and the screw speed was 60 rpm. The extrudate was cut into the pellet form and dried in an oven at 60°C for 24 hrs. Finally, the compounds were kept in the desiccator until being used.

Table 3.2 The formulation of PLA composites

Materials	PLA (wt.%)	MCC (wt.%)	BioMax® Strong 120 (phr)
PLA-neat	100	-	-
PLA-Bi	100	-	2
PLA-1.25MCC	98.75	1.25	-
PLA-2.5MCC	97.50	2.50	-
PLA-5MCC	95.00	5.00	-
PLA-10MCC	90.00	10.0	-
PLA-1.25MCC-Bi	98.75	1.25	2
PLA-2.5MCC-Bi	97.50	2.50	2
PLA-5MCC-Bi	95.00	5.00	2
PLA-10MCC-Bi	90.00	10.00	2
PLA-1.25MCC-Si	98.75	1.25	-
PLA-2.5MCC-Si	97.50	2.50	-
PLA-5MCC-Si	95.00	5.00	-
PLA-10MCC-Si	90.00	10.00	-
PLA-1.25MCC-Si-Bi	98.75	1.25	2
PLA-2.5MCC-Si-Bi	97.50	2.50	2
PLA-5MCC-Si-Bi	95.00	5.00	2
PLA-10MCC-Si-Bi	90.00	10.00	2

MCC-Si: Microcrystalline cellulose treated with APS

3.1.2 **PLA/MCC Composites fabrication**

Frist, the compound pellets were kept in the oven at 60 °C for 24 hrs. before fabrication to remove any moisture that had been absorbed during the storage. And then, the compounds were fabricated by compression molding and the processing parameters were shown in Table 3.3. The thickness of the prepared composites was 1.00 mm. After fabrication, the composite sheets were kept at room temperature before being tested the properties.

Table 3.3 The fabrication processing parameters

Parameters	Value
Temperature (°C)	180
Pressure (psi)	100
Pre-heat time (s)	300
Press before vent (s)	10
Venting (time)	2
Final press (s)	180
Cooling (s)	300

3.2 Characterization and testing

3.2.1 **Characterization of untreated and treated microcrystalline cellulose**

3.2.1.1 **Crystallinity**

The crystallinity of microcrystalline cellulose was determined by X-ray diffractometer. The powders were laid on the sample holder and analyzed under plateau condition with scan speed of 5°/min with a 2θ range of 5°-50°.

3.2.1.2 **Thermal properties**

Thermogravimetric analyzer was employed to determine the degradation temperature of microcrystalline cellulose. The TGA was carried out under nitrogen atmosphere at a heating rate of 10°C/min from 30°C to 500°C. Before doing the test, the sample was dried in a hot air oven at 60°C for 24 hours and approximate weight of sample was 8-10 mg. The onset of degradation temperature for sample was recorded.

3.2.1.3 **Functional group**

Fourier transformed infrared spectroscopy spectra were obtained with the Nicolet 6700 FT-IR Spectrometer (Thermo Scientific, UAS). Approximate 2 mg Samples of the APS treated and untreated MCC were grounded and dispersed in a KBr (28 mg) matrix. A KBr pellet was then formed by compression at the pressure of about 200 MPa. Spectra with samples were obtained from 64 scans scanning of the wave number 4000 to 400 cm^{-1}.

3.2.2 **Mechanical properties of PLA/MCC composites**

3.2.2.1 **Tensile properties**

The composites samples were cut into the dumbbell shape and kept at 25°C for 24 hours before testing. The tensile strength, elongation at break and Young‘s modulus were determined according to ASTM D 638 using a crosshead speed of 12.5 mm/min with 1,000 N load cell and a gauge length of 10 cm. Five of each sample were tested and averaged.

3.2.2.2 **Flexural properties**

The three-point bending of composites samples were carried out by universal testing machine according to ASTM D790 with a crosshead speed of 12.5 mm/min and a span length of 10 cm. Five specimens of rectangular sample (1.5x15 cm^2) were tested and averaged.

3.2.3 **Thermal properties**

3.2.3.1 **Thermogravimetric analysis (TGA)**

The thermal stability and degradation temperature (Td) were obtained by using a thermogravimetric analyzer. Approximately 8-10 mg of the sample was cut from the composites sheet with a heateing at a rate of 10°C/min from 30°C to 500°C under nitrogen atmosphere with a flow rate of 5 ml/min. The onset of degradation temperature for each sample was recorded.

3.2.3.2 **Differential scanning calorimetry (DSC)**

The composites samples were sliced (8-10 mg) from the compression molded specimen and encapsulated in a hermetically sealed aluminum pan. The samples was first heated from 50°C to 200°C, kept isothermal for 1 min, cooled to 50°C to remove any previous thermal history, and finally reheated to 200°C with a heating rate and cooling rate of 10°C/min. The melting temperature (Tm) and heat of fusion (ΔHf) of samples were obtained from the maximum peak and the area under the peak. The heat of fusion was used to calculate the crystallinity of each sample form the equation:

$$Crystallinity(\%x_c) = \frac{\Delta H_m - \Delta H_{CC}}{\Delta H_m^0 \times w} \times 100 \qquad \text{Equation 3.1}$$

Where:

$\%x_c$ = degree of crystallinity

ΔH_m = heat of fusion of sample

ΔH_m^0 = heat of fusion of fully crystalline poly(lactic acid)

w = weight fraction of poly(lactic acid) in sample

3.2.4 **Physical properties of PLA/MCC composites**

3.2.4.1 **Morphology**

The fractured surface were examined using electron microscopy (SEM) operated at 10 KV. All specimens were sputter coated with a thin layer of gold prior to examination. The comparison between micrographs of different specimens was made at the same level of magnification.

3.2.4.2 **Molecular weight**

Number and weight average molecular weights before and after biodegradation test of the PLA composites were determined by gel permeation chromatography on a THF GPC system with Shodex GPC KF-805L columns and a refractive index detector. THF was used as mobile phase with flow rate of 1 ml/min, and the temperature of column was controlled at 40°C. Calibration was performed with polystyrene standards with molecular weights from 5,840 to 1,350,000. To minimize relative deviation caused by the GPC instrument, all the measurements were carried out at one time.

3.2.4.3 **Water absorption**

The composite sheets were cut into the size of 2.5 x 2.5 cm^2 and were dried at 50°C for 24 hours. After that, the weighed sheets (W_1) were immersed in distilled water at 25°C for 2 and 24 hours according to ASTM D570. The samples were removed from the water, blotted with tissue paper to remove surface water, and then weighed (W_2) the sample again. Three specimen for each sample were tested and averaged. The percentage of water absorption was calculated according to the following equation:

$$\%Water\ absorption = \frac{W_2 - W_1}{W_1} \times 100 \qquad \text{Equation 3.2}$$

Where:

W_1 = dried weight (g), W_2 = wet weight (g)

3.2.5 **Biodegradability test of the PLA/MCC composites**

3.2.5.1 **Gravimetric measurement respirometric (GMR) System**

The biodegradability of composites was tested by using an in-house built Gravimetric Measurement Respirometric (GMR) System based on draft ISO 14855-2. A GMR system consists of six bioreactors, one for blank (compost), one for positive control (compost with cellulose powder), and four for sample (compost with crushed PLA composites). In the system, pressurized air was passed through a column containing soda lime to make it CO_2 free. Later, the air in bubbled through a flask containing deionized water to maintain the humidity in the compost mixture and in the reaction constant. The bioreactor was heated by water bath and maintained the temperature at 58±2°C. Air is pressed through each bioreactor and later through an ammonia eliminator which containing 1.0 M H_2SO_4. After that, the air was passed through the moisture remover column 1 and column 2 which containing silica gel and silica gel mix calcium chloride, respectively. Finally, moisture and ammonia free was passed through a CO_2 trap column 3 and column 4 which containing sodium hydroxide on support and calcium chloride, respectively. A schematic representation of the GMR system with a single bioreactor and column connection is shown in Figure 3.2

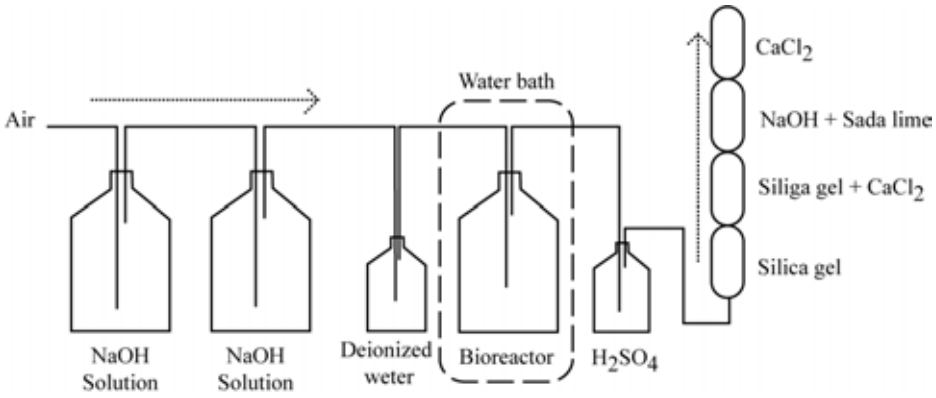

Figure 3.2 The schematic of GMR system

For the bioreactor, initially, a non-woven polyester fabric was placed at the bottom of the reaction column followed by the mixture. The ratio of sample: compost was 1:10. The CO_2 generated by biodegradation in the reaction column was measured by the weight gain seen in column 3 and column 4. The

percentage mineralization was further calculated by comparing the amount of carbon dioxide in the positive control and the sample with blank by the following equation []:

$$\%mineralization = \frac{gCO_2 - gCO_{2b}}{g_{materials} \times (\%C_{material}/100) \times (44/12)} \quad \text{Equation 3.3}$$

where

gCO_2 = amount of evolved carbon dioxide in grams from the sample and the positive control;

gCO_{2b} = amount of evolved carbon dioxide in grams from the blank;

$g_{material}$ = mass of the sample;

$\%C_{material}$ = percentage organic carbon content of the sample obtained from CHON/S analyzer.

3.2.5.2 **Aerobic biodegradability of plastic materials in an aqueous medium**

Activated sludge was supplied by Bangkok wastewater treatment office, Siphaya, Bangkok. The test system was setup according to ISO 14852 consist of four flasks, one for blank that containing the activated sludge, two for sample (activated sludge with testing materials) and positive flask that containing activated sludge and microcrystalline cellulose. In the system, the air was pump through a carbon dioxide trapping flask containing 2.0 M NaOH solution to make it CO_2 free. After that, the air was checked the carbon dioxide again with carbon dioxide indicator flask (0.1 M $Ba(OH)_2$) before pass trough the test flask. The test flasks were shaken and heated at 30°C. Finally, the air was passed through the twice of carbon dioxide trapping flask which containing 1.0 M $Ba(OH)_2$. A schematic representation of the test system with a single bioreactor and flask connection is shown in Figure 3.3.

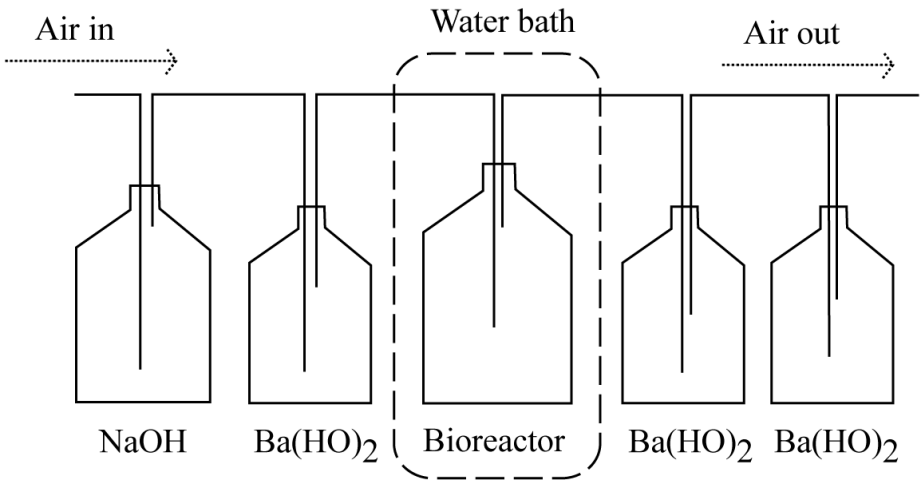

Figure 3.3 The schematic of aqueous medium test system.

After biodegradation, the CO_2 produced will react with the barium hydroxide and was precipitated as barium carbonate ($BaCO_3$). The amount of CO_2 evolved was determined by titrating the remaining $Ba(OH)_2$ with hydrochloric acid (HCl). The calculate the mass of CO_2 trapped in the absorber bottle was calculated using the follow equation:

$$m = \left[\frac{2C_B \times V_B^0}{C_A} - V_A \times \frac{V_B^t}{V_B^Z}\right] \times C_A \times 22 \qquad \text{Equation 3.4}$$

Where

m = mass of CO_2 Trapped in the absorber bottle;

C_A = exact concentration of the HCl solution;

C_B = exact concentration of the $Ba(OH)_2$ solution;

V_B^0 = volume of the $Ba(OH)_2$ solution at the beginning of the test;

V_B^t = volume of the $Ba(OH)_2$ solution at time t, before titration;

V_B^Z = volume of the aliquots of $Ba(OH)_2$ solution used for titration;

V_A = volume of the HCl solution used for titration;

22 = half the molecular mass of CO_2

Then, the percentage biodegradation can be calculated by the following equation:

$$D_t = \left[\frac{\sum(m_t) - \sum(m_b)}{ThCO_2}\right] \times 100 \qquad \text{Equation 3.5}$$

Where

D_t = percentage degradation;

$\sum m_t$ = amount of carbon dioxide evolved in test flask between the start of the test and time t;

$\sum m_b$ = amount of carbon dioxide evolved in blank flask between the start of the test and time t;

$ThCO_2$ = amount of carbon dioxide evolved in test flask between the start of the test and time t;

3.2.5.3 **Landfill biodegradation test**

Landfill test was performed to evaluate biodegradation of the PLA/MCC composites. The composites sheets were cut into the size of 2.5 x 5.0 cm^2 and were weighed. The samples were buried at 5 cm depth under the surface of the soil, at Physical Resources Management, Chulalongkorn University. The samples were collected every 7 days. After removal, the samples were brushed softly, washed with distilled water and dried under vacuum at 60°C for 24 hours before testing. Measurement of biodegradability was evaluated as percentage weight remaining, morphology and the molecular weight.

3.2.5.4 **Seawater biodegradation test**

The biodegradation of composites took place in the gulf of Thailand water in Arng-sila, Chonburi. The samples were located in a special basket at 1 m depth under the surface of the sea. Three replicates of each composites sheet with the size of 2.5 x 5.0 cm^2 were tested. After removal, the samples were washed with distilled water and dried under vacuum at 60°C for 24 hours before testing. Mesurement of biodegradability was evaluated as percentage weight remaining and the molecular weight.

CHAPTER 4

Results and discussion

In this research, the preparation of surface modified microcrystalline cellulose (MCC) reinforcing polylactic acid (PLA) was studied. The results were analyzed and divided into four parts follows:

1. Preparation of microcrystalline cellulose from coir fiber
2. Characterization of silane treated and Untreated microcrystalline cellulose
3. Evaluation of properties of polylactic acid composites
4. Evaluation of biodegradability of polylactic acid composites

4.4 Preparation of microcrystalline cellulose from coir fiber

MCC was prepared form coir fiber by dignifying, bleaching hydrolysis and grounding, respectively. The Figure 4.1 shows the appearance of coir at each step. The coir after delignification shows the dark brown color and after bleaching the fiber exhibited yellowish colors. The fiber after hydrolysis the color of fiber is brown and the fiber strength is very low.

(a)  (b)  (c) 

Figure 4.1 Appearance of coir after (a) delignification (b) bleaching (c) hydrolysis

4.5 Characterization of silane treated and untreated microcrystalline cellulose

Microcrystalline cellulose (MCC) was modified by 3-aminopropyl triethoxy silane (APS) before reforcing in polylactic acid. The properties of APS treated and untreated MCC were investigated and compare as follow.

4.5.1 Morphology

After treatment of MCC with APS, the surface morphology of treated MCC was examined by scanning electron microscope. The SEM micrographs of treated and untreated MCC are shown in Figure 4.1. From the SEM micrographs, the surfaces morphology of MCC is different. The MCC from coir fiber displayed rod-shape morphology with its aspect ratio of approximately 2.5-4. The average particle size is about 50-200 μm. Comparing between the surface of untreated and treated MCC, the surface of treated MCC was rougher, covering by a layer of silane coupling agent. Obviously its average partical size and aspect ratio were also greater than the untreated MCC. The treatment of silane coupling will be confirmed by FTIR.

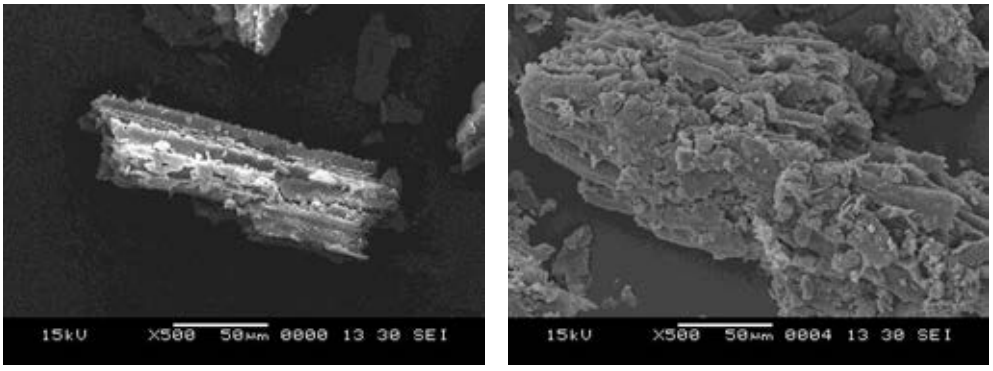

Figure 4.1 SEM micrographs of (a) untreated microcrystalline cellulose, (b) treated microcrystalline cellulose

4.5.2 Crystallinity

X-ray diffractograms of the untreated and APS treated MCC are shown in Figure 4.2. As can be seen, all the samples showed the characteristic peak of cellulose, The MCC showed crystallinity peak at 2θ = 22.23º and amorphous peak at 2θ = 16.37º The increasing of intensity peak at 2θ = 22.23º of treated MCC can be described by the scattering of Si-O-Si, which treated on the surface of MCC had a similar diffraction angle of cellulose and its an impact to increase the intensity of XRD pattern and can be attributed to the silane was treated on the surface of MCC.

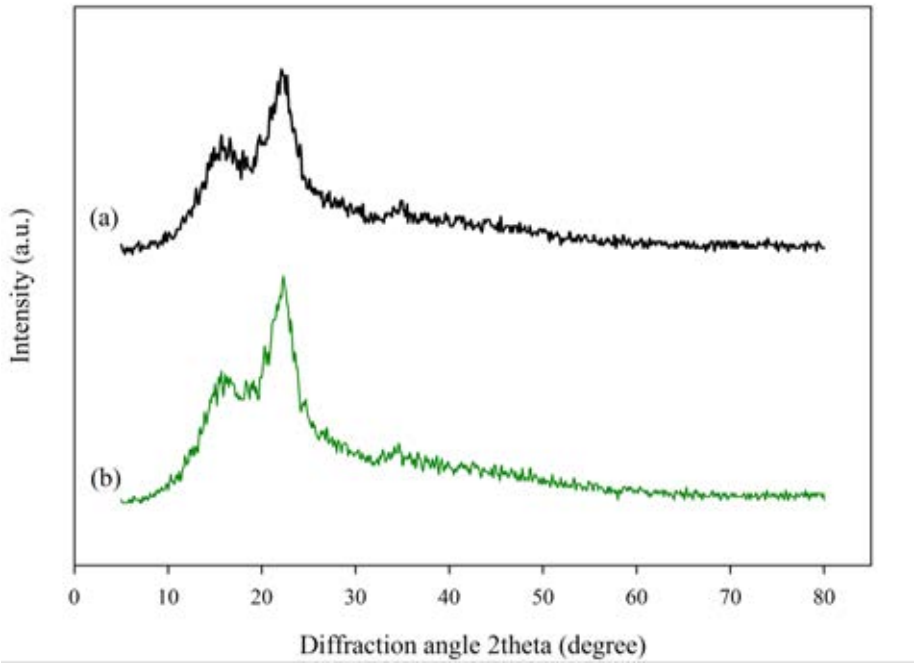

Figure 4.2 XRD diffractogram patterns of (a) untreated MCC (b) APS treated MCC

4.5.3 Thermal property

Thermal stability and decomposition temperature were investigated by thermogravimetric analyzer (TGA). Figure. 4.3 shows the TGA thermograms and derivative thermograms (DTG) of the untreated and treated microcrystalline cellulose with 3-aminopropyl triethoxy silane (APS). The thermal decomposition behavior of the untreated microcrystalline cellulose was observed over the wide range of temperature, consisting of three stages. The first decomposition stage occurred in the temperature range of 80 – 100 °C is attributed to the evaporation of water that absorbed by cellulose. The second main decomposition stage occurred in the temperature range of 250 – 390 °C is the characteristic of the thermal decomposition of cellulose [5]. The third decomposition stage observed near 420 °C is due to the thermal decomposition of lignin [46].

Thermograms of APS treated microcrystalline showed that the first decomposition stage (80 – 100 °C) exhibited higher percentage weight loss than the untreated microcrystalline cellulose because of the hydrophilic behavior of silanol group which was treated onto the surface of microcrystalline cellulose. The second decomposition stage (150 – 220 °C) was attributed to the thermal decomposition of hemi cellulose [46]. The third decomposition stage was observed above 300 °C and this weight loss was attributed to the decomposition of cellulose, lignin, and grafted silane.

In general, the thermal decomposition of inorganic filler, such as amino silane, is detect at the temperature range of 300 – 600 °C. In this case, the weight residue of treated microcrystalline cellulose was higher than the untreated microcrystalline cellulose, the result was attributed to the presence of grafted silane, which does not decompose under nitrogen atmosphere [47]. The treatment of the silane was also confirmed by FTIR analysis.

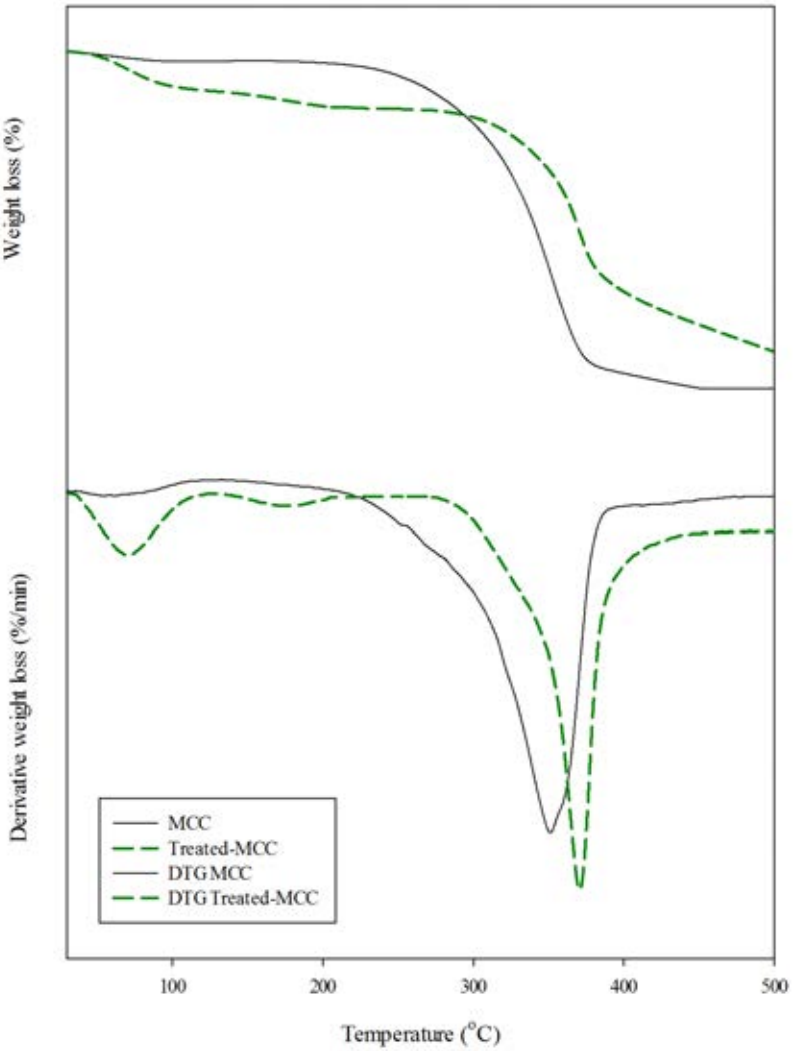

Figure 4.3 TGA thermograms and derivative thermograms for untreated and APS treated microcrystalline cellulose

4.5.4 Functional group

The FTIR spectra for microcrystalline cellulose and APS treated microcrystalline cellulose are shown in Figure 4.4 for the spectrum of the microcrystalline cellulose, Figure 4.4(a) shows the strong and broad peak at 3420 cm^{-1}, which is the characteristic absorption peak of the hydroxyl group in the main chain of cellulose. The wave number at 2930 cm^{-1} is assigned as the stretching of alkane group in cellulose structure. The complex absorption peak at 1500 – 400 cm^{-1} is related to the structure of cellulose, especially the strong peak at 1032 cm^{-1} corresponding to the C-O group.

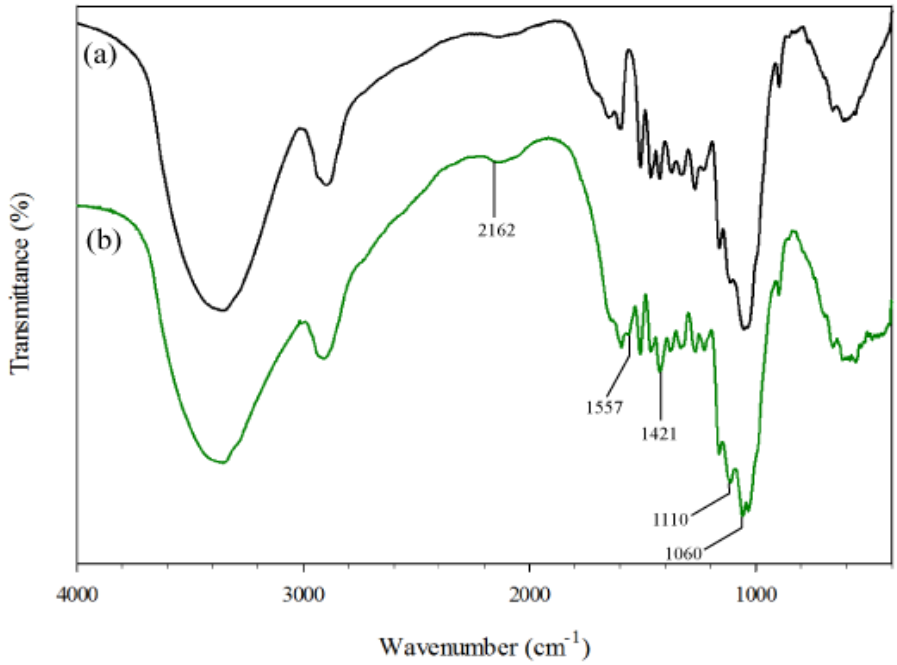

Figure 4.4 FTIR spectra of (a) microcrystalline cellulose (b) treated microcrystalline cellulose with APS.

For the spectrum of the treated MCC with APS, Figure 4.4(b), showed peak changes at 2162 cm^{-1} which is assigned as Si-OH stretching [46]. The wave number at 1557 and 1421 cm^{-1} are assigned as NH bending in the functional group of silane coupling agent [46], while the peak at 1204 and 1060 cm^{-1} are assigned as Si-O-Si of the self-condensation of silanol group at the surface of cellulose. The wave number at 1110 cm^{-1} corresponding to Si-Cellulose, indicated that surface of microcrystalline cellulose was treated with APS.

From these results, the surface modification of MCC by APS can be confirmed by FTIR spectra. The chemically surface-modified of microcrystalline would be expected to enhance adhesion between fibers and polymer matrix for composite with increasing compatibility.

4.6 Evaluation of properties of polylactic acid composites

4.6.1 Mechanical properties

4.6.1.1 Tensile properties

- *Effect of MCC content and surface treatment.*

The tensile properties of PLA composites were measured by universal testing machines, LLOYD LR100K. The tensile properties of PLA composites, with various contents of untreated and APS treated microcrystalline cellulose, are shown in Figure 4.5. From Figure 4.5(a), the maximum tensile strength of PLA composites containing 1.25, 2.5, and 5 wt.% of microcrystalline cellulose yielded valued of 58.24, 57.40, and 56.16 MPa, respectively. The decrease in tensile strength of PLA/MCC composite was not significantly obvious when the microcrystalline cellulose content was increased up to 5 wt.%, but when increasing the microcrystalline cellulose content up to 10 wt.%, the lowest tensile strength was observed. The tensile strength of 10 wt.% MCC composites was decreased to 40.14 MPA or about 34.4%, compared with neat PLA, which indicated of poor adhesion between the microcrystalline cellulose and the PLA matrix. Consequently, the stress is not transferred from the matrix to the stronger fiber.

Pilla et al. [44] have studied PLA/pine wood flour composites and reported a tensile strength of 55.5 MPa with a 20 wt.% pine wood flour content. These results are agreed with those of the 5 wt.% of microcrystalline cellulose composites.

Comparing between the composites reinforced with silane treated and untreated microcrystalline cellulose, the tensile strength of silane treated microcrystalline cellulose composites shown the slight improvement of the strength property. The tensile strength of 10 wt.% of treated surface microcrystalline cellulose was increased to 41.28 MPa. The silane treated microcrystalline cellulose polylactic composite exhibited an enhanced stress compared with PLA composites containing untreated microcrystalline cellulose. This result may be attributed to the improvement

of interfacial adhesion between microcrystalline cellulose and PLA matrix and will be confirmed by scanning electron microscope.

Figure 4.5(b) shows the elongation at break of polylactic acid composites containing 1.25 to 10 wt.% of untreated and APS treated microcrystalline cellulose. The elongation at break of polylactic acid composites was decreased when increasing content of microcrystalline cellulose comparing with the neat PLA. The values of elongation at break decrease from 3.4 % (neat PLA) to 2.3% and 2.65% for 10 wt.% untreated and silane treated microcrystalline cellulose, respectively.

The decreasing in elongation at break may be attributed to the fact that the microcrystalline cellulose particle acted as stress concentrator [47] and reduced the chain deformability of polymer matrix [49]. Hence, the surface silane treatment of microcrystalline cellulose also did not improve the elongation at break of composites because the treatment improved only the interfacial adhesion and was not effected to the deformability of polymer chain.

Figure 4.5(c) shows the Young‘s modulus as a function of MCC content and comparing between untreated and APS treated MCC. It clearly shows that increased MCC content has a positive effect on composites modulus compare to neat PLA, and obviously presented the highest Young‘s modulus of 3.53, 3.78 GPa at 5 wt% untreat and treated MCC, respectively. However, when increasing the MCC content to 10 wt.% (treat and untreated), the Young‘s moduli of composite were decreased and these results may be attributed to the agglomeration of MCC and will be confirmed by scanning electron microscope

(a)

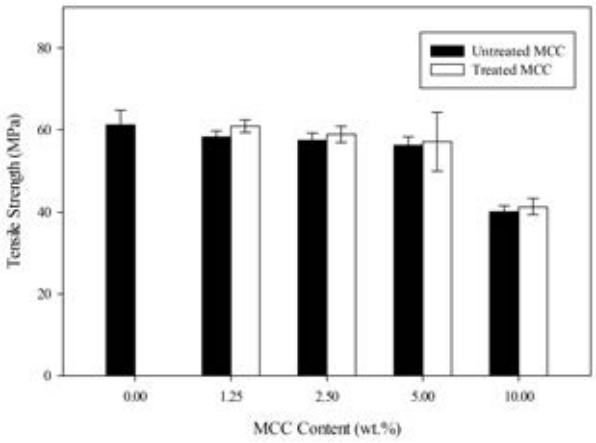

(b)

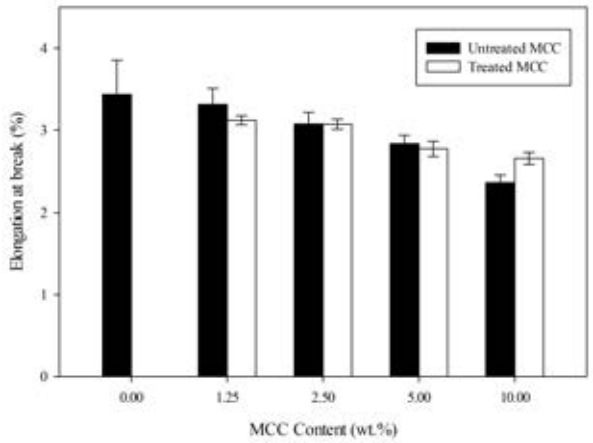

(c)

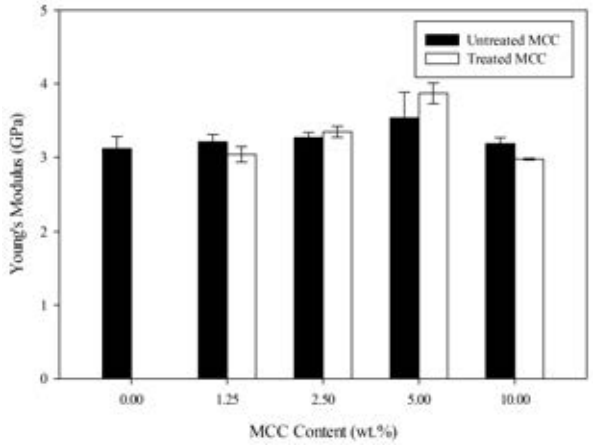

Figure 4.5 Mechanical properties of PLA/MCC composites comparing between APS treated MCC and untreated MCC (a) tensile strength (b) elongation at break (c) Young‘s modulus.

- Effect of modification resin.

The tensile strength of PLA blended with 2 phr of Biomax® Strong 120 at various MCC loadings is shown in Figure 4.6(a) and the results show that the tensile strength of neat PLA slightly decreases from 61.2 to 56.3 MPa when adding 2 phr of Biomax® and this result due to the fact that elastomeric nature of the Biomax® with low strength and modulus effect to the tensile strength properties. Comparing between adding and non-adding Biomax® of composites at various MCC loading, the tensile strength of composites shows the similar result, when increasing the MCC content the tensile strength of composites slightly decreases. From this results may be attributed to the fact that, the Biomax® dose not effect to the tensile strength properties of composites.

Figure 4.6(b) shows the effect of Biomax® on the elongation at break of composites at various MCC contents. The elongation at break of PLA/MCC-Bi composites is higher than that of PLA/MCC composites because the toughness behavior of Biomax® which can reduce the brittleness and increase chain mobility of PLA [31]. The elongation at break of PLA/MCC-Bi composite containing 10 wt% MCC is increased upto 21.72% compared with the non-Biomax® composites. From the result, can be indicated that the adding 2 phr of Biomax® enhance the elongation at break of PLA/MCC composites.

The Young‘s moduli of PLA/MCC and PLA/MCC-Bi composites are shown in Figure 4.6(c). The results show the slight decrease of modulus value of composites when blending the Biomax® into the PLA matrix and these results can be indicated that the low modulus of Biomax® contributed to the Young‘s modulus of PLA/MCC-Bi composites.

(a)

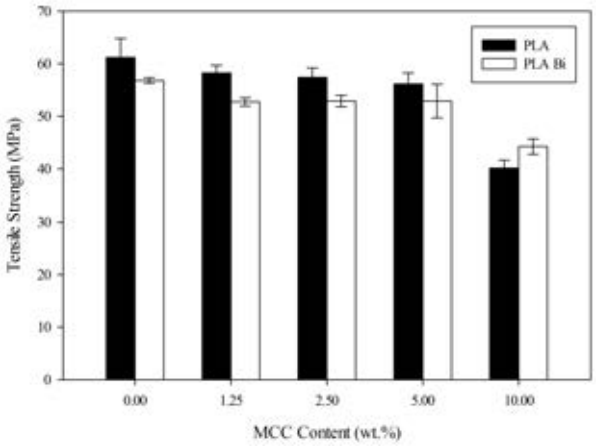

(b)

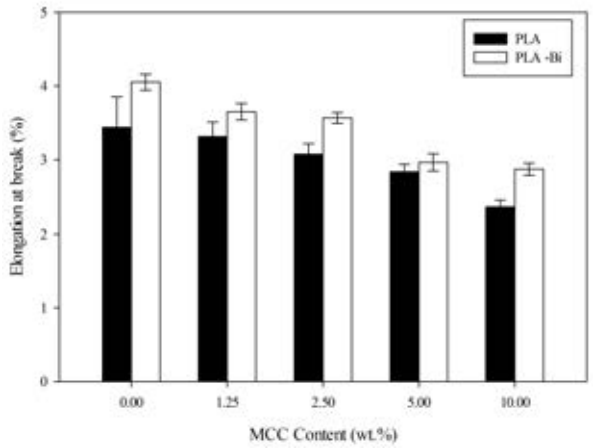

(c)

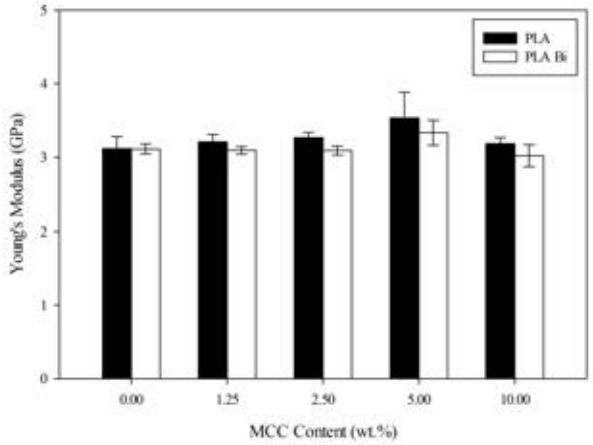

Figure 4.6 Effect of modification resin (Biomax® strong 120) on Mechanical properties of PLA/MCC composite (a) tensile strength (b) elongation at break (c) Young‘s modulus.

- *Effect of surface treatment and modification resin.*

The effect of APS treated MCC and Biomax® on mechanical properties of PLA Composites (PLA/MCC-Si-Bi) at various MCC contents are investigated. The tensile strengths of PLA/MCC-Si-Bi are shown in Figure 4.7. PLA/MCC-Si-Bi composites containing 1.25, 2.5 and 5 wt% of APS treated MCC with Biomax® yieled tensile strength valued of 62.81, 63.13, and 67.105 MPa, respectively, which were higher than those of PLA and PLA/MCC composites. Paricularly, the tensile strength of PLA/MCC-Si-Bi with 5 wt.% of 67.10 MPa yielded the highest value. The elongation of PLA/MCC-Si-Bi composites were obviously enhanced compared with PLA/MCC composites. The highest value of the elongaton at break was observed at 1.25 wt% of MCC-Si-Bi composites. The Young's modulus of composite exhibited the hightest value at 5 wt% of MCC-Si-Bi compostites with the value of 3.72 GPa.

The mechanical performance of composites is expected to depend on the following factors [50]: 1.) Adhesion between MCC and PLA matrix 2.) MCC content 3.) Aspect ratio of MCC 4.) Fiber orientation 5.) The degree of crystallinity of polymer matrix. The decreasing of strength is attributed to the poor stress transfer across the interphase, which means that there is practically no interfacial bonding between the MCC and the PLA matrix. The poor adhesion between the matrix and fiber initiates a lot of micro voids at the MCC matrix interface, and the stress transfer to the fiber which is the load bearing entities becomes inefficient leading to low strength values [51]. In this research, the 3-aminoproply triethoxy silane was chosen to be a coupling agent, which improves interfacial adhesion between fiber and polymer matrix. Figure 4.8 shows the reaction between MCC and PLA matrix with APS coupling agent. From the tensile strength results, it was shown that the APS enhanced the interfacial adhesion between the interface, leading an increase in the strength properties of PLA/MCC composites. This effect is in fact became significant when using with Biomax®.

The higher in elongation at break can be explained based on the crystallinity of polymer matrix. The addition of Biomax® to PLA is attributed to a decrease of chain stiffness and crystallinity of PLA because the Biomax® acts as the

rubber particle that inhibits the crystallization and increases chain mobility of PLA and these results will be confirmed by DSC.

(a)

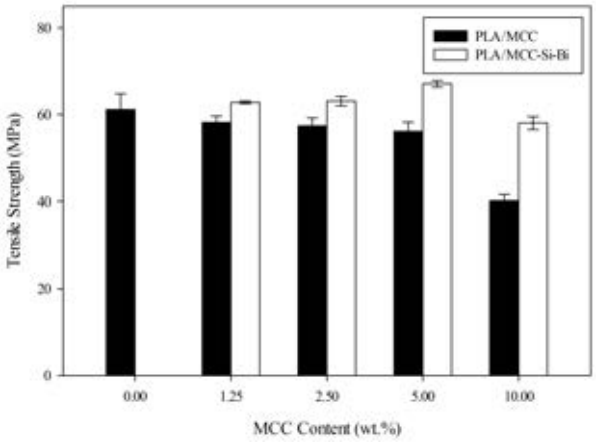

(b)

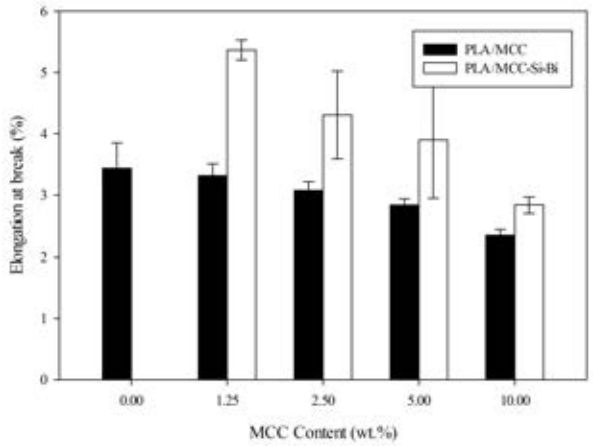

(c)

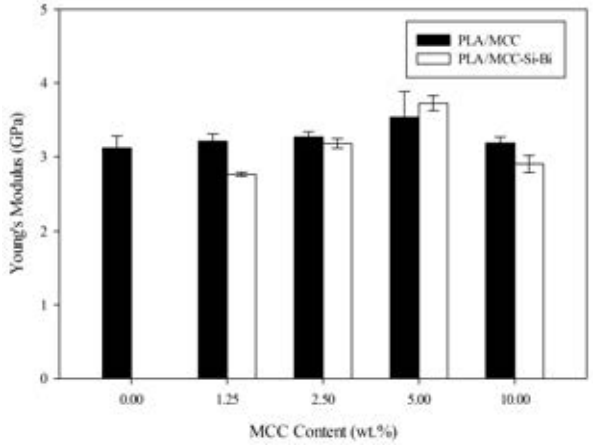

Figure 4.7 Effect of coupling agent and modification resin on mechanical properties (a) tensile strength (b) elongation at break (c) Young‘s modulus.

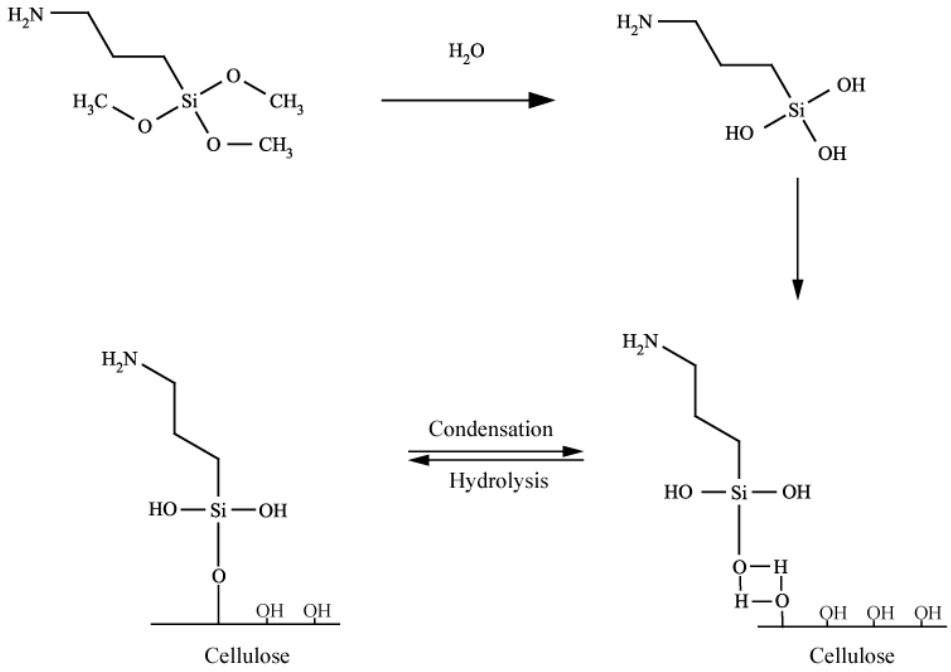

Figure 4.8 Schematic of the APS treatment reaction

4.6.1.2 Flexural properties

The flexural properties of PLA composites containing various MCC contents is shown in Table 4.1. The neat PLA matrix reached a value of 73.27 MPa, while the PLA composites containing 1.25, 2.5, 5, and 10 wt.% of untreated MCC revealed a flexural strength value of 66.65, 61.49, 63.88 and 61.72 MPa, respectively. This result indicated that the flexural strength of PLA composites were reduced with increasing the MCC content and can be attributed, to the poor stress transfer between matrix and the stress concentrator from MCC

To improve the stress transferring, APS was used as surface-modified agent. The flexural strength of PLA containing APS treated MCC (PLA-MCC-Si) was increased comparing to the untreated MCC/PLA composites. For example, the flexural strength of the APS treated MCC/PLA composites (PLA/MCC-Si) containing 10 wt.% MCC-Si (71.46 MPa) was 15% greater than its counterpart (PLA-10MCC). These results can be indicated that the APS MCC surface treatment significantly improved the interfacial adhesion and enhance stress transfer between fiber and matrix similar result have been found from other previous work. For

instance, Huda et al. [38] have studied PLA composites reinforce with kenaf fiber. They compared between the flexural strength of untreated kenaf fiber and APS treated fiber and the results shown that the APS enhanced the flexural strength of PLA/kenaf composites.

The addition of Biomax® also affected to the flexural strength. The flexural strength value of neat PLA was decreased from 73.27 MPa to 66.26 MPa (PLA-Bi). However, the tested samples were not broken at 20 mm. Among the PLA/MCC composites with 2 phr Biomax®, the sample can be bended to 20 mm. when MCC loading was increased up to 5 wt.%. This result is due to the fact that the Biomax® acts as toughening agent and improve toughness of PLA matrix [24].

The flexural strengths of PLA/MCC composites containing APS treated MCC and Biomax® are shown in the last group of Table 4.1 (PLA-MCC-Si-Bi). The interfacial adhesion was improved by APS and the toughness of matrix was enhanced by Biomax®. All of tested samples were unbroken when bended to 20 mm.

Table 4.1 Flexural strength of PLA/MCC composites

Materials	*Flexural strength (MPa)*	*S.D.*	*Remark*
PLA	73.27	1.07	B
PLA-Bi	66.26	1.40	NB
PLA-1.25MCC	66.65	1.37	B
PLA-2.5MCC	61.49	0.82	B
PLA-5MCC	63.88	1.75	B
PLA-10MCC	61.72	1.78	B
PLA-1.25MCC-Si	64.48	0.95	NB
PLA-2.5MCC-Si	68.37	1.45	NB
PLA-5MCC-Si	69.75	0.96	B
PLA-10MCC-Si	71.46	1.66	B
PLA-1.25MCC-Bi	65.45	0.94	NB
PLA-2.5MCC-Bi	59.28	1.65	NB
PLA-5MCC-Bi	61.74	1.45	NB
PLA-10MCC-Bi	56.04	1.66	B
PLA-1.25MCC-Si-Bi	52.93	1.05	NB
PLA-2.5MCC-Si-Bi	53.82	1.76	NB
PLA-5MCC-Si-Bi	55.52	1.47	NB
PLA-10MCC-Si-Bi	55.53	0.90	NB

4.6.2 Thermal properties

4.6.2.1 Thermogravimetric analysis

The TGA and DTG thermogams were obtained from TGA/SDTA851^e METTLER, USA. Samples weights of 8 mg were placed on an open aluminum pan and were heated from 30 to 500 °C with a heating rate of 10 °C/min under nitrogen atmosphere. Table 4.2 shows the detail of thermal stability of PLA/MCC composites at various MCC contents. The first group is presented the effect of Biomax® on the thermal stability. The initial degradation temperature (T_i) of neat PLA is increased from 339.46 °C to 344.18 °C when adding 2 phr of Biomax®. This result is attributed to the higher degradation temperature of Biomax® strong 120 which can slightly improve the thermal stability of PLA. The TGA thermogram of Biomax® strong 120 is shown in Figure 4.9.

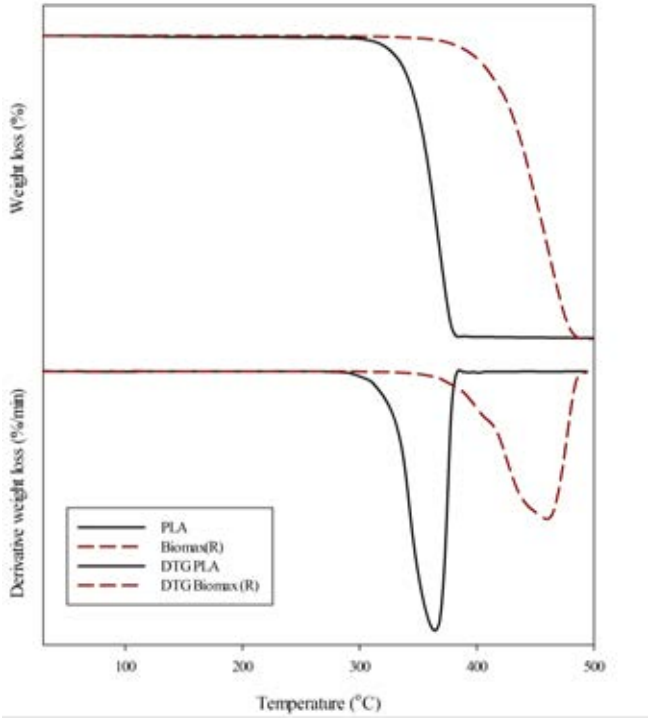

Figure 4.9 TGA thermograms and derivative thermograms of PLA and Biomax®

The effect of MCC loading on thermal stability is shown in the second group. The maximum degradation temperatures (T_{DM}) of PLA/MCC composites are decrease with increasing the MCC content, the T_{DM} of PLA/MCC composite is reducing from 373.52 °C (neat PLA) to 367.94 °C (10 wt.% of MCC) However, the weight residue (W_R) of PLA/MCC composites which representing the char yields of composites, are all higher than that of the neat PLA. These results expose that the addition of MCC to PLA effectively increase the char yield of sample. The char yield is directly correlated to the efficiency of the flame retardation in polymer [51].

The third group shows the effect of APS treated MCC. The haft decomposition weight (T_{50}) of PLA/MCC-Si composites are shown in Table 4.2 The T_{50} of PLA/MCC-Si composites exhibits higher temperature than that of the PLA/MCC composites. The T_{50} of PLA composites containing 10 wt.% MCC-Si increased to 359.0 °C, comparing with untreated MCC/PLA composites. This result is due to the higher thermal stability of APS MCC treated than the untreated MCC contributed to the greater thermal stability of the APS treated MCC/PLA composites.

The Effect of Biomax® on the PLA/MCC composites with vaious MCC contents is shown in fourth group in Table 4.2. The results show the similar trend with those of the PLA/MCC composites but the TAG and DTG thermograms of this group are different from those of the PLA/MCC composites. The TGA and DTG thermograms are shown in Figure 4.9. As shown, the TGA consists of two main stages. The first main stage was appeared within the same range of PLA/MCC composites at any MCC contents. The second stage was observed only in this group, other the onset of this stage started at 400 °C and ended at 422 °C. The result can be attributed to the decomposition of Biomax® which was observed at the higher temperature than that of PLA/MCC composites.

The final group displays the effect of Biomax® and APS trated MCC. The thermal stability of this group shows the characteristic of the third and fourth group. The initial decomposition temperatures were compared with PLA compsites; which is resulted from the effect of APS treated MCC. The two-stage decomposition temperature was also observed, which related to the decomposition of Biomax®. The TGA and DTG of PLA/MCC composite, the effect of MCC content, APS MCC surface treatment and Biomax®, show in Figure

Table 4.2 Thermal stability of PLA/MCC composites

Materials	T_i (℃)	T_{50} (℃)	T_{DM} (℃)	W_R (%)
PLA	339.46	361.0	373.52	0.57
PLA-Bi	344.18	363.0	377.50	0.24
PLA-1.25MCC	330.41	351.0	369.09	1.87
PLA-2.5MCC	333.08	353.0	370.66	1.39
PLA-5MCC	333.80	355.0	369.98	3.77
PLA-10MCC	330.98	353.0	367.94	5.18
PLA-1.25MCC-Si	340.88	358.5	374.21	1.14
PLA-2.5MCC-Si	340.03	359.5	375.61	1.36
PLA-5MCC-Si	341.04	360.5	374.04	2.28
PLA-10MCC-Si	338.55	359.0	375.05	3.07
PLA-1.25MCC-Bi	328.30	349.5	367.73	1.95
PLA-2.5MCC-Bi	331.93	352.0	368.78	2.19
PLA-5MCC-Bi	331.80	352.5	369.09	2.74
PLA-10MCC-Bi	332.28	353.5	369.57	5.15
PLA-1.25MCC-Si-Bi	336.46	348.0	374.64	1.23
PLA-2.5MCC-Si-Bi	338.69	358.0	373.29	2.19
PLA-5MCC-Si-Bi	339.50	359.5	373.92	3.51
PLA-10MCC-Si-Bi	336.36	355.5	370.36	6.46

4.6.2.2 Differential scanning calorimetry

The crystallization behaviors of PLA/MCC composites were studies using DSC. The Figure 4.11 shows the DSC thermograms obtained from the second heating scan. As can be seen in Figure 4.11(a), a double-melting peak was obtained for the neat PLA, the melting peak at low temperature (T_{ml}) of neat PLA obviously separated from high temperature (T_{mh}). This characteristic may be attributed to two different types of the lamellar structure (e.g., the difference thickness of lamellar and size of the spherulites) formed during the crystallization process[52]. In the figure 4.11(b-e), shows the effect of MCC content on thermal behavior of PLA/MCC composites. The present of the filler induced changes in the melting characteristic of composites. The double-melting peak was merged into single melting peak with increasing the MCC content. This result can be indicated that the MCC has ability to be a heterogeneous nucleating agent and improve crystallization rate of PLA because the major crystalline region can be completely form at cooling step when MCC content is increased, so, the cold crystallization is to reduced.

The crystallinity of PLA composites increases when increasing the MCC content and the percentage of crystallinity of PLA/MCC composites are shown in Table 4.3. Moreover, the MCC contents also affected to the melting temperature of composites. The melting temperature of PLA/MCC composites was increased from 171.3 ºC (neat PLA) to 176.7 ºC (10 wt.% MCC). The shifting in melting temperature can be attributed to the spherulites of PLA forming into the larger size, and this result will be confirm and discussion in crystallinity part which investigated by X-ray driffactometor.

The addition of 2 phr of Biomax® also affected to the melting behavior of PLA composites. The DSC thermograms of PLA/MCC composites blended with 2 phr of Biomax® are shown in Figure 4.12. When adding Biomax®, the merging of two melting peak into one peak, which indicating a decrease in enthalpy of melting peak, was observed and the cold crystallinzation peak was shifted towards higher temperature. This is because the Biomax® acts as a polymeric plasticizer which can increase amorphous region and inhibit the crystallization of PLA. However, when increasing the MCC content, the ability of MCC to improve the

crystalline region as mentioned earlier is competitive with Biomax®, so the synergism of these two materials is shown in the DSC thermogram of PLA/MCC-Bi containing 10 wt.% of MCC (Figure 4.12 (f)).

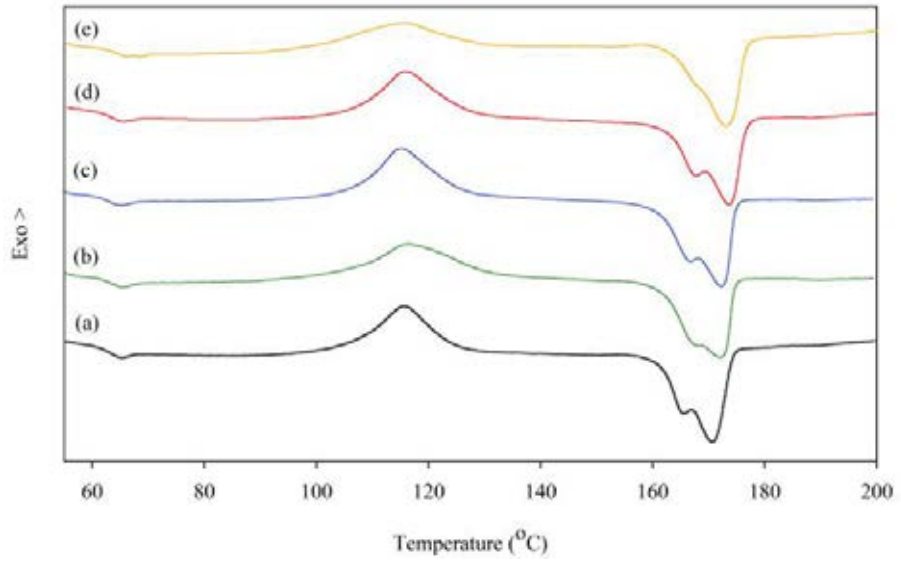

Figure 4.11 DSC thermograms of PLA composites at various MCC containing content (a) 0, (b) 1.25, (c) 2.5, (d) 5 and (e) 10 wt%.

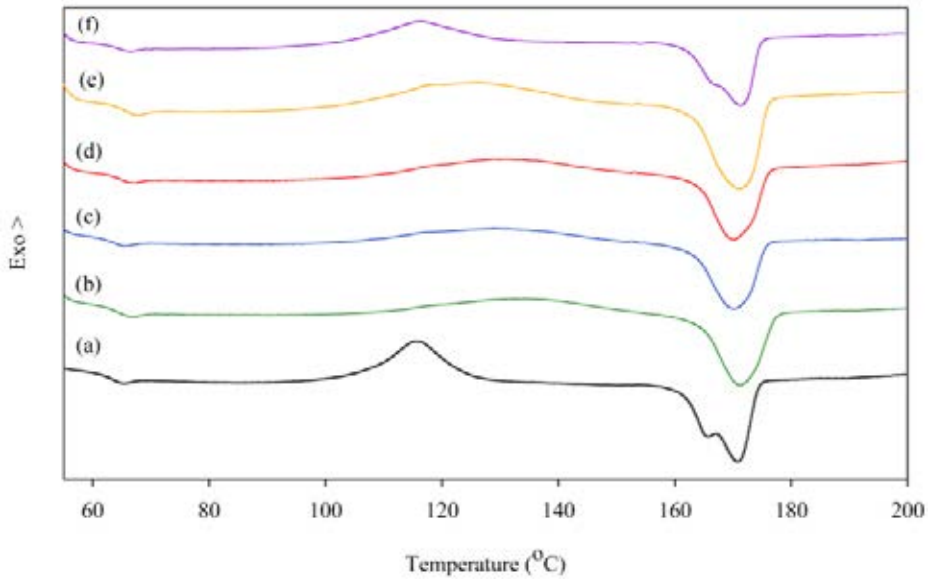

Figure 4.12 DSC thermograms of PLA composites with 2 phr of Biomax® at various MCC containing contents (a) neat PLA, (b) PLA-Bi, (c)1.25, (d) 2.5, (e) 5 and (f) 10 wt%.

Moreover, the DSC thermograms of PLA/MCC composites which containing APS treated MCC at various contents are shown in Figure 4.13. The thermal transition of PLA reinforced with APS treated MCC composites shows the similar behavior to the untreated MCC composites. The melting temperature of PLA shifted towards higher temperature with increasing the MCC content and the double melting peak changed into single melting peak. So, these results can be suggested that silane treatment of the surface of MCC had no effected on thermal transition behavior of PLA/MCC composite.

Figure 4.14 shows the effect of Biomax® and APS surface treatment of MCC (PLA-MCC-Si-Bi) on thermal transition behavior of PLA composite at various ratios of MCC. The DSC thermograms of this group show similar to these characteristic of PLA-MCC-Bi (Figure 14.12) composites because the thermal behavior of composites was affected by Biomax® only.

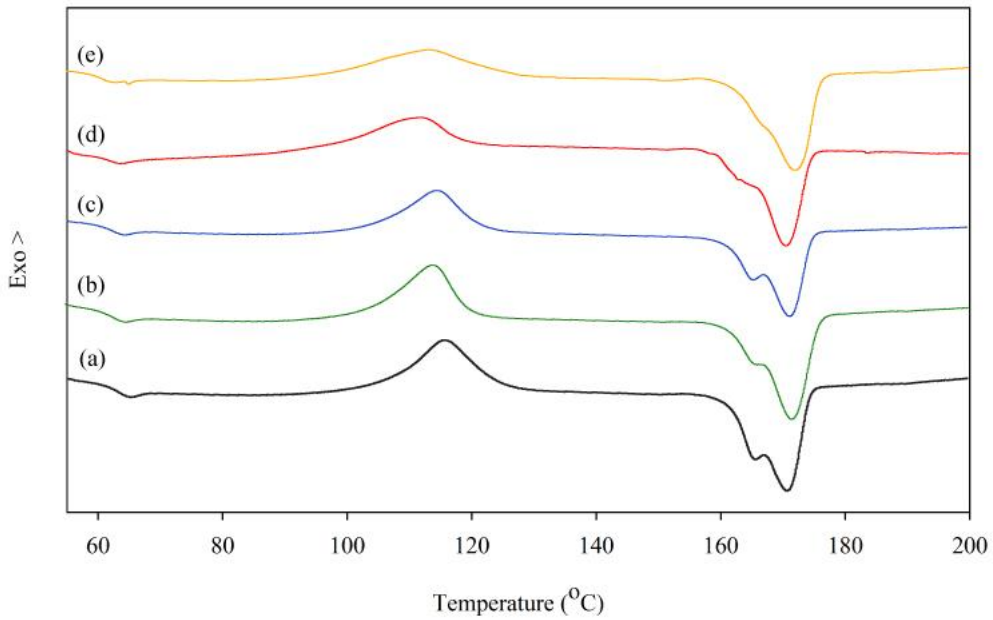

Figure 4.13 DSC thermograms of PLA composites at various APS treated MCC content at (a) 0, (b) 1.25, (c) 2.5, (d) 5 and (e) 10 wt%.

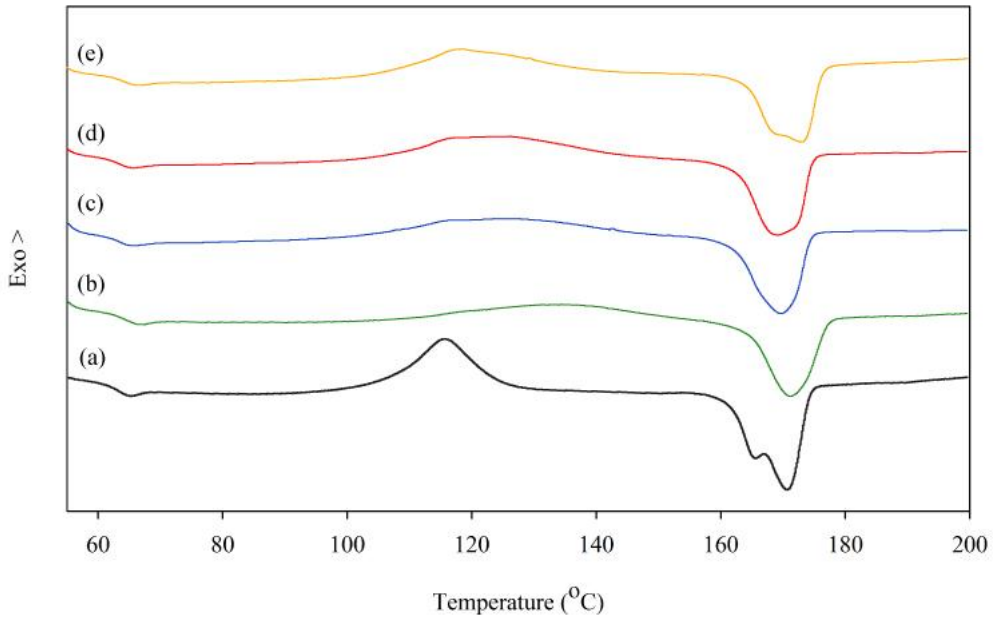

Figure 4.14 DSC thermograms of PLA composites with 2 phr of Biomax® at various APS treated MCC contents (a) neat PLA, (b) 1.25, (c) 2.5, (d) 5 and (e) 10 wt%.

Table 4.2 Detail thermal properties of PLA/MCC composites

Materials	T_g (℃)	T_m (℃)		T_{cc} (℃)	ΔHm (J/g)	χ_c(%)
		T_{mL}	T_{mH}			
PLA	61.65	164.04	169.76	113.41	39.96	4.09
PLA-Bi	59.16	165.46	170.84	114.97	36.44	2.48
PLA-1.25MCC	61.37	165.27	169.81	115.43	40.28	4.53
PLA-2.5MCC	61.40	165.38	170.29	114.40	41.30	6.51
PLA-5MCC	61.04	166.65	171.95	113.50	40.83	7.29
PLA-10MCC	61.09	170.72		113.14	41.13	12.82
PLA-1.25MCC-Bi	62.17	168.65		127.75	36.23	4.66
PLA-2.5MCC-Bi	62.98	168.29		127.22	37.73	3.13
PLA-5MCC-Bi	61.85	168.75		122.63	36.48	5.88
PLA-10MCC-Bi	61.53	164.66	169.47	124.24	38.51	8.19
PLA-1.25MCC-Si	63.19	164.53	170.80	113.60	39.01	5.47
PLA-2.5MCC-Si	61.79	164.82	170.27	113.71	36.89	6.13
PLA-5MCC-Si	62.28	163.48	169.52	110.78	39.65	8.20
PLA-10MCC-Si	61.32	170.32		112.97	38.74	11.43
PLA-1.25MCC-Si-Bi	62.87	169.96		131.92	34.95	7.07
PLA-2.5MCC-Si-Bi	61.96	167.99		123.73	39.79	5.36
PLA-5MCC-Si-Bi	62.5	167.46		124.87	37.30	8.83
PLA-10MCC-Si-Bi	63.2	167.43	171.31	116.92	35.56	10.20

4.6.3 Physical properties

4.6.3.1 Morphology

The fractured surface of the composites specimens was studied to understand the failure mechanism and also verified the interfacial adhesion between fiber and PLA matrix. The fractured surfaces of PLA/MCC composites are displayed in figure 4.15 – 4.19. Figure 4.15 is a fractured surface of neat PLA (a) and PLA with 2 phr of Biomax®. Their fractured surfaces are different, the fractured surface of neat PLA is smooth, while that of the PLA blended with Biomax is immiscible (Figure 14.5(b)), and the phase separation was observed. The particles of Biomax® were well disperse in a PLA matrix and act as rubber particle which improve the toughness of PLA.

Figure 4.16 shows the fracture surfaced of PLA/MCC composites at various MCC contents. These observations indicate that there is no interfacial adhesion between fiber and matrix. The SEM micrographs show several micro gaps between MCC and matrix. These the micro gaps between fiber and matrix result in poor stress transfer which is affected to the lower in strength properties and of the PLA composites. The agglomeration of MCC was also observed at 10 wt.% of MCC loading and this is the cause of the dramatically decrease in tensile strength.

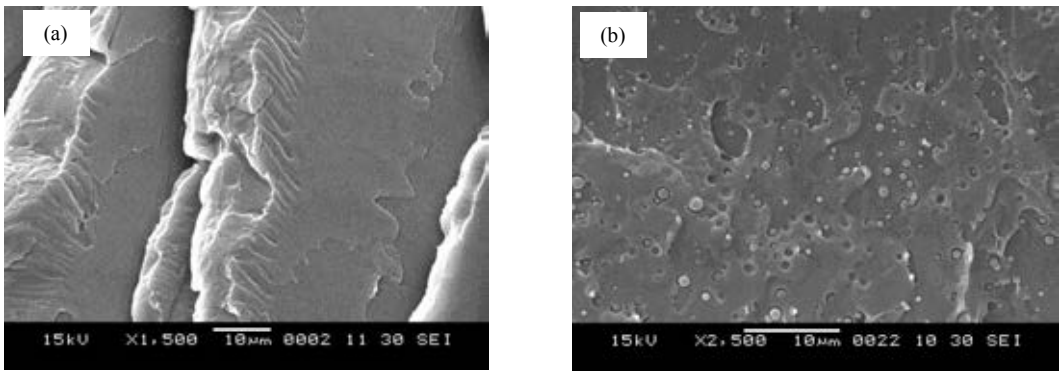

Figure 4.15 SEM micrographs of (a) Neat PLA, (b) PLA with 2phr Biomax®

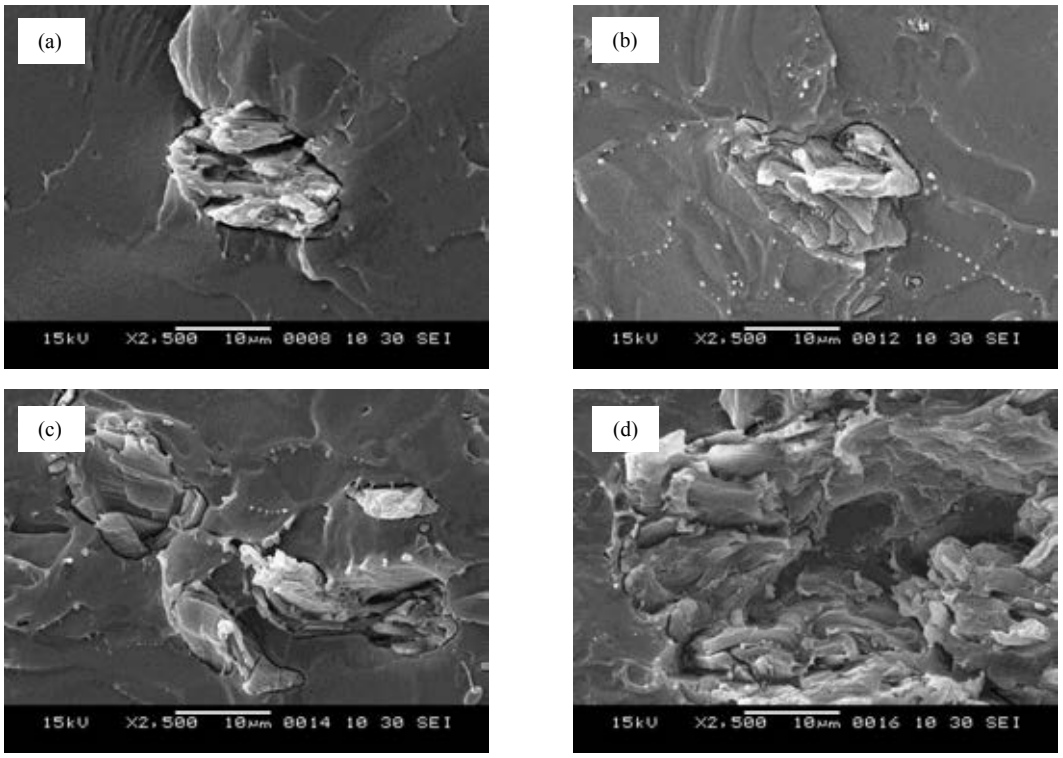

Figure 4.16 SEM micrographs of PLA reinforced with untreated MCC at (a) 1.25, (b) 2.50, (c) 5.00, (d) 10 wt.%

The fractured surface of PLA/MCC with 2 phr of Biomax® at various MCC contents are shown in Figure 4.17. The micro gaps between fiber and matrix stills remaining and the Biomax® micro particles are uniformly disperse in PLA matrix. From the SEM micrographs it can be indicated that the Biomax® improve the matrix properties by dispersing into the PLA matrix and acts as the rubber particle which improve the toughness of PLA matrix. However, the interfacial adhesion is still poor and needed to be improved.

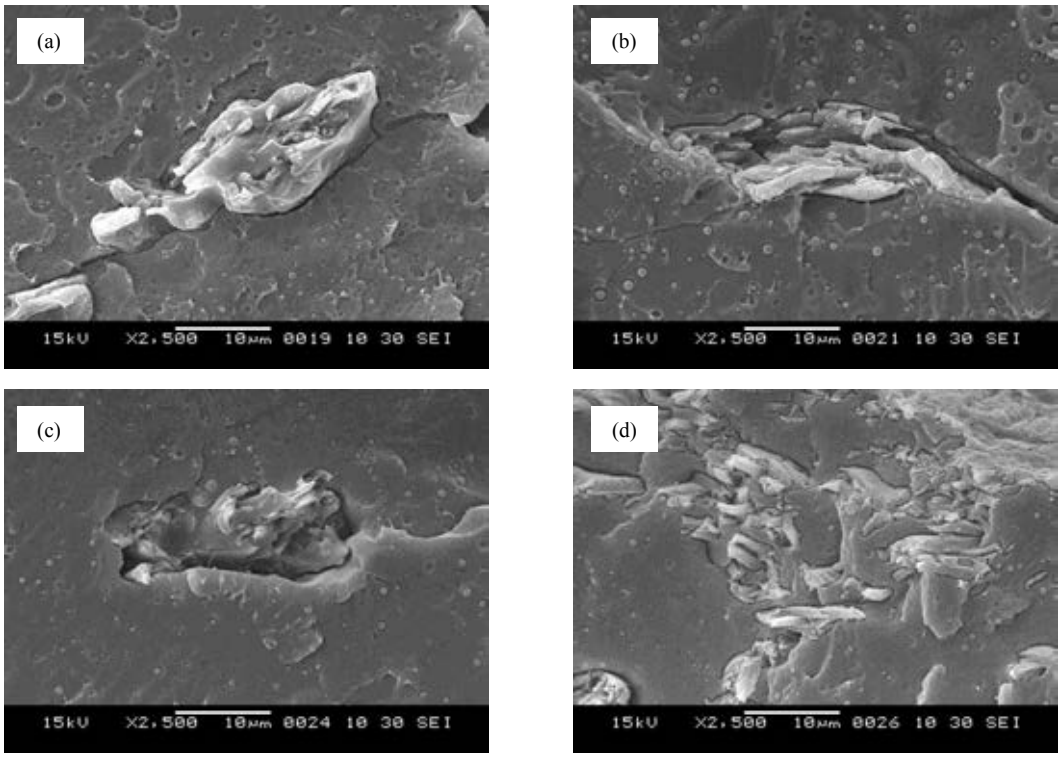

Figure 4.17 SEM micrographs of PLA/MCC with 2 phr of Biomax® at various MCC contents (a) 1.25, (b) 2.50, (c) 5.00, (d) 10 wt.%

Figure 4.18 shows the fractured surface of PLA/MCC composites which containing APS treated MCC. The morphologies of silane treated MCC composites are different from the untreated MCC (Figure 4.16). The SEM micrographs show no micro gaps between fiber and PLA interface, the treated MCC is well wet with the PLA matrix. These results can be indicated that the treatment of MCC with APS is an efficient approach to improve the interfacial adhesion between fiber and polymer matrix; as a result the stress transfer between the interfaced is enhanced attributing to the improve in mechanical properties.

The SEM micrographs of PLA/MCC with 2 phr of Biomax® at various ratios of APS treated MCC are shows in Figure 4.19. The cooperation between Biomax® and silane surface treatment is shown its dominant characteristic. The rubber particles were observed and also well dispersed in PLA matrix, contributing to the grates in elongation at break of this composites group. The wetting of polymer matrix around the fiber by APS surface treatment can be indicated that the fiber and matrix have an interaction to each other. These results are in good agreement with the increase in mechanical properties as previously discussed.

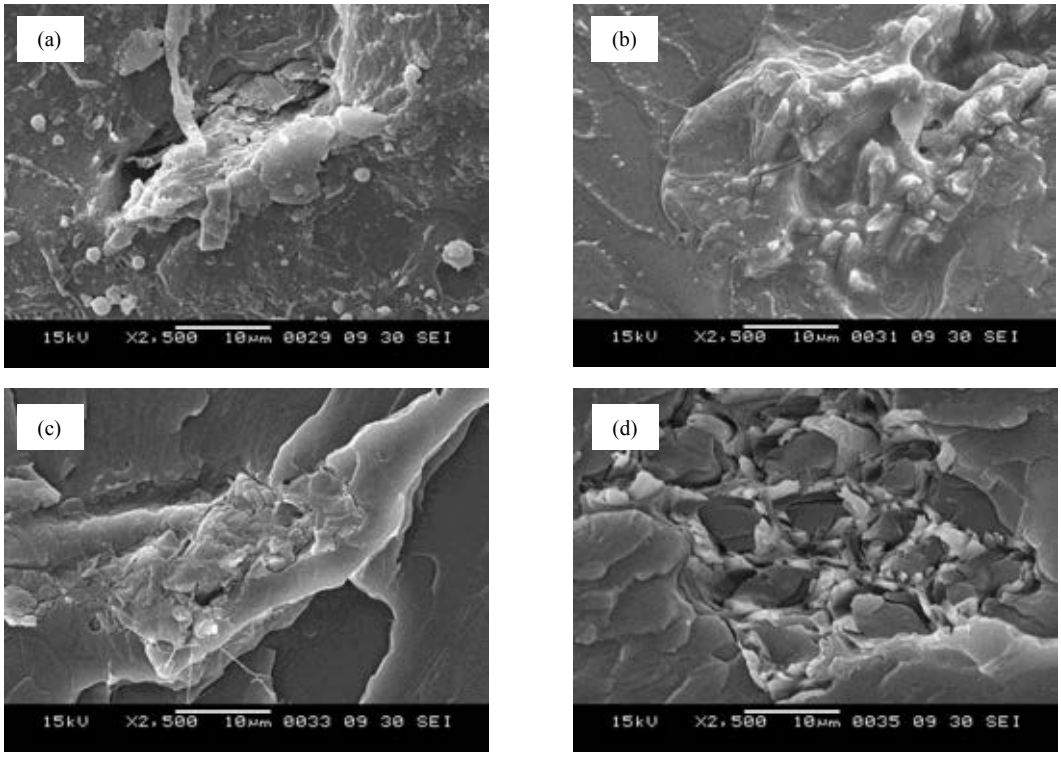

Figure 4.18 SEM micrographs of PLA reinforced APS treated MCCC at (a) 1.25, (b) 2.50, (c) 5.00, (d) 10 wt.%

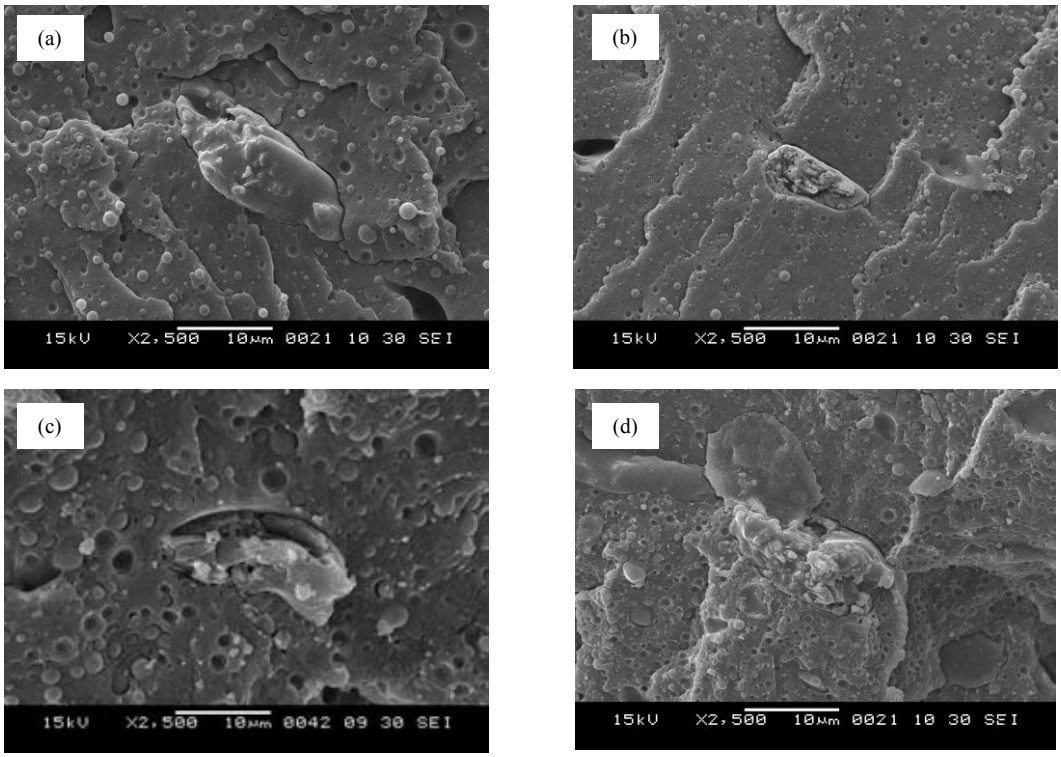

Figure 4.19 SEM micrographs of PLA/MCC with 2 phr of Biomax® at various APS treated MCC contents (a) 1.25, (b) 2.50, (c) 5.00, (d) 10 wt.%

4.6.3.2 Water absorption

Percentages water absorption of PLA/MCC composites are reported in Figure 4.20 as a function of MCC contents. The water absorption of 1.4 %. A moisture uptake was observed for all the specimens within 24 hours. The absorption of water is related to its rate of diffusion into the composites. Wang et al. [53] also reported that the water absorption of neat PLA was at approximately 1%. The higher in water absorption values in the PLA/MCC composites can be attributed to the hydrophilic nature of the MCC by the presence of an abundance of hydroxyl groups, which are available for interaction with the water molecules. So, the water absorptions of PLA composites are increased up to 1.4% (5 wt%) with increasing the MCC content. Biomax® has an effect no the water PLA composite by decreasing the water absorption in samples. This result is due to the fact that Biomax® is a hydrophobic material with the long chain hydrocarbon in its structure, so the hydrophobic behavior of the PLA composites increased. The APS treated MCC also has an influence on the water absorption of the composites. As the interface of treated MCC was well wet by the PLA matrix, the micro gaps around the

fiber and matrix decreased. Consequently, water molecules can hardly diffuse into the composites; thus the water absorption of PLA composites containing APS treated MCC was decreased

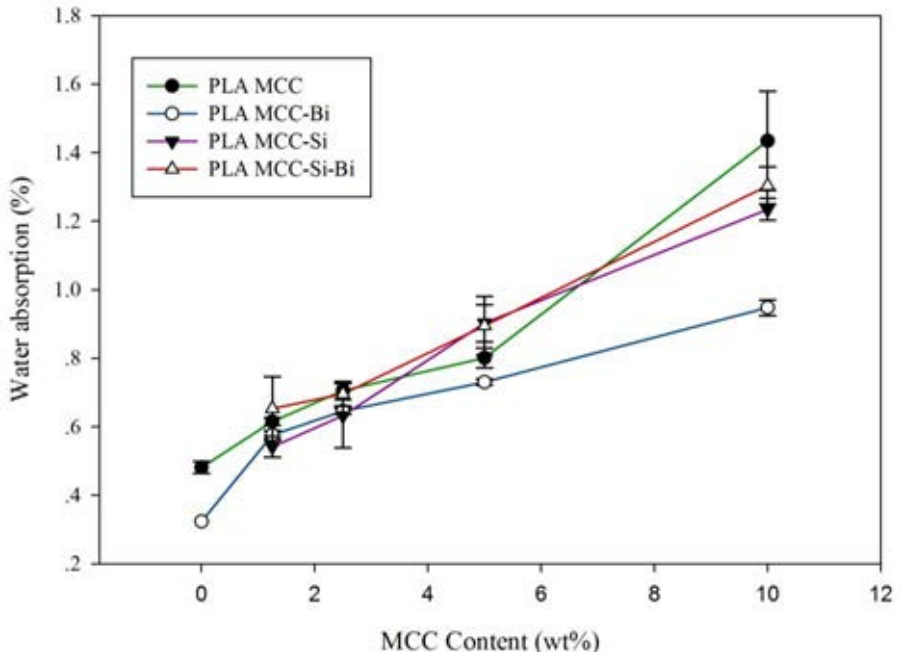

Figure 4.20 Water absorption of PLA/MCC composites.

4.6.3.3 Crystallinity

The neat PLA, MCC and APS treated MCC were characterized by X-ray diffraction to study the effect of MCC content on the crystallinity of PLA. X-ray diffraction patterns of neat PLA, MCC and APS treated MCC are shown in Figure 4.21. For PLA a narrow peak at 2θ at 16.37 represents an amorphous nature and it can be considered as in a semi-crystalline phase. The MCC and untreated MCC show the peak at 2θ = 15.69 and 22.23, which are characteristic peaks of cellulose structure, representing the crystalline nature of this reinforcement. Other researches have also reported the same results for MCC from X-ray analysis [53,54]. To obtain the high performance composite with MCC, the high crystallinity of MCC is required [55].

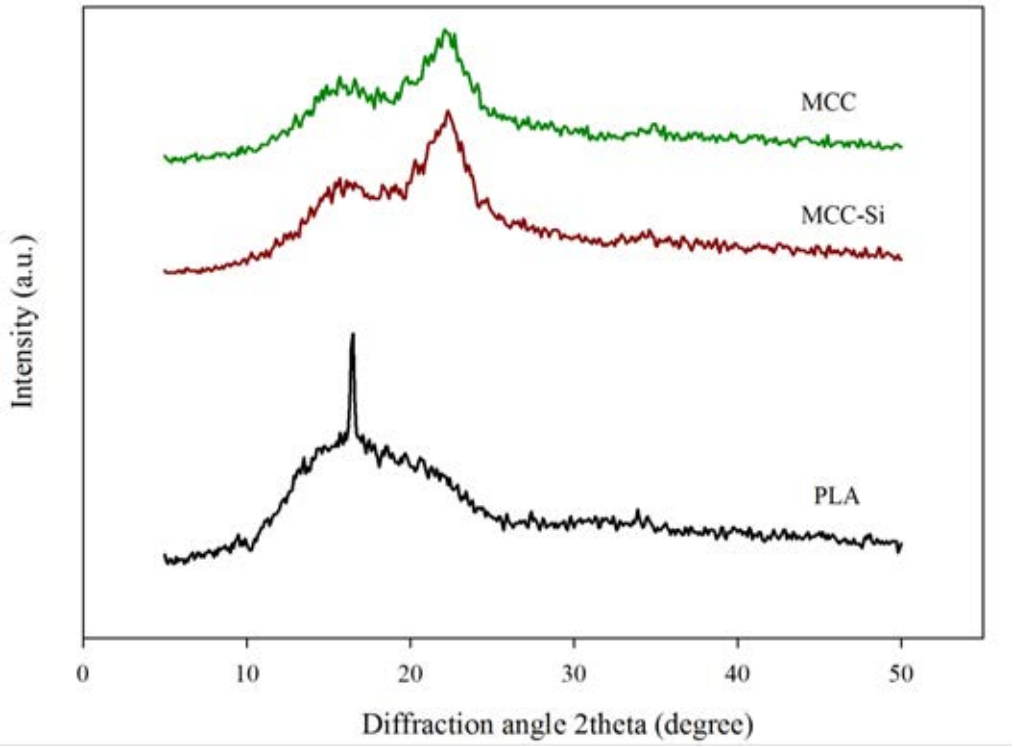

Figure 4.21 X-ray diffraction patterns of raw materials

From Figure 4.22, the effect of MCC content on the crystallinity of the system is shown. The peak at 2θ = 16.37º is the most prominent and is indicative of PLA crystallinity. The XRD data indicate that the low crystallinty and the peak due to PLA and MCC are weak. Comparing with neat PLA, the low intensity of PLA/MCC composites is possibly explained by a low level of matrix crystallinity developed due to fast cooling rate during the extrusion and compression. As the MCC content increased, the increasing in intensity of the peaks at 2θ = 22.23º is observed and the results can be attributed to the effect of crystallinity of cellulose which is merging with the crystalline part of PLA and enhancing the crystalline of composites. The total peak intensity of composites is increased with increasing the MCC content. The PLA/MCC-Bi, PLA/MCC-Si and PLA/MCC-Si-Bi composites are showing the similar result.

In all cases, it can be seen that the magnitude of the peaks indicating crystallinity of the composite is lower than that of the PLA and the reinforcement used. This probably results from the mixing of reinforcement with PLA and fabrication process, which rendered in the random orientation of the reinforcement. The crystallinity of reinforcement having random arrangement is expected to be less than the case when the reinforcement is oriented in a plane. This type of observation was reported by Wallenberger and coworkers [56] who have been working with tunicin whiskers filled composites.

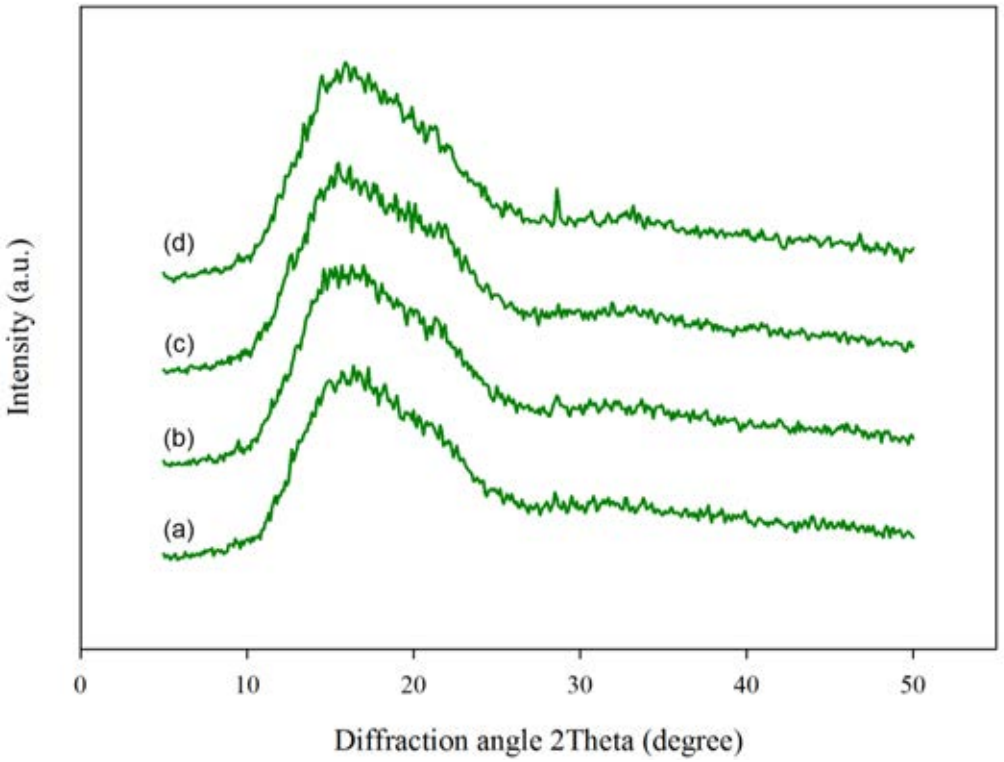

Figure 4.22 X-ray diffraction patterns PLA/MCC composites at various MCC contents (a) 1.25, (b) 2.50, (c) 5.00, (d) 10 wt.%

4.7 Biodegradability

Poly(lactic acid) (PLA) is the first polymer based on renewable raw materials commercialized at a large scale. It is a compostable material, meeting the specifications of international standards. However, the biodegradation behaviour of PLA in soil is not clear [57]. To our knowledge, there has been no studies available concerning the behavior of PLA in soil.

Polylactic acid (PLA) is fully biodegradable when composted in a large-scale operation with temperatures of 60 and above. The first stage of degradation of PLA (two weeks) is via hydrolysis to water-soluble compounds and lactic acid, then metabolization by microorganisms into carbon dioxide, water and biomass proceeds [58].

PLA is largely resistant to attack by microorganisms in soil or sewage under ambient conditions. The polymer must first be hydrolyzed at elevated temperatures approximately 58 °C to reduce the molecular weight before biodegradation can commence. Thus, PLA will not degrade in typical garden compost. Under typical use and storage conditions PLA is quite stable.

As mentioned, the primary mechanism of degradation of PLA is hydrolysis, catalyzed by temperature, followed by bacterial attack on the fragmented residues. Many studies concern biodegradation of PLA in different environments such as aquatic system, soil, compost. Therefore, in this research, the real condition (land fill, sea water) and simulated condition (ISO 14855-2, ISO 14852) were used to investigate the biodegradability of PLA/MCC composites.

4.7.1 ISO 14855-2

A biodegradation test was performed using the gravimetric measurement respirometryic (GMR) system in a controlled compost at 58±2ºC as shown in Figure. 4.23. Neat PLA and PLA/5MCC-Si-Bi composites were used to investigate the biodegradability. The effects of APS MCC surface treatment and Biomax® Strong 120 were studied by comparing the results between neat PLA and PLA/5MCC-Si-Bi. The polymer sample powder (10 g of Neat PLA, PLA, 5MCC-Si-Bi and cellulose) was well mixed in the activated compost 100 g and transferred to a reaction vessel. A compost with no sample was used as a blank to determine the respiration activity of this compost. Biodegradation tests were performed at 58±2ºC with air (CO_2-free) flow for 40 days. The activated compost used in this study produced approximately 50 mg CO_2 per gram of volatile solids of this compost over the first 10 days. In almost all cases, the number of experimental replicates of the blank or sample was two (duplicate). The produced CO_2 amounts were measured once a day by measuring the weights of an absorption column for carbon dioxide (column 1 and 2) and an absorption column for water (column 3 and 4). The percentage of biodegradation was calculated from the produced CO_2 amount, which was cancelled, respiration CO_2 amount determined from a blank. The absorbed CO_2 amounts for the absorption columns were reached to 40% of the theoretical absorption capacity, and the chemicals (soda lime and soda talc) inside the columns were changed. This test method is based on the ISO 14855-2.

The GMR system with the absorption columns is shown in Figure. 4.23. This evaluation system for the biodegradation uses the CO_2 trap system with CO2 absorption columns. This GMR mechanism is as follows. At first, room air is purged into the carbon dioxide trap (2.0 M NaOH) to remove CO_2 in the air as shown in Fig. 4.23. This air is moisturized (water) and purged into the reaction vessel controlled at 58 using a thermosensor and water bath. The air with the produced CO_2 from biodegradation of the samples is poured into the ammonia trap (0.1 M H_2SO_4) to remove the produced ammonia from the compost for obtaining an accurate carbon balance using a gravimetric measurement. The air with its CO_2 is poured into dehumidifying traps (Silica gel and CaCl) to remove the moisture from the stream in air for an accurate carbon weight balance and then poured into an absorption column

of carbon dioxide and an absorption column of water. In these two columns with NaOH on support and soda lime (NaOH immobilized to slaked lime), the produced CO_2 is completely absorbed by the reactions indicated as Equation 4.1.

$$CO_2 + 2NaOH \rightarrow Na_2CO_3 + H_2O \qquad \textbf{Equation 4.1}$$

The produced H_2O is simultaneously trapped in these two columns. According to this reaction, the weight of these two columns is increased the same as the weight of the produced CO_2. In this way, the produced CO_2 amount is easily obtained by a gravimetric measurement. Once a day, the weights of these two columns are measured. From the increasing amount of these two columns for a sample and a blank, and the theoretical CO_2 amount, the percentages of biodegradations can be calculated as follows.

$$\%mineralization = \frac{gCO_2 - gCO_{2b}}{g_{materials} \times (\%C_{material}/100) \times (44/12)} \qquad \textbf{Equation 4.2}$$

where

gCO_2 = amount of evolved carbon dioxide in grams from the sample and the positive control;

gCO_{2b} = amount of evolved carbon dioxide in grams from the blank;

$g_{material}$ = mass of the sample;

$\%C_{material}$ = percentage organic carbon content of the sample obtained from CHON/S analyzer.

Figure. 4.24. Shows the biodegradation of PLA, PLA5MCC-Si-Bi and cellulose powders by the GMR system in controlled compost at 58ºC. The PLA powders were used for the biodegradation test. After about 30 days of incubation at 58ºC, the degree of biodegradation reached 60%. It was postulated that the molecular weight of PLA decreased by hydrolysis during the period of induction. If the molecular weight of PLA reached the value (PLA oligomer), which can be metabolized by microorganisms in the compost, the biodegradation of PLA was actively done then much CO2 was evolved. The high rate of CO_2 evolve was observed about 14 days. At the first period (1-14 days), PLA 5%MCC-Si-Bi composites is shown higher biodegradation rate than neat PLA because the hydrophilic behavior of 5%MCC-Si-Bi is greater than neat PLA, so, the polymer chain can be hydrolyzed more than neat PLA. For the second period (15-30 days), the biodegradation rates of two samples are similar rate. And final period, the percentage of biodegradation going to the close value at 80.2% and 78.2% for neat PLA and PLA 5%MCC-Si-Bi respectively.

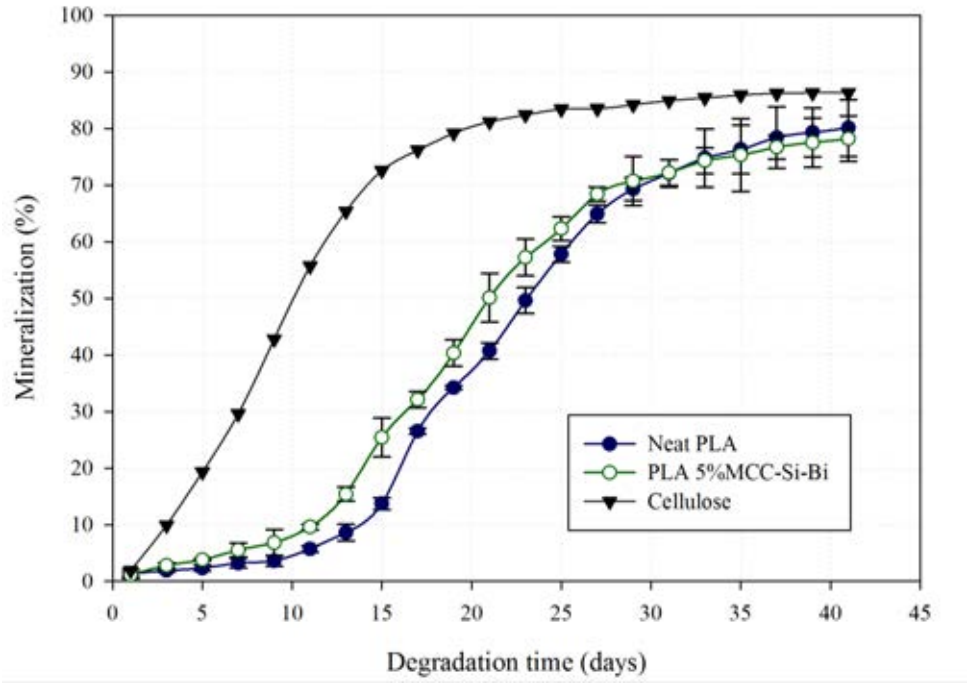

Figure 4.24 Biodegradability of PLA composites by GMR systems

4.7.2 ISO 14852

According to ISO 14852, the biodegradation rate is calculated by comparing the experimentally determined amount of evolved CO_2 from degraded materials with the theoretical amount of evolved CO_2. The detection device shown in Figure 4.25 was designed according to ISO 14852 and is composed of an air pump, air CO_2 absorption bottles, a bioreactor, and evolved CO_2 absorption bottles. The air was passed through the absorption bottles containing NaOH and $Ba(OH)_2$ solution to eliminate CO_2. The CO_2-free air entered the bioreactor that containing sample and activated sludge and the degradation reaction was carried out using a water bath, which was controlled the temperature at 30 ºC and shaking during the reaction. Evolved CO_2 from the degraded materials was absorbed by $Ba(OH)_2$ (0.1 M) in the absorption bottles and the $BaCO_3$ was collected by titration with 0.1 M HCl to calculate the quantity of evolved CO_2. The produced CO_2 is completely absorbed by the reactions indicated as Equation 4.3 and 4.4.

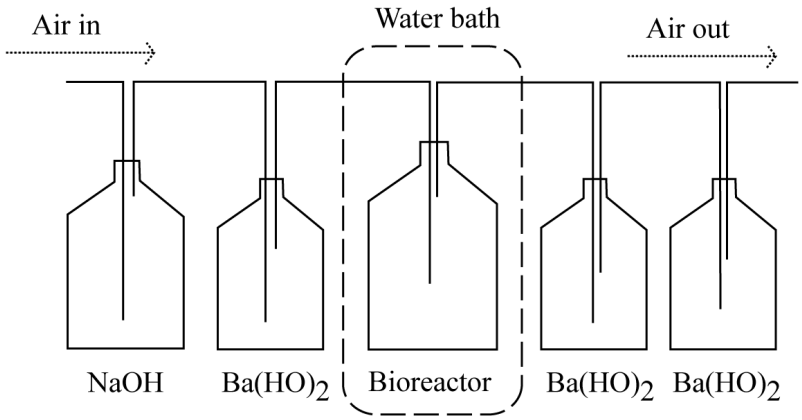

Figure 4.25 The schematic of aqueous medium test system.

$CO_2 + Ba(OH)_2 \rightarrow BaCO_3 + H_2O$ **Equation 4.3**

then

$Ba(OH)_2 + 2HCl \rightarrow BaCl_2 + 2H_2O$ **Equation 4.4**

To verify the accuracy of the degradation results obtained with the microbial community, this research used the standard ISO 14852 method to determine biodegradability of the materials. For this experiment, the microorganism source is an activated sludge. The activity of the degrading bacteria in the activated sludge was not completely the same as that in the natural. However, the degradation state of these materials in the natural environment can be compared with the experiment where the activated sludge was used as the biodegrading environment.

The results showed that cellulose had the highest biodegradation rate and reached 60% on the 30 days of degradation. During the 30 days in test system the neat PLA and PLA-MMC-Si-Bi reached 37.6% and 42.1%, respectively. The biodegradation curve could be seen from Figure. 4.26. Similar to the results obtaining from the GMR system, The PLA-5MCC-Si-Bi had higher biodegradability rate than the neat PLA for the whole period of time, due to its greater hydrophilic nature from MCC content. However, from these results, the biodegradability of the neat PLA and its was lower volume than the biodegradability which were tested by GMR system because the sum of carbon in test materials is not converted to CO_2 but it also converted to dissolved organic carbon (DOC) [59]. So, the test results from this method are lower than those from GMR system; nevertheless, this method can be used to confirm the biodegradation characteristic of materials.

The test results and the experience also confirm that the test method is suitable even when the test material is not water-soluble. Biochemical oxygen demand and carbon conversion are obvious indicators of biodegradation processes and can be measured precisely and reproducibly even for poorly water-soluble materials. Measurement of the exhaust gas requires tight connections. The disadvantage of the this analytical method is that the absorption of CO_2 in barium hydroxide solution is the frequent handling of concentrated alkaline solutions and the possibility of losing CO_2 if the absorption capacity of the solution is saturated. For low degradation rates the CO_2 concentrations becomes small and the gas flow in such a test system is generally very low. The tests may be improved in future, as there is a considerable potential for automation and the handling of the test data by computer, which significantly improves their performance and evaluation.

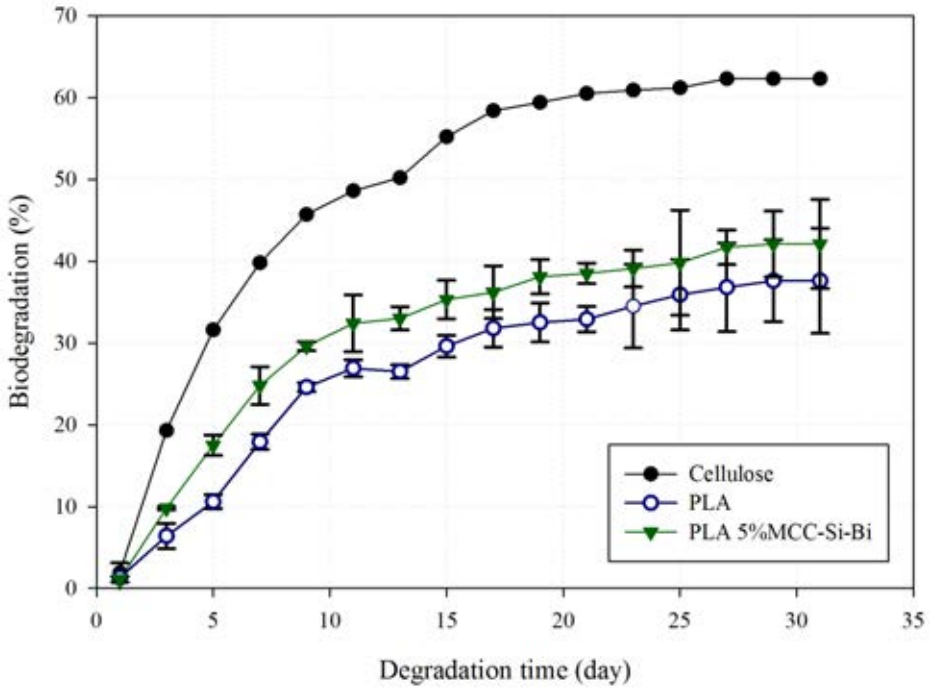

Figure 4.26 Biodegradability of PLA composites by aqueous medium test system.

4.7.3 Landfill test

4.7.3.1 Appearance

The biodegradability of neat PLA and PLA composites was studied by real composting condition test at the composting department of Chulalongkorn University. Figure 4.27 displays that the neat PLA had a smooth surface with high transparency at the initial time (Figure 4.27 (a)). After 15 days, the transparency of sample was decrease and after 30 days the white spot was observed and the PLA sheet tended to crack easily. The brown polymer matrix was noticed at the degradation time of 45 days (Figure 4.27 (d)) and cracking easier then the pervious sample at 30 days. This result shows that the enzymatic degradation occurred at this time and makes the polymer matrix going to brown.

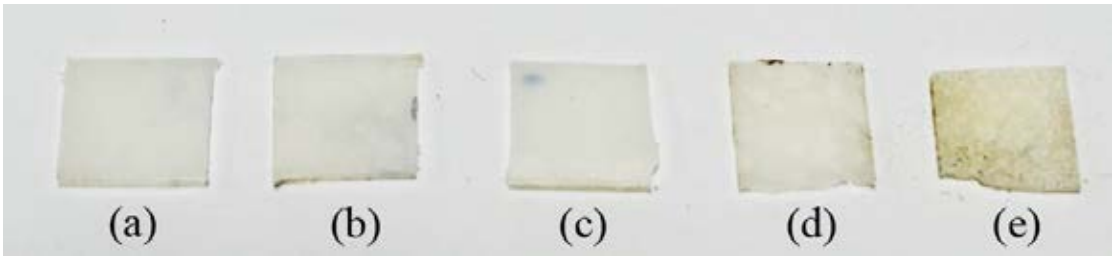

Figure 4.27 Appearance of degraded neat PLA (a) 0 day (b) 7 days, (c) 15 days, (d) 30 days, (e) 45 days.

Figure 4.28 shows the physical appearance of PLA composites with various MCC contents at 45 days. The 10 wt.% of MCC/PLA composite shows greater amounts of white spot and lowest strength comparing with the other samples. The biodegradability of PLA composites increased with increasing the MCC content and these results is due to the water which was absorbed into the PLA matrix through the micro gaps between MCC and matrix, that can hydrolyze PLA matrix into to the lower molecular weight faster than the composites with low MCC content.

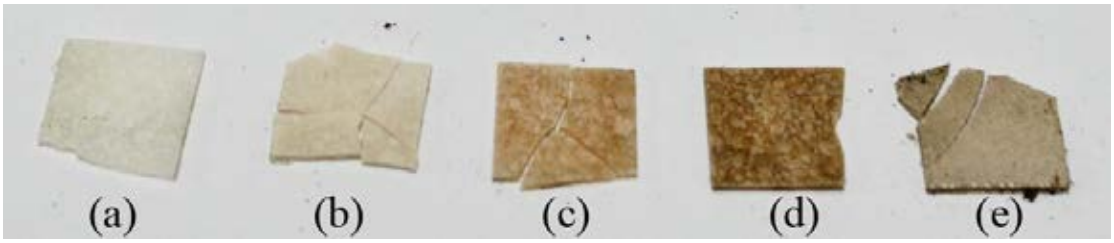

Figure 4.28 Appearance of degraded PLA with various contains MCC contents (a) 0 %, (b) 1.25%, (c) 2.5%, (d) 5%, (e) 10% at 45 days of biodegradation.

Comparing with the neat PLA as shown in Figure 4.29., The PLA with 2 phr Biomax® shows lower brittleness and whiter color than the neat PLA This may be attributed to the toughness and color of Biomax® itself. In addition, this results is due to the higher hydrophobic behavior of Biomax® which is influenced on the biodegradability by decreasing the water absorption rate of PLA.

Figure 4.29 Appearance of neat PLA (left) and PLA with 2 phr Biomax® (right) at 45 days of biodegradation.

The effect of APS MCC surface treatment on the biodegradability is shown in Figure 4.30. The appearance of surface treated MCC and untreated MCC/PLA composites is quite similar. The micro cracks as well as white spot and darkness color were observed in both samples. From this result, the APS surfaced treatment of MCC was not significant effect on the appearance of PLA composites.

Figure 4.30 Appearance of 5 wt.% MCC/PLA composites (left) untreated MCC and (right) APS treated MCC at 45 days of biodegradation.

4.7.3.2 Morphology

Figure 4.31 shows SEM micrographs of surface and fractured surface of neat PLA after buried for 15, 30 and 45 days in real composting condition. The fractured surface morphology of PLA at 15 days exhibited higher surface roughness than the surface of PLA before testing (0 day). This result indicates that the PLA was probably at the beginning stage of degradation mechanism. After 30 days, the rougher surface and some micro pores of PLA were observed. Furthermore, These micro pores became denser and larger upon increasing the burial time, as obviously noticed from the sample degraded for 45 days. This result shows that the biodegradation of PLA is not confined only on the surface but the bulk polymer matrix also changed; as a results the mechanism, of biodegradation for PLA is bulk degradation.

Figure 4.32 presents SEM micrographs of the composites at various MCC contents at 45 days of burial in compost. All of the PLA composites show several micro pores, particularly at the fractured surface. The surface roughness of PLA composites increases with increasing MCC content and the 10 wt.% of MCC the PLA composites displayed the erosion of surface by microorganisms.

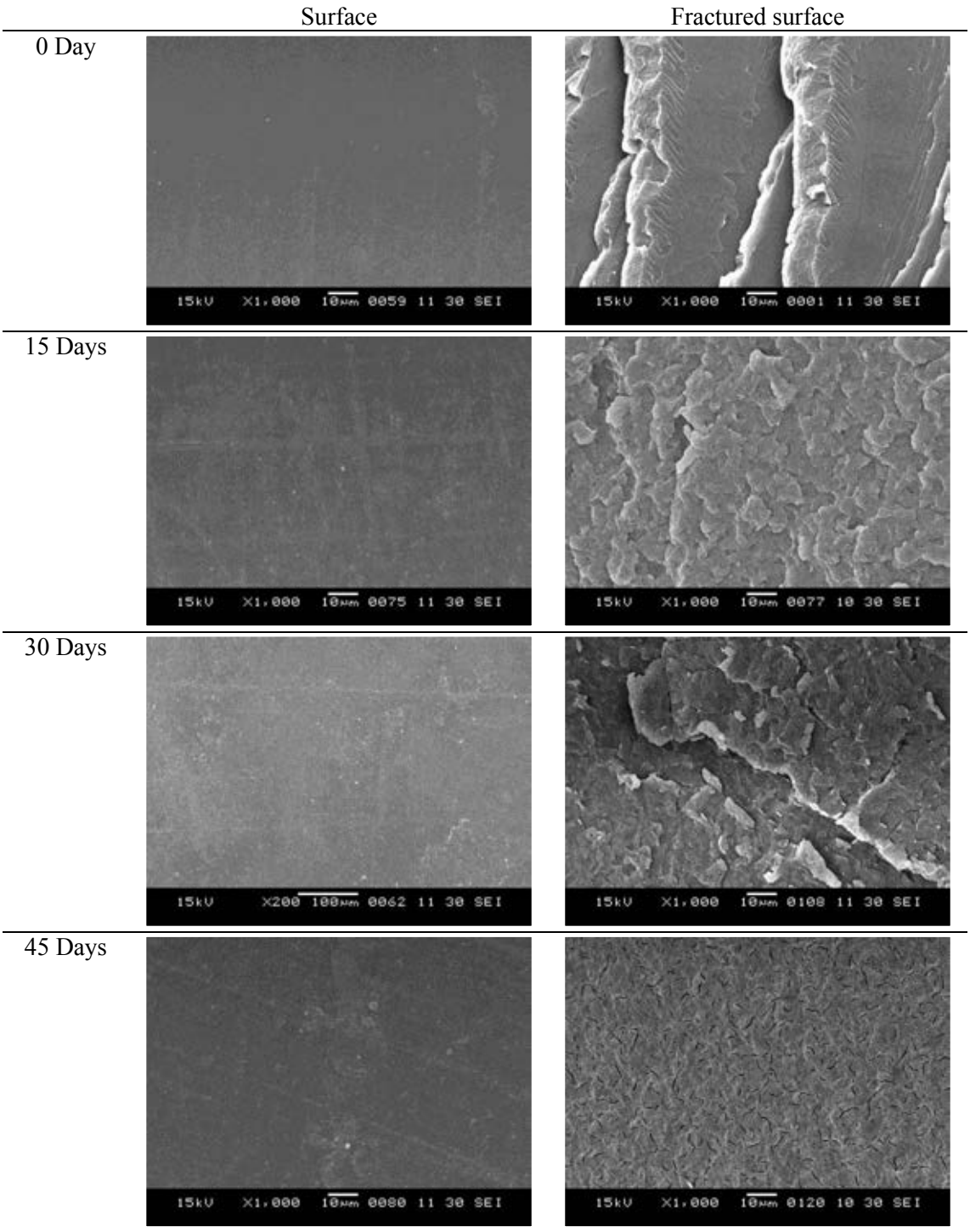

Figure 4.31 SEM micrographs of neat PLA at various degradation time

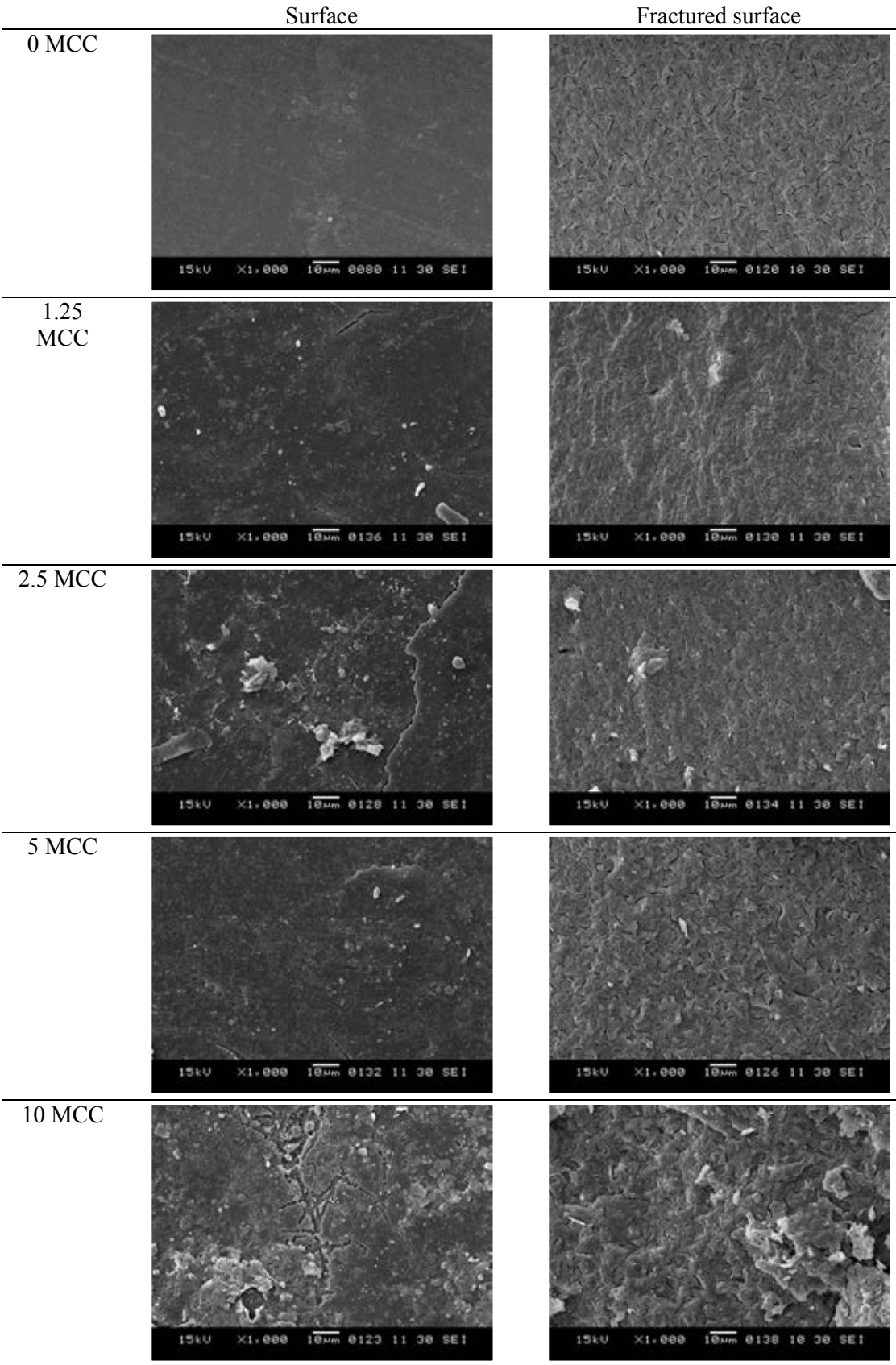

Figure 4.32 SEM micrographs of PLA/MCC composites after 45 days

In Figure 4.33, its surface roughness was less than that of the neat PLA. In addition, the micro pores in the fractured surface of PLA-Bi were smaller than those of the neat PLA because of the hydrophobic behavior of Biomax® decreasing water absorption content of the PLA-Bi composite.

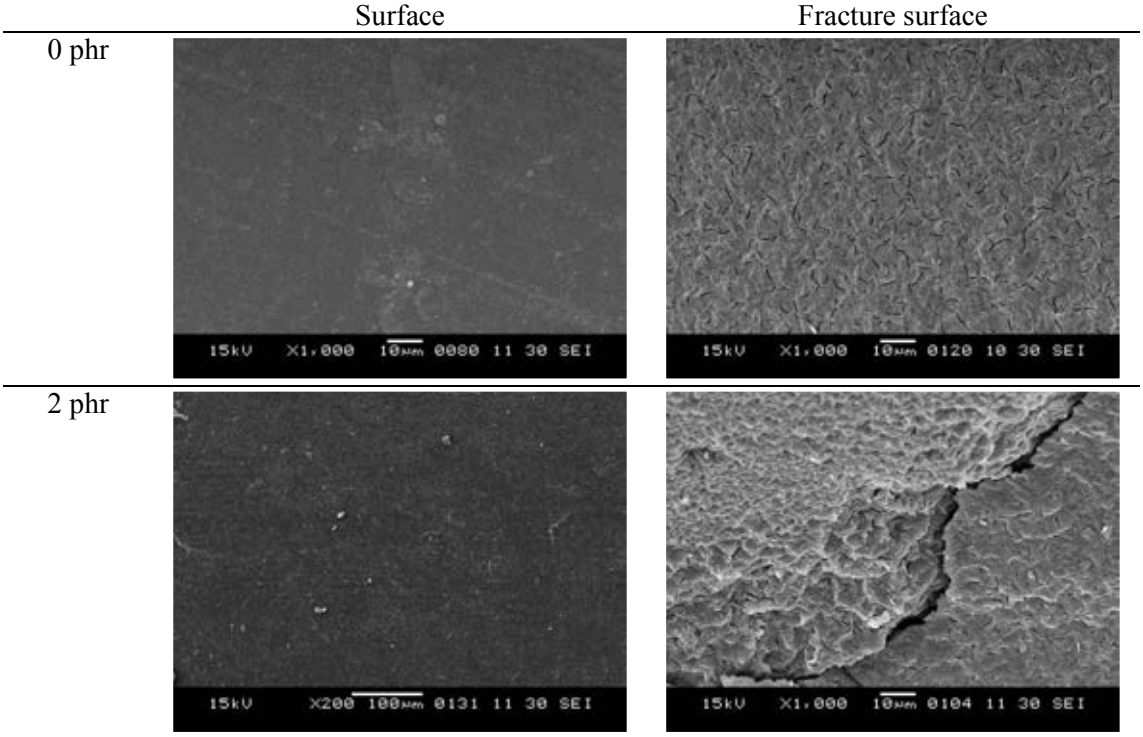

Figure 4.33 SEM micrographs of (top) neat PLA and (bottom) PLA-Bi after 45 days of biodegradation

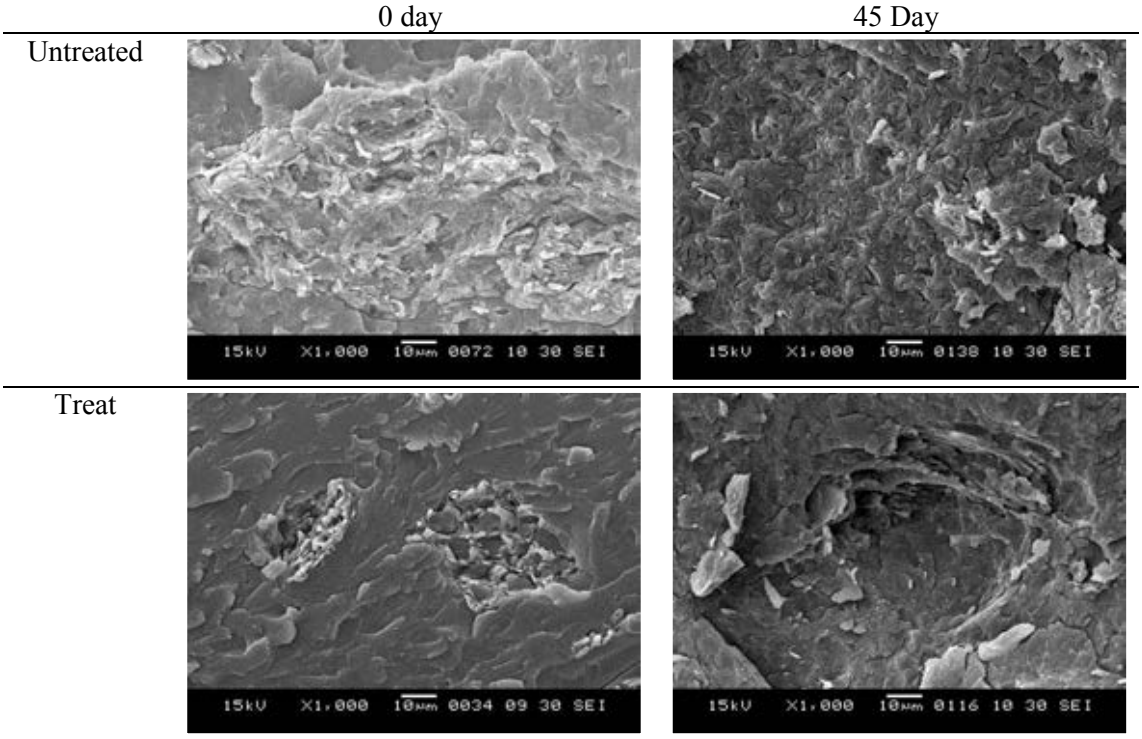

Figure 4.34 SEM micrograph of 45 days degraded 5 wt.% of untreated and APS treated MCC/PLA composites.

4.7.3.3 Weight loss

Considering the effect of time, Figure 4.35 - 4.37 illustrate that the percent weight remaining of all the composites decreased as a function of time and amount of MCC.

Figure 4.35 showed the percent of weight remaining of PLA/MCC composites at various MCC contents. From this figure, weight of neat PLA decreased to 72.6 % at 45 days. When adding the MCC, the weight remaining of PLA composite decreased with increasing the MCC content and this result can be attributed to water absorption properties of the composites. The absorbed water in the materials allows the microorganism to grow and utilize the materials as energy source. The result in section 4.2.3.2 shows that the hydrophilic of PLA composites increased while the MCC contents increased. This behavior caused a reduction in the % weight remaining of PLA composites.

Considering the effect of Biomax®, as shown in Figure 4.36, although PLA-Bi has lower hydrophilic properties than the neat PLA, % weight remaining of neat PLA and PLA-Bi composites id not different, this may be due to the low amount of Biomax® in the composite.

Comparing between APS surface treatment and Biomax®, the Figure 4.37 showed the percentage remaining of 5 wt.% MCC composites. From this figure, PLA with 5 wt.% APS treated MCC composites and 2 phr of Biomax® shows the largest weight remaining and the result can be attributed mainly to the effect of surface treatment which reduce the micro gaps be tween the interface, leading the lower amount of absorbed water.

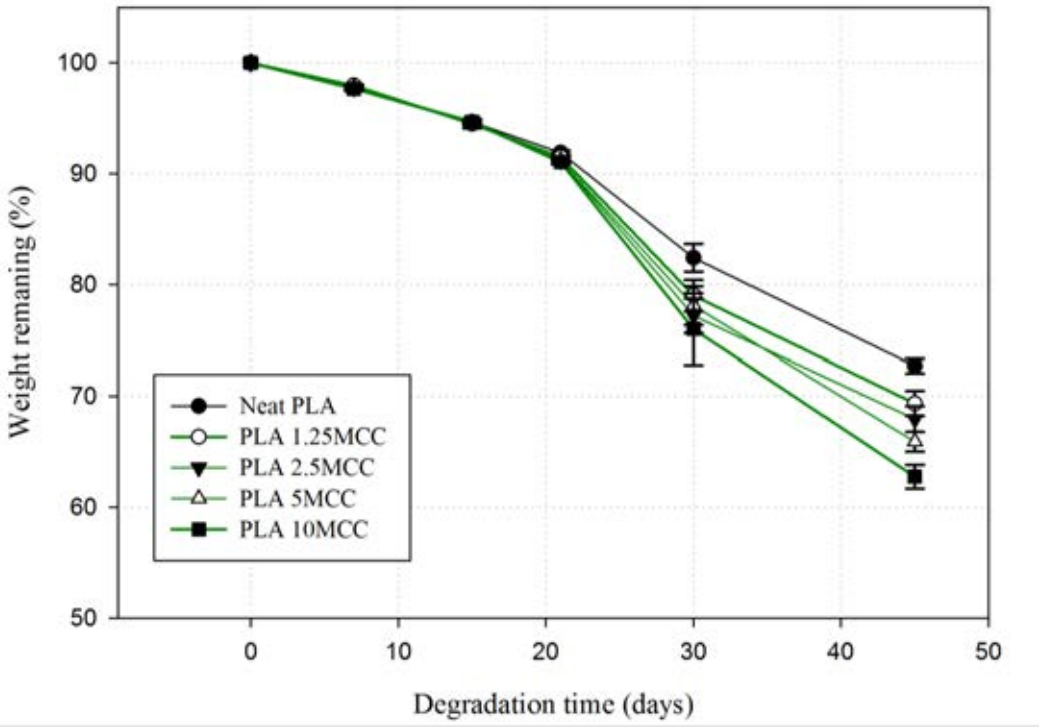

Figure 4.35 Weight remaining of degraded PLA/MCC composite at various MCC contents as a function of time.

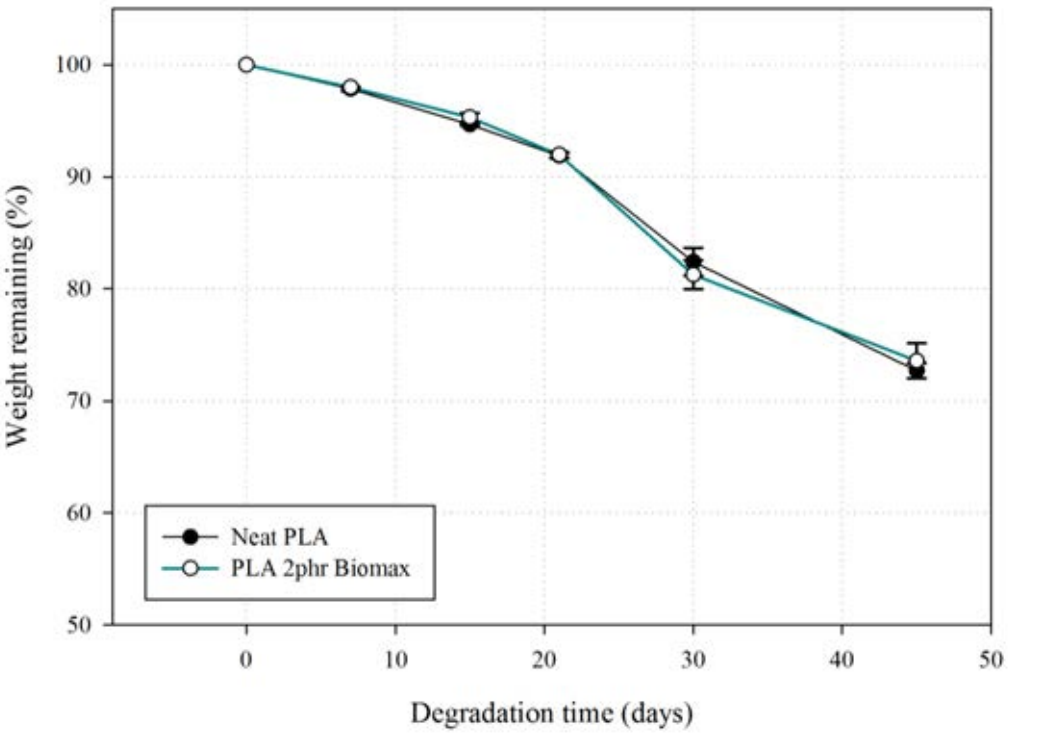

Figure 4.36. Weight remaining of degraded neat PLA and PLA-Biomax® as a function of time.

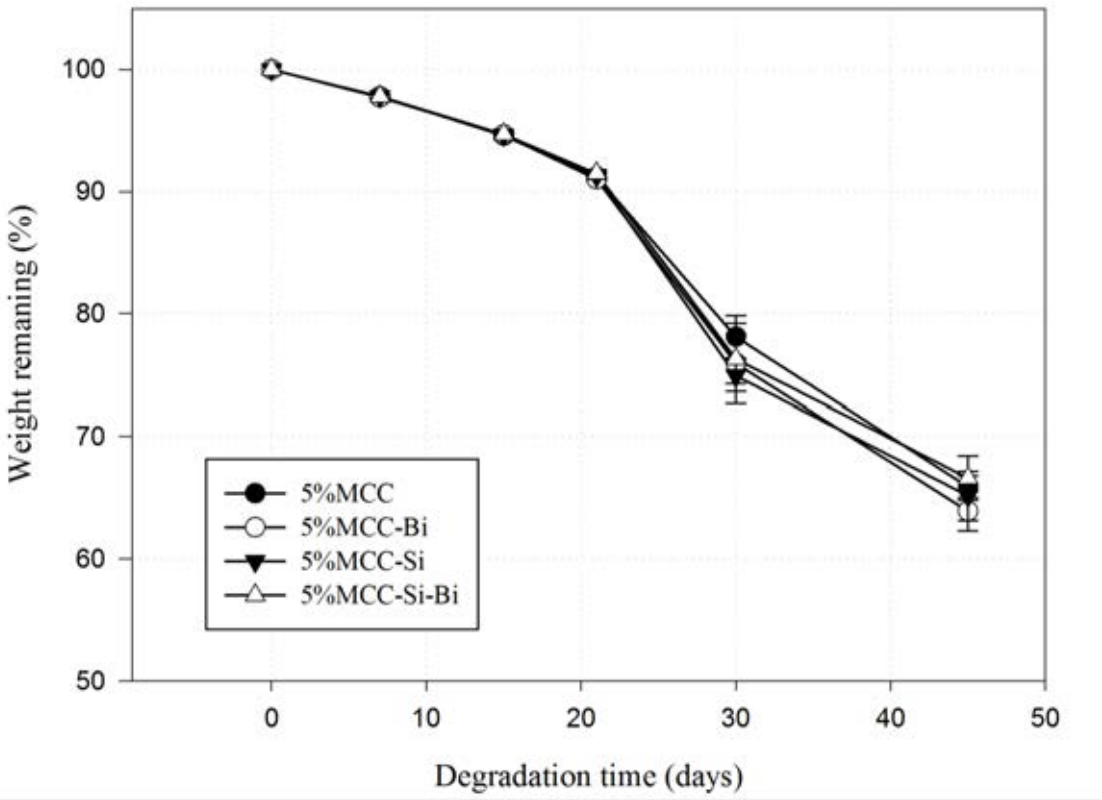

Figure 4.37 Weight remaining of PLA composite at 5 wt.% MCC as a function of time.

4.4.4.3 Molecular weight

Molecular weight is one of the most important parameters to estimate biodegradability. The molecular weights of the PLA component in composite specimens unburied and after exposure to compost for 7, 15, 30 and 45 days are shown in Figure 4.38-4.39. Figure 4.38 shows the number average molecular weight (Mn) of neat PLA after exposure to compost. From this figure, the dramatical decrease of molecular weight of PLA/MCC composites is higher than neat PLA, this result can be attributed to the high rate of hydrolysis of PLA/MCC composites which is influenced from the hydrophilic behavior of MCC in PLA/MCC composites. After that, the molecular weight still decrease.

Figure 4.39 shows the effect of APS surface treatment and Biomax® on biodegradability of PLA-5MCC composites. The molecular weights of PLA-5MCC composites show the similar trend. The fast decreasing in molecular weight were observed in all PLA/MCC composites. It seen that both fiber surface treatment and Biomax® had no effect on the decrease in molecular weight of PLA.

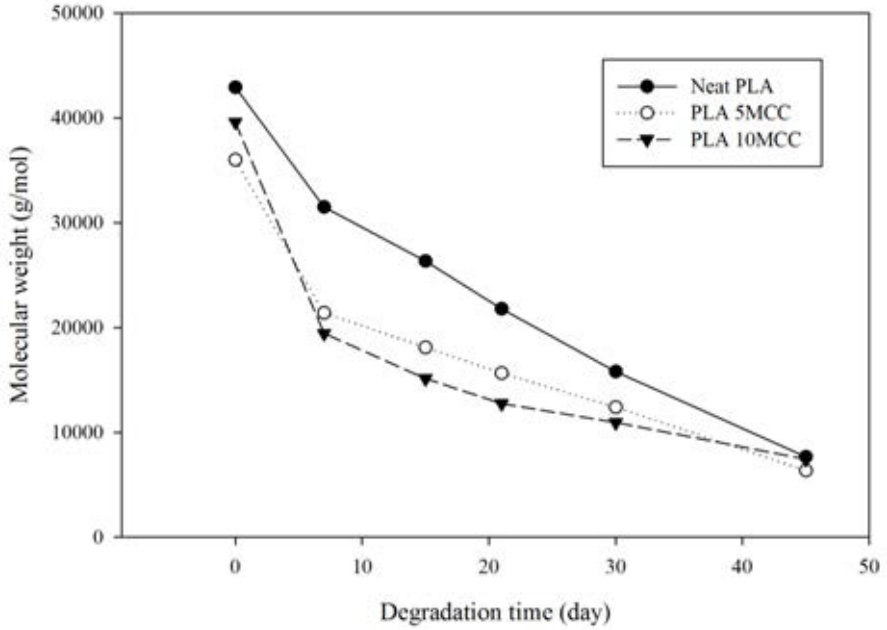

Figure 4.38 Biodegradability of PLA/MCC composites at various MCC containing

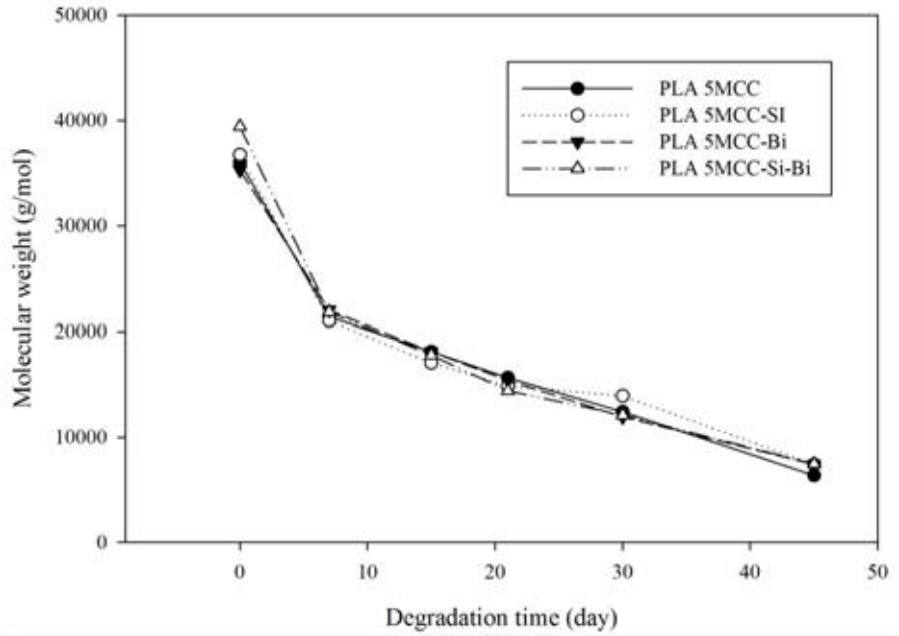

Figure 4.39 Effect of APS surface treatment and Biomax® on Biodegradability of PLA/MCC composite

4.7.4 Seawater test

Seawater is a very complicated environment for degradation because microorganisms, animals, salt, sunlight, fluctuation of water, rain etc. all play a part in degradation in nature [60]. The aim of this test was the estimation of degradability of different types of PLA/MCC composites in seawater. The samples were soaked in seawater at the depth of 1 m from the water surface. The samples after soaking for 30 days at Arng-sila, Chonburi are shown in Figure 4.40.

Figure 4.41 shows the weight losses of neat-PLA and PLA/MCC composites biodegraded statically in the seawater as a function of degradation time. Weight loss (%) were determined using an electronic balance and were shown in Figure 4.41. Weight of clean and dried samples of PLA/MCC composites after incubation in seawater was compared with those before incubation. Surisingly no significant weight loss of the neat-PLA and PLA/MCC composites was observed after biodegradation for 4 weeks. The percentage of weight loss estimated by gravimetric is comparable with the result reported by Hideto Tsuji, Kaori Suzuyoshi [60] for those biodegraded in seawater, but were very similar with each other when river water was used as a degradation medium.

The unchanged in weight of PLA/MCC composites can be attributed to the unsuitable the degradation environments because the degradation of PLA will occur under the two major factors. First, the polymer chains have to be hydrolyzed by water, which is catalyzed by temperature. For this test, the testing occurred in August, which is in the rainy season of Thailand. In August, 2011, the total number of rainy days at test filed was about 15-18 days, higher than July about 5-8 days [61]. So, the temperature of seawater was not high enough to catalyze the hydrolysis process. Secondly, follow by the attraction of microorganism to the fragment polymer chain. Consequence, the biodegradable of PLA was not occurring in this environment condition.

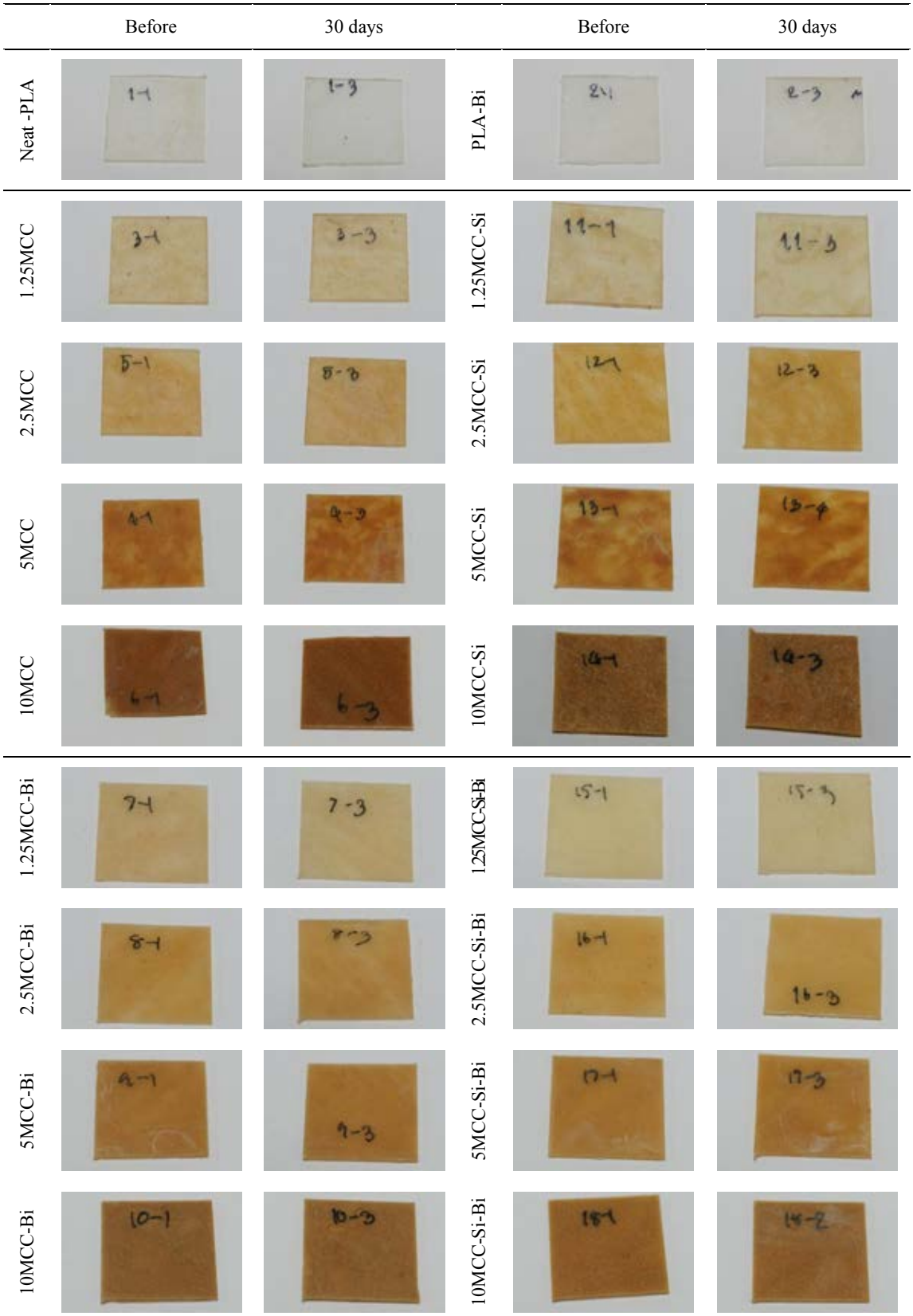

Figure 4.40 Appearance of PLA/MCC composites before and after soaking in seawater for 30 days.

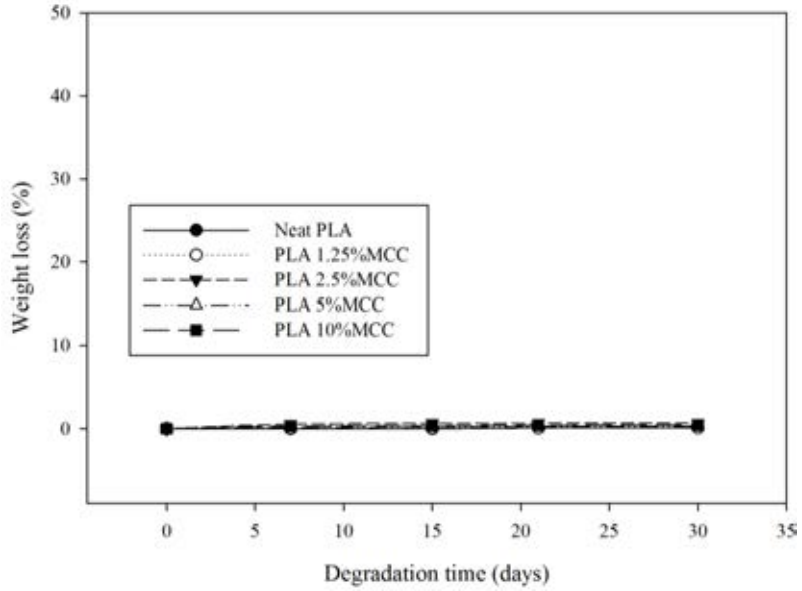

Figure 4.41 Weight loss of PLA composite after soak in seawater.

CHAPTER 5

Conclusions

Polylactic acid composites reinforced with microcrystalline cellulose were studied. The coir fibers were used to prepare microcrystalline cellulose by acid hydrolysis. In order to obtain microcrystalline cellulose, coir fibers were delignified, bleached, and hydrolyzed, respectively. Subsequently, the prepared microcrystalline cellulose was treated with 3-amiopropyl triethoxy silane (APS) to improve interfacial adhesion between fiber and polymer matrix. Treated and untreated microcrystalline cellulose were mixed at 0-10 wt.% with polylactic acid by twin-screw extruder and fabricated into test specimens by compression molding. Biomax ® strong 120 was used as modification resin at 2 phr. The effects of fiber loading, fiber surface treatment, and modification resin on mechanical, physical, thermal, and biodegradable properties of PLA/MCC composites were investigated. The results are summarized as follows.

1. The average size of prepared microcrystalline cellulose is 200 μm and the rod like shape is found.

2. The fiber surface treatment of microcrystalline cellulose by 3-amiopropyl triethoxy silane was confirmed by FT-IR and XRD. The characteristic of APS treated microcrystalline cellulose is shown by the existence of the wave number at 2162, 1557, 1421, 1110 cm^{-1}. For XRD diffraction pattern, the intensity peak of APS treated microcrystalline cellulose is higher than that of the untreated one. The treatment of microcrystalline enhances thermal stability of microcrystalline cellulose.

3. The polylactic acid composites reinforced with APS treated and untreated microcrystalline cellulose at various ratios were prepared. The neat PLA also prepared at the same processing condition of the composites as a reference material. Polylactic acid blended with 2 phr of Biomax® strong 120 was prepared and the effect of this modification resin was investigated.

4. For mechanical properties, the addition of microcrystalline cellulose in polylactic acid improved Young‘s modulus by 22% with 5 wt.% of microcrystalline cellulose loading. While the tensile strength and elongation at break decreased 34.4% and 2.65% respectively, upon adding 10 wt.% of microcrystalline cellulose. However,

the elongation at break and flexural strength can be enhanced by blending polylactic acid and its composites with 2 phr of Biomax®. In addition, APS surface treatment improved interfacial adhesion of microcrystalline cellulose and PLA matrix and enhanced tensile strength of the composites, as support by SEM analysis. In this work, the polylactic acid with 5 wt.% of microcrystalline cellulose and 2 phr of Biomax® exhibited the best mechanical properties compare with all other prepared composites.

5. The thermal stability of composites was decreased with increasing microcrystalline cellulose content. However, APS treated microcrystalline cellulose enhanced the thermal stability, while Biomax® had no significant effect no the thermal stability of the polylactic acid composites.

6. The percentage of water absorption was increased with increasing microcrystalline cellulose content and showed the increasing of hydrophilic behavior of polylactic acid composites.

7. The X-ray diffraction pattern of polylactic acid composites shows the characteristic of PLA at $2\theta = 16.37°$. When increasing the microcrystalline cellulose, the diffraction pattern also shows the characteristic of microcrystalline at $2\theta = 22.23°$.

8. The biodegradability of polylactic acid/microcrystalline composites was tested by simulated and real condition. GMR system was used to investigate the percentage of biodegradation of neat PLA and PLA-5MCC-Si-Bi and %biodegradability reached the values of 80.1% and 78.2%, respectively at 40 days of test period. The aqueous medium test system, which set up according to ISO 14852, was used to determine biodegradability of composites in activated sludge. Neat PLA and PLA-5MCC-Si-Bi reached the value of 37.6% and 42.1%, respectively,

9. The biodegradability in landfill condition was determined by following the changes in weight loss, molecular weight, and morphology. The weight remaining of composites was decreased with increasing microcrystalline cellulose content and biodegradation time. The APS treated microcrystalline cellulose had slight effect on the biodegradability. Similarly, Biomax® had no significant effect on the biodegradability of composites in landfill condition.

10. The sea water biodegradation test was used to determine the biodegradability of PLA/MCC composites in aqueous medium under real condition. Surprisingly, all of the test composites were not degraded in sea water upon soaking the sample for 30 days.

REFFERENCES

[1] Nolasco-Hipolito, C., Matsunaka, T., Kobayashi, G., Sonomoto, K., and Ishizaki, A. Synchronised fresh cell bioreactor system for continuous L (+) lactic acid production using Lactococcus lactis IO-1 in hydrolysed sago starch. Bioscience Bioengineering 93 (2002): 281–287.

[2] Carrasco, F., Pag s, P., G mez-P rez, J., Santana, O.O., and Maspoch, M.L. Kinetics of the thermal decomposition of processed poly(lactic acid). Polymer Degradation and Stability Article in press (2010):1-7.

[3] Gajria, A. M., Dave, V., Gross R. A., and McCarthy, S. P. Miscibility and biodegradability of blends of poly (lactic acid) and poly (vinyl acetate). Polymer 37 (1996): 437-444.

[4] Kulkarni, R. K., Moore, E. G., Hegyeli, A. F., and Leonard, F. Biodegradable poly(lactic acid) polymers. Journal of Biomedical. Material Research 5 (1971):169-181

[5] John M.J., and Thomas, S. Biofibres and biocomposites. Carbohydrate Polymers. 71. (2008):343–364.

[6] Tummala, P., Mohanty, A. K., Misra, M., and Drzal, L. T. Proceedings of 14th international conference on composite materials ICCM-14. (2003)

[7] Reddy, N., and Yang, Y. Structure and properties of high quality natural cellulose fibers from cornstalks. Polymer, 46 (2005): 5494–5500.

[8] Food And Agriculture Organization of the United Nations. Economic And Social Department. Statistics Division. (September 2, 2010). FAOSTAT – Production – Crops [Selected annual data]. (14 April 2011)

[9] Brian, E. G., Ashman, F., Dendy, D.A.V., and Jarman, C.G. Coconut palm products: their processing in developing countries. Food and Agicultural orgazination of the united nations, Rome, Italy 1975.

[10] Mohd Edeerozey A.M., and Hazizan M. A. Material Letter. 61 (2007)., 20-23

[11] Scandola, M., Frisoni, G., and Baiardo, M. Chemically Modified Cellulosic Reinforcements. in Book of Abstracts 219th ACS National Meeting, Washington, D.C., American Chemical Society. (2000)

[12] Klaus, F., Stoyko F., and Zhong Z. Polymer composite, from nano to macro scale. Springer, Berlin. 1966.

[13] Rothon, R. N. Particle-filled polymer composites, 2nd edition. Rapra Technology, Shrews- bury, UK. 1989.

[14] Hollaway, L. Handbook of polymer composites for engineers. Woodhead, Cambridge,UK. 1985.

[15] Cripps, A. Fibre-reinforced polymer composites in construction. CIRIA, London, UK. 1987.

[16] Mel, M., Schwart, Z. Composites Materials: Volume I, Prentice Hall PTR, New Jersy, USA. 1996.

[17] De, S.K., White, J.R. Short fibre-polymer composites. Woodhead, Cambridge, UK. 1984.

[18] Smith R. Biodegradable polymers for industrial applications, Woodhead Publishing, Cambridge, UK. 2005.

[19] Averous L., Boquillon, N. Biocomposites based on plasticized starch: Thermal and mechanical behaviours. Carbohydrate Polymers, 56, (2004): 111–122.

[20] Moore G.F., Saunders S.M., Advances in Biodegradable Polymers, Rapra Technology Ltd. 9, (1997):17-31.

[21] DarteÂe, M. Quality achievements in PLA based plastics. International Congress & Trade Show The Industrial Applications of Bioplastics, 3rd, 4th and 5th February. 2002.

[22] Nampoothiri, K. M., Nair, N. R., Rojan, P. J. An overview of the recent developments in polylactide (PLA) research. Bioresource Technology. 101. (2010): 8493–8501.

[23] Sarasua, J.R., Prud'homme, R.E., Wisniewski, M., LeBorgne, A., and Spassky, N. Crystallization and melting behavior of polylactides. Macromolecules 31 (1998): 3895– 3905.

[24] Technical data sheet. Biomax® Strong 120. Dupont. USA. (2010)

[25] Nevell, T. P., & Zeronian, S. H. Cellulose chemistry and its applications. Wiley, New York. 1985.

[26] Paralikar, K.M., and Bhatawdekar, S.P., Microcrystalline cellulose from bagasse pulp. Biological wastes, 24, (1988):75-77.

[27] Sakhawy, M., and Hassab, L. M. Physical and mechanical properties of microcrystalline cellulose prepared from agricultural residues. Jouranl of Carbohydraye polymer 67 (2006): 1-10.

[28] Plackett, D., Andersen, T. L., Pedersen, W. B., and Nielsen, L. Biodegradable composites based on L-polylactide and jute fibres, Composite Science Technology 63 (2003):1287-1296.

[29] Oksman, K., Skrifvars, M., and Selin, J.F. Natural fibres as reinforcement in polylactic acid (PLA) composites. Composite Science Technology 63 (2002):1317-1324.

[30] Scho Ènweitz C. New functional biopolymer-natural fibre-composites from agricultural resources. Consolidated progress report for EU FAIR CT98-3919, 2001.

[31] Lanzilotta, C., Pipino, A., and Lips, D. New functional biopolymer composites from agricultural resources. Proceedings of the Annual Technical Conference of the Society of Plastic Engineers 60 (2002):2185-2189.

[32] Nishino, T., Hirao, K., Kotera, M., Nakamae, K., and Inagaki, H. Kenaf reinforced biodegradable composites. Composite Science Technology 63 (2002):1281-1286.

[33] Shibata, M., Ozawa, K., Teramoto, N., Yosomiy,a R., and Takeishi, H. Biocomposites made from short abaca fiber and biodegradable polyesters. Macromolecule Materials Engineering 288 (2003):35-43.

[34] Huda, M.S., Drzal, L.T., Mohanty, A.K., and Misra, M. The effect of silane treated- and untreated-talc on the mechanical and physico-mechanical properties of poly(lactic acid)/newspaper fibers/talc hybrid composites. Composites Part B: Engineering 38 (2007):367–79.

[35] Jochen, G., and Andrzej, K.B. Alkali treatment of jute fibers: relationship between structure and mechanical properties. Journal Apply Polymer Science. 71. (1999):623–9.

[36] Singh, B., Verma, A., and Gupta, M. Studies on adsorptive interaction between natural fiber and coupling agents. Journal Apply Polymer Science 70 (1998):1847–1858.

[37] Dupraz, A.M.P., de Wijn, Jr. V.D., Meer, S.A.T., and de Groot K. Character-ization of silane-treated hydroxyapatite powders for use as filler in biodegradable composites. Journal Biomedical Materials Research. 30 (1996):231–238.

[38] Huda, M. S., Drzal, L. T., Mohanty, A. K., and Misra, M. Effect of fiber surface-treatments on the properties of laminated biocomposites from poly(lactic acid) (PLA) and kenaf fibers, Composites Science and Technology 68. (2008):424–432.

[39] ISO 14855-2:2007. Determination of the Ultimate Aerobic Biodegradability of Plastic Materials Under Controlled Composting Conditions—Method by Analysis of Evolved Carbon Dioxide—Part 2: Gravimetric Measurement of Carbon Dioxide Evolved in a Laboratory-scale Test, Edition. International Standard Organization. 2007.

[40] ISO 14852: Determination of the ultimate aerobic biodegradability of plastic materials in an aqueous medium - Method by analysis of evolved carbon dioxide. 1999.

[41] Annette, C., Renouf, G., John, R., David, F. F., and Ruth, E. C. The effect of crystallinity on the deformation mechanism and bulk mechanical properties of PLLA. Biomaterials 26 (2005):5771–5782.

[42] Jun, T. K. and Seong, H. K. Improvement in the Mechanical Properties of Polylactide and Bamboo Fiber Biocomposites by Fiber Surface Modification. Macromolecular Research. 19 (2011):789-796.

[43] Ali, R., Marianne, L. T., Claire, P., and Agne, S. Comparison of the Thermal Degradation of Natural, Alkali-Treated and Silane-Treated Hemp Fibers Under Air and an Inert Atmosphere. Journal of Applied Polymer Science 112 (2009):226–234.

[44] Srikanth, P., Shaoqin, G., Eric O.N., Liqiang, Y., and Roger M. R. Polylactide-Recycled Wood Fiber Composites. Journal of Applied Polymer Science. 111 (2009):37–47.

[45] Tserki, V., Zafeiropoulos, N.E., Simon, F., and Panayiotou, C. A study of the effect of acetylation and propionylation surface treatments on natural fibres. Compos Part A: Apply Science Manufacture 36 (2005):1110–1118.

[46] Moyeenuddin, Sawpan, K. L., and Pickering, A. F. Effect of various chemical treatments on the fibre structure and tensile properties of industrial hemp fibres. Composites: Part A 42 (2011):888–895.

[47] Yeng, F. S., and Chien, C. H. Polylactic acid(PLA)/banana fiber(BF) biodegradation green composites. Journal of polymer research (2011).

[48] Varma, I.K., Anantha, K. S.R., and Krishnamoorthy, S. Effect of chemical treatment on density and crystallinity of jute fibers. Text Research Journal 59 (1989):368–370.

[49] Hughes, M, Sebe, G, Hague, J., Hill, C., Spear, M., and Mott, L. An investigation into the effects of micro-compressive defects on interphase behaviour in hemp-epoxy composites using half-fringe photoelasticity. Composites Interfaces 7 (2000):13–29.

[50] Dan, W., Shi-bin S., Zhan-qian S., and Myoung-Ku L. Evaluation of microcrystalline cellulose prepared from kenaf fibers. Journal of Industrial and Engineering Chemistry 16 (2010):152–156.

[51] Gassan, J., and Bledzki, A.K. Alkali treatment of jute fibers: relationship between structure and mechanical properties. Journal of Apply Polymer Science 71 (1999): 623–629.

[52] Kunal, D., Dipa, R., Indranil, B., Bandyopadhyay, N. R., Suparna S., Amar, K. M., and Manjusri, M. Crystalline Morphology of PLA/Clay Nanocomposite Films and Its Correlation with Other Properties. Journal of Applied Polymer Science 118 (2010):143–151.

[53] Wong, S., Shanks, R., and Hodzic, A., Poly(L-lactic acid) composites with flax fibres modified by plasticizer absorption. Polymer Engineering Science 43 (2003): 1566-1575.

[54] Mohanty, A. K., Misra, M. and Hinrichsen, G. Biofibres, biodegradable polymers and biocomposites: An overview. Macromol Material Enginerring, (2000):276-277,

[55] Tserki, V., Matzinos, P. and Panayiotou, C. Effect of compatibilization on the performance of biodegradable composites using cotton fibre waste as filler. Journal of Applied Polymer Science 88 (2003): 1825-1835.

[56] Wallenberger, F. T. and Weston, N. Natural fibres, plastics and composites, Dordrecht, Kluwer Academic. 2004.

[57] Martin, O., AveÂrous, L. Poly(lactic acid): plasticization and properties of biodegradable multiphase systems, Polymer 42 (2001): 6209-6219.

[58] Jun, C. L. Reactive blending of biodegradable polymer: PLA and starch, Journal of Polymer. Environment. 8 (2000): 33-37.

[59] Nathalie, L., Christophe, B., Christian, B., Michèle, Q., Françoise, S., José, E., Nava, S. Review Polymer biodegradation: Mechanisms and estimation techniques. Chemosphere 73 (2008):429–442.

[60] Marco, B., Jan, P., Eubelerb, S. Z., and Thomas P. K. Aerobic biodegradation of polyethylene glycols of different molecular weights in wastewater and seawater. Water research 42 (2008): 4791–4801.

[61] Thai Meteorological department[Online]. Available from: http://www.arcims.tmd .go.th/dailydata/ MonthRain.php [17 september 2011].

APPENDIX

Table A1 Percent weight loss of PLA/MCC composites in landfill at 7 day

Materials	1		%	2		%	3		%	X	SD
	Bf	Af		Bf	Af		Bf	Af			
PLA	2.4901	2.4430	1.93	2.4226	2.3718	2.14	2.4901	2.3657	2.34	2.14	0.21
PLA-Bi	2.6138	2.5633	1.97	2.6253	2.5743	1.98	2.6138	2.5698	2.03	1.99	0.03
PLA-1.25MCC	2.6135	2.5590	2.13	2.6113	2.5591	2.04	2.6135	2.5621	1.97	2.05	0.08
PLA-2.5MCC	2.5928	2.5340	2.32	2.5866	2.5334	2.1	2.5928	2.5353	2.34	2.25	0.13
PLA-5MCC	2.5965	2.5374	2.33	2.5629	2.5134	1.97	2.5965	2.5211	2.34	2.21	0.21
PLA-10MCC	2.5488	2.4905	2.34	2.5527	2.4897	2.53	2.5488	2.4973	2.11	2.33	0.21
PLA-1.25MCC-Bi	2.7672	2.7074	2.21	2.7678	2.7085	2.19	2.7672	2.71	1.92	2.11	0.16
PLA-2.5MCC-Bi	2.6500	2.5957	2.09	2.6409	2.583	2.24	2.6500	2.6043	2.18	2.17	0.08
PLA-5MCC-Bi	3.0473	2.9840	2.12	2.9541	2.884	2.43	3.0473	2.3403	2.32	2.29	0.16
PLA-10MCC-Bi	2.7128	2.6430	2.64	2.7970	2.7392	2.11	2.7128	2.8302	2.43	2.39	0.27
PLA-1.25MCC-Si	2.8935	2.8340	2.1	3.0013	2.9304	2.42	2.8935	2.1762	1.98	2.17	0.23
PLA-2.5MCC-Si	2.7455	2.6830	2.33	2.4844	2.4302	2.23	2.7455	2.334	2.01	2.19	0.16
PLA-5MCC-Si	2.4508	2.4032	1.98	2.8588	2.794	2.32	2.4508	2.3748	2.32	2.21	0.20
PLA-10MCC-Si	2.2015	2.1493	2.43	2.5685	2.5049	2.54	2.2015	2.3845	2.74	2.57	0.16
PLA-1.25MCC-Si-Bi	2.8046	2.7493	2.01	2.9345	2.8739	2.11	2.8046	2.794	1.98	2.03	0.07
PLA-2.5MCC-Si-Bi	2.6946	2.6392	2.1	2.6550	2.5943	2.34	2.6946	2.443	1.73	2.06	0.31
PLA-5MCC-Si-Bi	2.6945	2.6329	2.34	2.9328	2.8739	2.05	2.6945	2.3454	2.23	2.21	0.15
PLA-10MCC-Si-Bi	2.8041	2.7403	2.33	3.0524	2.9832	2.32	2.8041	2.4958	2.53	2.39	0.12

Table A2 Percent weight loss of PLA/MCC composites in landfill at 15 day

Materials	1		%	2		%	3		%	X	SD
	Bf	Af		Bf	Af		Bf	Af			
PLA	2.3351	2.2129	5.23	2.3868	2.2599	5.32	2.4484	2.3152	5.44	5.33	0.11
PLA-Bi	2.6666	2.5338	4.98	2.8117	2.6748	4.87	2.6574	2.5450	4.23	4.69	0.41
PLA-1.25MCC	2.5195	2.3882	5.21	2.5208	2.3867	5.32	2.6418	2.4838	5.98	5.50	0.42
PLA-2.5MCC	2.4942	2.3670	5.1	2.5495	2.4133	5.34	2.6152	2.4758	5.33	5.26	0.14
PLA-5MCC	2.5541	2.4154	5.43	2.6107	2.4638	5.63	2.5946	2.4589	5.23	5.43	0.20
PLA-10MCC	2.4745	2.3456	5.21	2.8921	2.7293	5.63	2.5701	2.4362	5.21	5.35	0.24
PLA-1.25MCC-Bi	2.4511	2.3229	5.23	2.5055	2.3807	4.98	2.7960	2.6556	5.02	5.08	0.13
PLA-2.5MCC-Bi	2.5430	2.4072	5.34	2.5994	2.4611	5.32	2.6664	2.5280	5.19	5.28	0.08
PLA-5MCC-Bi	2.8393	2.6795	5.63	2.5906	2.4575	5.14	2.9772	2.8197	5.29	5.35	0.25
PLA-10MCC-Bi	2.7507	2.6074	5.21	2.5293	2.3983	5.18	2.8277	2.6772	5.32	5.24	0.07
PLA-1.25MCC-Si	2.4661	2.3421	5.03	2.7257	2.5834	5.22	3.0251	2.8681	5.19	5.15	0.10
PLA-2.5MCC-Si	2.8294	2.6783	5.34	2.5753	2.4355	5.43	2.5087	2.3803	5.12	5.30	0.16
PLA-5MCC-Si	2.5344	2.3996	5.32	2.9023	2.7458	5.39	2.8842	2.7302	5.34	5.35	0.04
PLA-10MCC-Si	2.6968	2.5439	5.67	2.7566	2.6099	5.32	2.5858	2.4454	5.43	5.47	0.18
PLA-1.25MCC-Si-Bi	2.8850	2.7315	5.32	2.9490	2.8033	4.94	2.9667	2.8083	5.34	5.20	0.23
PLA-2.5MCC-Si-Bi	2.3926	2.2653	5.32	2.4456	2.3182	5.21	2.6781	2.5327	5.43	5.32	0.11
PLA-5MCC-Si-Bi	2.8294	2.6769	5.39	2.8921	2.7383	5.32	2.9667	2.8131	5.18	5.30	0.11
PLA-10MCC-Si-Bi	2.9370	2.7775	5.43	3.0021	2.8466	5.18	3.0796	2.9160	5.31	5.31	0.13

Table A3 Percent weight loss of PLA/MCC composites in landfill at 21 day

Materials	1		%	2		%	3		%	X	SD
	Bf	Af		Bf	Af		Bf	Af			
PLA	2.6233	2.4163	7.89	2.3713	2.1788	8.12	2.3547	2.1583	8.34	8.12	0.23
PLA-Bi	2.7525	2.5367	7.84	2.7935	2.5717	7.94	2.5578	2.3450	8.32	8.03	0.25
PLA-1.25MCC	2.7479	2.5217	8.23	2.5044	2.2855	8.74	2.5502	2.3324	8.54	8.50	0.26
PLA-2.5MCC	2.7210	2.4802	8.85	2.5329	2.3131	8.68	2.5235	2.2976	8.95	8.83	0.14
PLA-5MCC	2.7247	2.4947	8.44	2.5938	2.3593	9.04	2.5094	2.2863	8.89	8.79	0.31
PLA-10MCC	2.6743	2.4325	9.04	2.8734	2.6116	9.11	2.4857	2.2684	8.74	8.96	0.20
PLA-1.25MCC-Bi	2.9072	2.6589	8.54	2.4892	2.2657	8.98	2.6974	2.4724	8.34	8.62	0.33
PLA-2.5MCC-Bi	2.7873	2.5523	8.43	2.5825	2.3496	9.02	2.5922	2.3506	9.32	8.92	0.45
PLA-5MCC-Bi	3.2042	2.9146	9.04	2.5738	2.3440	8.93	2.3294	2.1193	9.02	9.00	0.06
PLA-10MCC-Bi	2.8381	2.5701	9.44	2.5129	2.2732	9.54	2.8170	2.5790	8.45	9.14	0.60
PLA-1.25MCC-Si	3.0431	2.7988	8.03	2.7080	2.4797	8.43	2.1661	1.9776	8.7	8.39	0.34
PLA-2.5MCC-Si	2.8810	2.6263	8.84	2.5586	2.3404	8.53	2.3231	2.1326	8.2	8.52	0.32
PLA-5MCC-Si	2.5806	2.3491	8.97	2.8834	2.6404	8.43	2.3637	2.1571	8.74	8.71	0.27
PLA-10MCC-Si	2.3079	2.1007	8.98	2.7387	2.4884	9.14	2.3734	2.1707	8.54	8.89	0.31
PLA-1.25MCC-Si-Bi	2.9522	2.6909	8.85	2.9298	2.6653	9.03	2.7810	2.5218	9.32	9.07	0.24
PLA-2.5MCC-Si-Bi	2.8340	2.5803	8.95	2.4297	2.2137	8.89	2.4316	2.2050	9.32	9.05	0.23
PLA-5MCC-Si-Bi	2.8272	2.5827	8.65	2.8734	2.6389	8.16	2.3345	2.1316	8.69	8.50	0.30
PLA-10MCC-Si-Bi	2.9425	2.6909	8.55	2.9826	2.6954	9.63	2.4842	2.2748	8.43	8.87	0.66

Table A4 Percent weight loss of PLA/MCC composites in landfill at 30 day

Materials	1		%	2		%	3		%	X	SD
	Bf	Af		Bf	Af		Bf	Af			
PLA	2.3637	1.9160	18.94	2.3637	1.9543	17.32	2.6832	2.2408	16.49	17.58	1.25
PLA-Bi	2.6992	2.1721	19.53	2.6992	2.2342	17.23	2.8154	2.2683	19.43	18.73	1.30
PLA-1.25MCC	2.5503	2.0066	21.32	2.5503	1.9844	22.19	2.8106	2.2645	19.43	20.98	1.41
PLA-2.5MCC	2.5247	1.9607	22.34	2.5247	1.9812	21.53	2.7832	2.1005	24.53	22.80	1.55
PLA-5MCC	2.5854	1.9693	23.83	2.5854	2.0572	20.43	2.7869	2.1897	21.43	21.90	1.75
PLA-10MCC	2.5048	1.8701	25.34	2.5048	1.8450	26.34	2.7354	2.1796	20.32	24.00	3.23
PLA-1.25MCC-Bi	2.4812	1.8996	23.44	2.4812	1.9820	20.12	2.9736	2.2567	24.11	22.56	2.14
PLA-2.5MCC-Bi	2.5742	1.9196	25.43	2.5742	2.0508	20.33	2.8510	2.2146	22.32	22.69	2.57
PLA-5MCC-Bi	2.8741	2.1432	25.43	2.8741	2.1145	26.43	3.2774	2.6108	20.34	24.07	3.27
PLA-10MCC-Bi	2.7844	2.1599	22.43	2.7844	2.0789	25.34	2.9029	2.2228	23.43	23.73	1.48
PLA-1.25MCC-Si	2.4963	1.9918	20.21	2.4963	1.9387	22.34	3.1127	2.4456	21.43	21.33	1.07
PLA-2.5MCC-Si	2.8641	2.2248	22.32	2.8641	2.1389	25.32	2.9468	2.2564	23.43	23.69	1.52
PLA-5MCC-Si	2.5655	1.8846	26.54	2.5655	1.9411	24.34	2.6395	1.9973	24.33	25.07	1.27
PLA-10MCC-Si	2.7298	2.0351	25.45	2.7298	2.1746	20.34	2.3607	1.6921	28.32	24.70	4.04
PLA-1.25MCC-Si-Bi	2.9204	2.3270	20.32	2.9204	2.3264	20.34	3.0197	2.3122	23.43	21.36	1.79
PLA-2.5MCC-Si-Bi	2.4219	1.9147	20.94	2.4219	1.8569	23.33	2.8987	2.1932	24.34	22.87	1.75
PLA-5MCC-Si-Bi	2.8641	2.1386	25.33	2.8641	2.2500	21.44	2.8918	2.1879	24.34	23.70	2.02
PLA-10MCC-Si-Bi	2.9730	2.2202	25.32	2.9730	2.1997	26.01	3.0098	2.3013	23.54	24.96	1.27

Table A4 Percent weight loss of PLA/MCC composites in landfill at 30 day

Materials	1		%	2		%	3		%	X	SD
	Bf	Af		Bf	Af		Bf	Af			
PLA	2.3262	1.6598	28.65	2.5131	1.8112	27.93	2.8877	1.6598	25.34	27.30	0.67
PLA-Bi	2.5269	1.8333	27.45	2.7300	2.0641	24.39	3.0299	1.8333	27.43	26.42	1.56
PLA-1.25MCC	2.5194	1.7578	30.23	2.7218	1.8418	32.33	3.0248	1.7578	29.43	30.66	1.11
PLA-2.5MCC	2.4930	1.6868	32.34	2.6933	1.8791	30.23	2.9953	1.6868	33.64	32.07	1.15
PLA-5MCC	2.4790	1.6498	33.45	2.6782	1.8121	32.34	2.9993	1.6498	36.54	34.11	0.89
PLA-10MCC	2.4556	1.5584	36.54	2.6529	1.6276	38.65	2.9438	1.5584	36.54	37.24	1.07
PLA-1.25MCC-Bi	2.6648	1.8534	30.45	2.8789	1.8909	34.32	3.2002	1.8534	32.34	32.37	1.94
PLA-2.5MCC-Bi	2.5609	1.7583	31.34	2.7666	1.8135	34.45	3.0682	1.7583	32.34	32.71	1.56
PLA-5MCC-Bi	2.3013	1.5320	33.43	2.4862	1.5805	36.43	3.5272	1.5320	38.43	36.09	1.64
PLA-10MCC-Bi	2.7830	1.7602	36.75	3.0066	1.8812	37.43	3.1241	1.7602	36.23	36.80	0.38
PLA-1.25MCC-Si	2.1399	1.4218	33.56	2.3118	1.4435	37.56	3.3499	1.4218	37.65	36.25	2.04
PLA-2.5MCC-Si	2.2951	1.5024	34.54	2.4795	1.5514	37.43	3.1714	1.5024	33.74	35.23	1.51
PLA-5MCC-Si	2.3352	1.4866	36.34	2.5228	1.7069	32.34	2.8407	1.4866	35.86	34.84	2.02
PLA-10MCC-Si	2.3447	1.5609	33.43	2.5331	1.7139	32.34	2.5405	1.5609	38.43	34.73	1.20
PLA-1.25MCC-Si-Bi	2.7474	1.8344	33.23	2.9681	2.0088	32.32	3.2498	1.8344	30.34	31.96	0.65
PLA-2.5MCC-Si-Bi	2.4023	1.5752	34.43	2.5953	1.7567	32.31	3.1196	1.5752	32.32	33.02	1.08
PLA-5MCC-Si-Bi	2.3063	1.5353	33.43	2.4916	1.5812	36.54	3.1122	1.5353	30.23	33.40	1.80
PLA-10MCC-Si-Bi	2.4542	1.6610	32.32	2.6514	1.6059	39.43	3.2391	1.6610	40.23	37.32	3.65

BIOGRAPHY

Mr. Tanawat Tayommai was born in Nakhonratchasima, Thailand on 23rd September 1986. He received his Bachelor's Degree of Science in Materials Science from Faculty of science, Chulalongkorn University in 2009. After that, He continued a further study in a Master Degree in the field of Applied Polymer and Textile Technology at department of Materials Science, Faculty of science, Chulalongkorn University in 2009, and ultimately completed the Degree of the Master of Science in Applied Polymer Science and Textile Technology in October 2011.